การเกิดสารประกอบระหว่างโคบอลต์กับตัวรองรับของตัวเร่งปฏิกิริยาโคบอลต์บนตัวรองรับไทเทเนีย

นางสาวจิตรลดา ศักดิ์ดามพ์นุสนธิ์

COBALT-SUPPORT COMPOUND FORMATION IN TITANIA-SUPPORTED COBALT CATALYSTS

Miss Chitlada Sakdamnuson

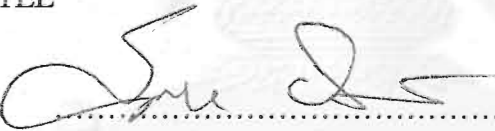Thesis Title   COBALT-SUPPORT COMPOUND FORMATION IN TITANIA SUPPORTED COBALT CATALYSTS
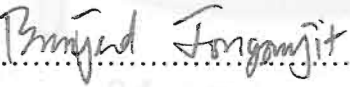
By   Miss Chitlada Sakdamnuson

Field of Study   Chemical Engineering

Thesis Advisor   Bunjerd Jongsomjit, Ph.D

Thesis Co-advisor   Professor Piyasan Praserthdam, Dr.Ing.
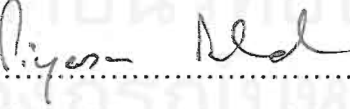
Accepted by the Faculty of Engineering, Chulalongkorn University in Partial Fulfillment of the Requirements for the Master's Degree

....Dean of Faculty of Engineering

(Professor Direk Lavansiri, Ph.D.)
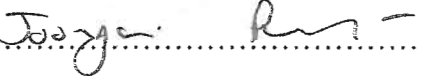
THESIS COMMITTEE

.... Chairman

(Associate Professor Suttichai Assabumrungrat, Ph.D.)

.... Thesis Advisor

(Bunjerd Jongsomjit, Ph.D.)

.... Thesis Co-advisor

(Professor Piyasan Praserthdam, Dr.Ing.)

.... Member

(Montree Wongsri, D.Sc.)

.... Member

(Joongjai Panpranot, Ph.D.)

จิตรลดา ศักดิ์ดามพ์นุสนธิ์: การเกิดสารประกอบระหว่างโคบอลต์กับตัวรองรับของตัวเร่ง
ปฏิกิริยาปฏิกิริยาโคบอลต์บนตัวรองรับไทเทเนีย (COBALT-SUPPORT COMPOUND
FORMATION IN TITANIA-SUPPORTED COBALT CATALYSTS) อ. ที่ปรึกษา :
ดร.บรรเจิด จงสมจิตร, อ. ที่ปรึกษาร่วม : ศ.ดร.ปิยะสาร ประเสริฐธรรม, 124 หน้า. ISBN
974-17-4477-3

สารประกอบระหว่างโคบอลต์กับตัวรองรับของตัวเร่งปฏิกิริยาโคบอลต์บนตัวรองรับไทเท
เนียพบในระหว่างการทำรีดักชันที่ภาวะมาตรฐานแสดงถึงค่าความสามารถในการรีดิวซ์ที่ลดลงของ
ตัวเร่งปฏิกิริยา สารประกอบที่เกิดขึ้นพบว่าไม่สามารถรีดิวซ์ได้ที่อุณหภูมิน้อยกว่า 800 องศา
เซลเซียสในการรีดักชันแบบโปรแกรมอุณหภูมิและแตกต่างจากโคบอลต์ไทเทเนต การทดสอบ
คุณลักษณะของสารประกอบระหว่างโคบอลต์กับตัวรองรับทำการศึกษาโดยใช้ การวัดพื้นที่ผิว การ
กระเจิงรังสีเอ็กซ์ การดูดซับด้วยไฮโดรเจน รามานสเปกโทรสโกปี การส่องผ่านด้วยกล้อง
จุลทรรศน์อิเล็กตรอน/การวัดการกระจายตัวของโลหะ และการรีดักชันแบบโปรแกรมอุณหภูมิ
การศึกษาผลของโครงสร้างผลึกของตัวรองรับไทเทเนีย ทำการเปรียบเทียบตัวรองรับไทเทเนียที่ใช้
ระหว่างเฟสแอนาเทสบริสุทธิ์ (T1) และ เฟสผสม; แอนาเทสและรูไทล์ (T2) ผลการศึกษาพบว่า
ความแตกต่างของตัวรองรับไทเทเนียมีผลต่อสมรรถนะของตัวเร่งปฏิกิริยา โดยเฉพาะอย่างยิ่งความ
ว่องไวและความเสถียรภาพ พบว่าความว่องไวของตัวเร่งปฏิกิริยาและความเสถียรภาพในปฏิกิริยา
คาร์บอนมอนคาร์บอนมอนอกไซด์ไฮโดรจิเนชันของตัวเร่งปฏิกิริยาโคบอลต์บนตัวรองรับ T2 สูง
กว่าตัวเร่งปฏิกิริยาโคบอลต์บนตัวรองรับ T1 ซึ่งอาจเป็นผลมาจากเฟสรูไทล์อาจช่วยสนับสนุน
ความว่องไวของตัวเร่งปฏิกิริยาและยับยั้งสารประกอบระหว่างโคบอลต์กับตัวรองรับ การเติมตัว
สนับสนุนรูทีเนียม มีผลทำให้ค่าความสามารถในการรีดิวซ์และความว่องไวของตัวเร่งปฏิกิริยา
เพิ่มขึ้น เมื่อมีรูทีเนียม การเกิดสารประกอบระหว่างโคบอลต์สปีชีส์กับตัวรองรับที่รีดิวซ์ได้ยาก
ลดลง อาจเป็นเพราะรูทีเนียมช่วยทำให้การทำรีดักชันของโคบอลต์ง่ายขึ้นที่อุณหภูมิต่ำกว่า
เนื่องจากผลของไฮโดรเจนสปิลโอเวอร์

ภาควิชา	วิศวกรรมเคมี	ลายมือชื่อนิสิต จิตรลดา ศักดิ์ดามพ์นุสนธิ์
สาขาวิชา	วิศวกรรมเคมี	ลายมือชื่ออาจารย์ที่ปรึกษา
ปีการศึกษา	2546	ลายมือชื่ออาจารย์ที่ปรึกษาร่วม

##4570253521: MAJOR CHEMICAL ENGINEERING

KEY WORD: SUPPORTED CATALYST/ COBALT CATALYST/ COBALT-SUPPORT COMPOUND/ TITANIA SUPPORT/ Co/TiO$_2$/ REDUCIBILITY/ CO HYDROGENATION

CHITLADA SAKDAMNUSON: COBALT-SUPPORT COMPOUND FORMATION IN TITANIA-SUPPORTED COBALT CATALYSTS. THESIS ADVISOR: BUNJERD JONGSOMJIT, Ph.D., THESIS COADVISOR: PROFESSOR PIYASAN PRASERTHDAM, Dr.Ing. 124 pp. ISBN: 974-17-4477-3

Co-support compound formation (Co-SCF) in Co/TiO$_2$ was found during standard reduction resulting in a lower reducibility of the catalyst. The compound formed is considered to be non-reducible at temperatures $< 800^{\circ}$C during TPR and different from CoTiO$_3$. The characteristics of Co-SCF were investigated using BET surface area, XRD, H$_2$ chemisorption, Raman spectroscopy, SEM/EDX and TPR. In addition, effects of crystalline form of the TiO$_2$ supports were also studied. A comparative study of titania supports used between the pure anatase phase (T1) and mixed phase; anatase and rutile (T2) was investigated. The results indicated the differences in titania support phases can affect the catalyst performance especially in the overall activity and stability. It was found that the overall activity and the stability in CO hydrogenation reaction of the Co/T2 catalysts was higher than that of Co/T1 catalysts. This is probably because rutile phase may help promoting the activity of the Co/TiO$_2$ catalysts and inhibiting Co-SCF. The addition of Ru promoter was found to enhance both reducibilities and the overall activities. When Ru promoter was present, the formation of Co-SCF decreased significantly due to hydrogen spillover effect.

Department......Chemical Engineering... Student's signature...Chitlada Sakdamnuson

Field of study...Chemical Engineering... Advisor's signature...Bunjerd Jongsomjit

Academic year.....2003.................. Co-advisor's signature...

ACKNOWLEDGEMENTS

CONTENTS

CONTENTS (CONT.)

CONTENTS (CONT.)

LIST OF TABLES

LIST OF TABLES

LIST OF FIGURES

高

LIST OF FIGURES

LIST OF FIGURES

CHAPTER I

INTRODUCTION

Research in heterogeneous catalysis involves in developing a better understanding of the catalytic properties and reactions. Catalysts are chemically and physically complex. In general, a supported catalyst consists of three components; a catalytic active phase, a support and/or a promoter. Catalyst properties are divided into three parts: physical, chemical and dynamic. Physical properties contain BET surface area, pore size distribution, pore diameter, morphology of particles and etc. Chemical properties involve acidity, hydrophobic-hydrophilic nature and etc. Dynamic properties relate to the catalytic behavior during reaction including activity and selectivity. Definitely, the catalyst compositions always have impacts on catalyst properties. In order to understand catalysis, the catalyst properties need to be elucidated.

Fischer-Tropch synthesis (FTS) is known as a carbon monoxide (CO) hydrogenation which is added hydrogen to carbon monoxide. Generally, the process is most widely used for synthesis of hydrocarbon waxes which are further cracked into gasoline and diesel fuel. Many transition metals of Group VIII can be used as catalysts for FTS such as iron (Fe), cobalt (Co), nickel (Ni) and ruthenium (Ru). However, supported cobalt catalysts are preferred due to their high activity for FTS based on natural gas, high selectivity to linear hydrocarbon and low activity for the competitive water-gas shift reaction (WGS). For Co catalysts, it is known that the reduced metal, rather than its oxides or carbides, is the most active phase in CO hydrogenation. However, compound formation between cobalt and the supports can occur during the catalyst activation and/or reaction conditions resulting in irreversible catalyst deactivation (Jongsomjit et al., 2001, 2002, 2003).

Besides alumina (Al_2O_3) and silica (SiO_2), titania (TiO_2) has been widely studied as the support for cobalt catalysts by many authors (Reuel and Bartholomew, 1984; Kraum and Baerns, 1999; Li et al., 2002; Jacobs et al., 2002; Madikizela and Coville, 2002). It was reported that Co-SCF in SiO_2 (Kogelbauer et al., 1995) and Al_2O_3 (Zhang et al. 1999; Jongsomjit et al., 2001, 2002, 2003) can occur during

standard reduction and resulted in a lower degree of reduction. However, Co-SCF in titania support has been rarely studied.

Moreover, promotion with a second metal such as Ru (Kogelbauer *et al.*, 1996; Zhang *et al.* 1999; Jongsomjit *et al.*, 2001; Tsubaki *et al.*, 2001; Panpranot *et al.*, 2002; Jacobs *et al.*, 2002; Sun *et al.*, 2002), Rh (Schanke *et al.*, 1995; Hilmen *et al.*, 1999), Re (Das *et al.*, 2003), Pt (Tsubaki *et al.*, 2001; Jacobs *et al.*, 2002; Sun *et al.*, 2002) and Pd (Tsubaki *et al.*, 2001; Sun *et al.*, 2002) as been reported to used on cobalt-based catalysts. It had been proposed that these metal promoters can increase the reducibility and dispersion of Co, preserve the activity by preventing the formation of coke, exhibit cluster and ligand effect and act as a source for hydrogen spillover (Jongsomjit *et al.*, 2001).

In this study, the nature of Co-SCF in titania-supported cobalt catalysts and its effect on the characteristics of the catalysts were the main focus. In addition, how the crystalline forms (anatase, rutile) of titania support affected the nature of Co-SCF and then provided a strategy to minimize Co-SCF in titania-supported cobalt catalysts using ruthenium (Ru) promotion. The study was scoped as follows:

1. Preparation of Co/TiO_2 (20 wt% Co) with and without Ru promotion using the incipient wetness impregnation method.

2. Catalyst pretreatment by standard reduction (350°C, 10 h, in H_2) with and without addition of water vapor during reduction.

3. Characterization of the catalyst samples using atomic absorption spectroscopy (AAS), BET surface area, X-ray diffraction (XRD), temperature-programmed reduction (TPR) thermal gravimetric analysis (TGA), H_2 chemisorption, scanning electron microscopy (SEM), energy dispersive X-ray spectroscopy (EDX) and Raman spectroscopy.

4. Reaction study of the catalyst samples in CO hydrogenation at 220°C and 1 atm in order to measure catalytic activity and selectivity.

CHAPTER II

LITERATURE REVIEWS

There are several studies of titania-supported catalysts. Many researchers have found knowledge about titania, especially supported cobalt catalyst in Fischer-Tropch synthesis. In this chapter, literature reviews on cobalt-support compound formation (Co-SCF), titania-supported cobalt catalysts and effects of noble metal promotion on supported cobalt catalysts are provided, respectively. These reports are very useful and will use to develop works for the future.

2.1 Cobalt-support compound formation (Co-SCF)

Kogelbauer *et al.* (1995) studied the formation of cobalt silicates on Co/SiO_2 under hydrothermal conditions. Hydrothermal treatment at $220^{\circ}C$ led to a catalyst with lower reducibility due to the formation of both reducible and nonreducible (at temperatures < $900^{\circ}C$) Co silicates. They also showed that silicate was formed in catalysts which had been used for FT synthesis. No significant change occurred upon hydrothermal treatment of calcined catalyst. The presence of air during the hydrothermal treatment inhibited the formation of silicate and they proposed that the formation of silicate was linked to the presence of metallic cobalt.

Zhang *et al.* (1999) investigated the impact of water vapor on the reducibility of $CoRu/Al_2O_3$ during the standard reduction procedure (H_2, $350^{\circ}C$, 10 h) and during TPR. They reported that water vapor has a significant effect on the reduction behavior of $CoRu/Al_2O_3$ catalysts. They also suggested that introduction of water vapor during standard reduction led to a decrease in the degree of reduction of cobalt probably in two ways: (i) inhibition of the reduction of well-dispersed CoO interacting with the alumina support possibly by increasing the Co-alumina interaction and (ii) facilitation of migration Co ions into probable tetrahedral sites of γ- Al_2O_3 to form a nonreducible ($\leq 900^{\circ}C$) spinel. Such an irreversible spinel formation resulted in a decrease in the amount of reduced cobalt metal atoms using conventional reduction procedures.

Jongsomjit *et al.* (2001) studied the nature of the Co-support compounds formed in alumina-supported cobalt catalysts during standard reduction and the effect of noble metal (Ru) promotion on their formation. They found that 3% added water vapor during reduction increased the amounts of nonreducible Co aluminate (at temperatures $\leq 900^{\circ}C$) formed. This compound formation caused changes in the characteristics of Co catalysts, especially their reducibilities and overall activity during FT synthesis. The addition of Ru promoter to Co catalysts increased both the overall Co^{o} dispersion and the reducibility. It was suggested that the Ru promoter not only facilitated the reduction of Co at lower temperatures, but also decreased the formation of Co strongly interacting with the alumina (Co_XO_Y-Al_2O_3) and nonreducible Co aluminate by minimizing the impact of water vapor on this formation.

Jongsomjit and Goodwin (2002) investigated the effect of the addition of CO during H_2 reduction on Co-support compound formation in a Co/Al_2O_3 catalyst. They have reported that the addition of CO during H_2 reduction of a 20% Co/Al_2O_3 catalyst produced specific activities about four times greater than when the catalyst reduced without CO addition. Most of this increase appeared to be due to increases in Co reducibility and dispersion. They also suggested that the effect of CO addition may be due to one or more of possibly three reasons: (i) CO may help to prevent the formation of Co species strongly interacting with the support, thereby facilitating its reduction, (ii) CO may decrease sintering of the Co metal resulting an increase in Co dispersion, and (iii) Co may block Co "aluminate" formation by minimizing the impact of water vapor even at low partial pressures.

Jongsomjit *et al.* (2003) synthesized the Zirconia (Zr)-modified alumina-supported Co catalysts by the sequential impregnation method. They studied the impact of Zr loading on the reducibility of Co in the absence and presence of water vapor. They reported that Zr modification of the alumina support had a significant impact on the catalyst properties: the overall activity during FT synthesis increased significantly upon Zr modification due to an increase in reducibility during standard reduction. Furthermore, the increase in reducibility appeared to have been caused by a decrease in the amount of Co-SCF. They also suggested that Zr modification may

have caused: (i) a stabilization of the alumina support by blocking Co "aluminate" formation and/or (ii) a minimization of the impact of water vapor in modifying the surface properties of alumina, thereby decreasing the ease of Co reaction with the alumina.

2.2 Titania-supported cobalt catalysts in CO hydrogenation

Reuel and Bartholomew (1984) studied the effect of support and dispersion on the CO hydrogenation activity/selectivity properties of cobalt. They found that the specific activity and selectivity of cobalt in CO hydrogenation is a function of support, dispersion, metal loading and preparation. The order of decreasing CO hydrogenation activity at 1 atm and 225°C for catalysts containing 3wt% cobalt was $Co/TiO_2 > Co/SiO_2 > Co/Al_2O_3 > Co/C > Co/ MgO$. The specific activity of cobalt best correlated with dispersion and extent of reduction. In the Co/Al_2O_3 system, activity and selectivity for high molecular weight hydrocarbons increased very significantly with increasing cobalt loading.

Ho *et al.* (1992) proposed to characterized the state and dispersion of cobalt in a series of Co/TiO_2 catalyst and investigated performance in benzene and CO hydrogenation. They reported that the cobalt phase in oxidic 0.5 and 1% cobalt catalysts was present as highly dispersed surface $CoTiO_3$. For catalysts having higher cobalt loading, discrete Co_3O_4 particles are formed in addition to surface $CoTiO_3$. Furthermore, ESCA data indicated that after reduction the cobalt metal particle size increased with increasing cobalt loading, but did not vary with reduction temperature (400-500°C). Hydrogen chemisorption was found to be activated and suppressed. The extent of hydrogen chemisorption suppression increased with increasing reduction temperatures and decreasing cobalt particle size. The turnover frequency (based on cobalt dispersion derived from ESCA) for benzene and CO hydrogenation decreased with increasing reduction temperatures and decreasing cobalt particle size.

Choi (1995) investigated the reduction of cobalt catalysts supported on Al_2O_3, SiO_2 and TiO_2 and the effect of metal loading on the reduction. He reported that the activation energy of reduction increased in the following order: $Co/SiO_2 > Co/Al_2O_3 >$

have caused: (i) a stabilization of the alumina support by blocking Co "aluminate" formation and/or (ii) a minimization of the impact of water vapor in modifying the surface properties of alumina, thereby decreasing the ease of Co reaction with the alumina.

2.2 Titania-supported cobalt catalysts in CO hydrogenation

Reuel and Bartholomew (1984) studied the effect of support and dispersion on the CO hydrogenation activity/selectivity properties of cobalt. They found that the specific activity and selectivity of cobalt in CO hydrogenation is a function of support, dispersion, metal loading and preparation. The order of decreasing CO hydrogenation activity at 1 atm and 225°C for catalysts containing 3wt% cobalt was $Co/TiO_2 > Co/SiO_2 > Co/Al_2O_3 > Co/C > Co/MgO$. The specific activity of cobalt best correlated with dispersion and extent of reduction. In the Co/Al_2O_3 system, activity and selectivity for high molecular weight hydrocarbons increased very significantly with increasing cobalt loading.

Ho *et al.* (1992) proposed to characterized the state and dispersion of cobalt in a series of Co/TiO_2 catalyst and investigated performance in benzene and CO hydrogenation. They reported that the cobalt phase in oxidic 0.5 and 1% cobalt catalysts was present as highly dispersed surface $CoTiO_3$. For catalysts having higher cobalt loading, discrete Co_3O_4 particles are formed in addition to surface $CoTiO_3$. Furthermore, ESCA data indicated that after reduction the cobalt metal particle size increased with increasing cobalt loading, but did not vary with reduction temperature (400-500°C). Hydrogen chemisorption was found to be activated and suppressed. The extent of hydrogen chemisorption suppression increased with increasing reduction temperatures and decreasing cobalt particle size. The turnover frequency (based on cobalt dispersion derived from ESCA) for benzene and CO hydrogenation decreased with increasing reduction temperatures and decreasing cobalt particle size.

Choi (1995) investigated the reduction of cobalt catalysts supported on Al_2O_3, SiO_2 and TiO_2 and the effect of metal loading on the reduction. He reported that the activation energy of reduction increased in the following order: $Co/SiO_2 > Co/Al_2O_3 >$

Co/TiO$_2$. For different metal loading, the catalyst with the higher loading was more readily reducible than with the lower metal loading.

Ho (1996) investigated the dehydroxylation and rehydroxylation properties of titania and the states of hydrogen adsorbed on titania supported cobalt catalysts. They reported that FTIR and TPD-MS data indicated hydroxyl groups were not completely removed at 500°C *in vacuo* and rehydration/rehydroxylation occurred under helium flow at room temperature. In addition, repeating dehydroxylation/ rehydroxylation treatments for ten times did not significantly modify the dehydroxylation/rehydroxylation property of titania surface. Desorption of hydrogen from titania was observed at 535°C after titania was reduced aboved 400°C. Besides, TPD data showed four types of hydrogen on 3% titania supported cobalt catalysts: hydrogen adsorbed on cobalt metal (desorption temperature around 100°C), reverse spillover hydrogen (150-250°C), hydrogen from H-TiO$_{2-x}$-Co interacting species (~330°C) and recombined hydrogen from Ti^{3+}-H on titania (~535°C). the absence of hydrogen desorption peak at 535°C for titania supported cobalt reduced above 400°C can be explained in terms of the migration of H-TiO$_{2-x}$ moieties onto cobalt metal surface during reduction. Removal of hydroxyl groups before high temperature reduction, enhanced the amount of hydrogen desorbed from cobalt metal. This indicated that hydroxyl groups played a role in the migration of H-TiO$_{2-x}$ species.

Duvenhage and Coville (1997, 2000) investigated Fe:Co/TiO$_2$ bimetallic catalysts for the Fischer-Tropsch reaction. They divided two parts of the study. For part I, they studied the synthesis, characterization and catalytic activity of a series of Fe:Co/TiO$_2$ catalysts in which the Fe:Co ratio was varied. They found that Fe/Co alloys are readily formed under mild condition on TiO$_2$ and the 1:1 Fe:Co catalyst performed optimal activity/selectivity catalyst characteristics when compared to other Fe:Co metal ratios.

For part II, they studied the influence of support calcination temperatures and catalyst calcination/reduction temperatures on the performance of a 1:1 Fe:Co/TiO$_2$ catalyst. They reported that the TiO$_2$ support calcination temperature (200-400°C) increased the stability of the final catalyst. In addiotion, the catalyst Fe:Co/TiO$_2$

calcination temperature (at constant reduction temperatures) wer not an important parameter in influencing the activity and product selectivity of the catalyst. Moreover, the reduction temperatures (at constant calcination temperature) of the $Fe:Co/TiO_2$ catalyst influenced the FT activity and selectivity. A low reduction temperature ($250^{\circ}C$) resulted in a highly dispersed and difficult to reduced catalyst. A high reduction temperature ($400^{\circ}C$) generated a catalyst with low dispersion and high reducibility, but poor activity. The higher reduction temperature generated catalysts with lower BET surface area and increased surface Fe content. They also found that the changes in reduction/calcination conditions used to generate the Fe:Co catalyst permits the methane and olefin yields to be manipulated within the constrained of the FT reaction.

Kraum and Baerns (1999) studied the influence of various cobalt compounds applied in the preparation of supported cobalt catalysts on their performance. From the impregnation and calcination procedures, X-ray diffraction (XRD) showed the formation of $CoTiO_3$ by the use of cobalt (III) acetyl acetonate (Co-ACAC3) as a precursor in Co/TiO_2 catalysts. They reported that this effect can be attributed be the migration of cobalt ions into the lattice, with the consecutive formation of titanate. Furthermore, the addition of Ru to the Co-ACAC3 catalyst influenced the phase composition. For Co-ACAC3-Ru, only Co_3O_4 was detected and no peaks corresponding to $CoTiO_3$ phase were present.

Curtis *et al.* (1999) synthesized TiO_2- and SiO_2-supported cobalt Fischer-Tropsch catalysts load with low concentration of sulfur (100-2000 ppm) from different sources (($NH_4)_2S$, $(NH4)_2SO_4$, and $(NH_4)_2SO_3$) and characterized using diffuse reflectance infrared fourier transform spectroscopy (DRIFTS) and TPR. They reported that, for the IR data, sulfur inhibits CO adsorption onto the surface of Co catalysts for a sulfur concentration studied possibly due to (i) site blockage and (ii) inhibited reduction of the catalysts. They also found that sulfur also affects the TiO_2- and SiO_2-supported cobalt catalysts during the Fischer-Tropsch reaction. The *in situ* F-T reactions, monitored by DRIFTS, further suggest that lower concentrations of sulfur (100 ppm) on TiO_2-supported cobalt catalysts improves catalysts activity. Besides, the surface of the silica supported catalysts decreased the intensity of the TPR peak related to reducible silicate.

Li and Coville (1999) studied the effect of small amounts of boron (0.02-1.5%) on the active phase/support interaction, the reduction capability and the activity of Co/TiO_2 catalysts in the FT reaction. They found that the introduction of boron into a 10 wt% Co/TiO_2 catalysts decreased the Co_3O_4 crystallite size in the oxidic catalyst. Moreover, the reducibility of the catalysts was found to decrease with increasing boron loading. For the reaction study, they reported that the CO conversion and overall hydrogenation rated decreased with decreasing ease of reducibility and decreasing cobalt dispersion caused by boron. However, the addition of B (< 0.1%) resulted in an increase in selectivity, less CH_4 production and an increase in the olefin/paraffin ratio. Furthermore, at high B loading, product selectivity shifted to the lower molecular weight hydrocarbons and CO_2 selectivity increased.

Riva *et al.* (2000) investigated metal-supported interaction in Co/SiO_2 and Co/TiO_2 catalysts and their effect on the dispersion and reducibility of cobalt. They found that the interaction is much stronger in the case of titania, as indicated by the formation of a surface compound between cobalt and titania that is more resistant to reduction than Co_3O_4. On the contrary the behavior of silica supported sample is very similar to that of unsupported Co_3O_4 under reduction treatments. Besides, the degree of interaction between cobalt and the support affected not only the response of cobalt to reduction, but also its dispersion. They also found that cobalt spread on titania during reduction and trended to sintering on silica.

Zennaro *et al.* (2000) studied kinetics of Fischer-Tropsch synthesis on titania-supported cobalt. They reported rates of CO hydrogenation on a well-characterized 11.7% Co/TiO_2 catalyst measured after 20h of reaction in a differential fixed-bed reactor at 20 atm, 180-240°C, and 5% conversion, over a range of reactant partial pressure, can be used to model precisely and accurately the kinetics of this reaction. In addition, turnover frequecies and rate constants determined from this study were in very good to excellence agreement with those obtained in previous studies of Co/TiO_2 and other cobalt-supported combination, when the data were normalized to the same conditions of temperature and partial pressure of the reactant. Based on this comparison it is concluded that CO conversion and the partial pressure of product

water have little effect on specific rate per catalytic site. They also found that the data of this and other studies are fitted fairly well by a simple power law expression of the form

$$-r_{CO} = kP_{H_2}^{0.74} P_{CO}^{-0.24}$$

Where k = 5.1x 10^{-3} s^{-1} at 200°C, P = 10atm, and H_2/CO = 2/1. However, the data of this study are best fitted by the simple Langmuir-Hinshelwood (LH) rated form,

$$-r_{CO} = aP_{H_2}^{0.74} /(1 + bP_{CO})^2$$

in comparison to fits of the same data by several other representative LH rate forms proposed in previous studies.

Brik *et al.* (2001) studied characterization of titania-supported cobalt and cobalt-phosphorus and investigated performance in ethane oxidative dehydrogenation (ODH). They found that at low cobalt loading, the sample was essentially covered by octahedral Co^{2+} ions, whereas at concentrations superior to 3.7 wt% formation of the Co3O4 spinel is observed. The best performance in ethane ODH was achieved at 550°C with the sample containing 7.6 wt% Co. In addition, the reaction began with a conversion of 33% and a selectivity around 75%, then it decreased to reach after 150 minutes on stream a stationary state at 22% of conversion and 60% selectivity. This loss of 30% of the initial activity may be associated with a decrease of the specific surface area and the concomitant formation of $CoTiO_3$ and Co_2TiO_4. Moreover, addition phosphorus led to a marked activity decrease, ascribed to the formation of cobalt-phosphorus compounds not active in the reaction.

Li and Coville (2001) studied the effect of a boron additive on the resistance of a titania supported cobalt catalyst to poisoning by sulfur for Fischer-Tropsch synthesis. They found that a low-level of sulfur addition (100, 200 ppm S) did not influence the activities of the catalysts with and without boron. The addition of high-level loading of sulfur (500 ppm S) resulted in a severe sulfur poisoning for the boron-free and boron-modified Co/TiO_2 catalysts. Furthermore, the modification of Co/TiO_2 by boron effectively retards the poisoning of sulfur (500 ppm S). The

reaction rate decreased by 50% for boron-free Co/TiO_2, while the reaction rate decreased by only 35% for 0.1 wt% boron-modified Co/TiO_2. They also confirmed that boron can act as 'S sponge' in the FT reaction.

Coville and Li (2002) studied effect of the boron source on titania supported cobalt Fischer-Tropsch catalysts. The 10 wt% Co/TiO_2 catalysts modified by different amounts of boron from boric acid, ammonium borate and carborane were synthesized. They found that the boron source had a profound influence on both the catalyst reducibility and the FT reaction. In addition, TPR and O_2 titration measurements indicated that the carborane-modified catalysts were reduced more easily than those modified by boric acid and ammonium borate. Furthermore, the addition of boron to Co/TiO_2 catalysts also decreased the activity substantially, although the effect varied for the different boron sources. The order of the effect was found to be boric acid > ammonium borate > carborane. They also reported that this order was the same as that of increasing reducibility and increasing metal dispersion. Indeed the effect led to a turnover frequency that remained constant and was unaffected by the addition of boron for all the catalysts.

Lin et al. (2002) studied the effect of water vapor on the catalytic properties of a ruthenium promoted Co/TiO_2 catalyst during FTS operated, in a continuously stirred tank reactor (CSTR) by adding water into the feed gas at varying space velocity. They found that at higher space velocities (SV = 4 NL g $cat^{-1}h^{-1}$), the addition of water did not have significant effect on the CO conversion. At lower space velocity (SV = 2 NL g $cat^{-1}h^{-1}$), the addition of water decrease the CO conversion; however, the decrease was reversible with the catalyst quickly recovering the activity that it exhibited prior to water addition. Moreover, at high CO conversion (space velocity of SV = 1 NL g $cat^{-1}h^{-1}$) the addition of water resulted in a catalyst permanent deactivation. The methane selectivity was not influence by water addition, but the CO_2 selectivity was increased with water addition.

Voβ et al. (2002) investigated the structural, chemical and electronic properties of Co and Co/Mn catalysts supported on Al_2O_3, SiO_2 and TiO_2 by a combination of different methods such as TEM, XRD, XPS, TPR and TPO. They

reported that temperature-programmed reduction and oxidation reveal the formation of various oxides in dependence on temperature. In case of the alumina- and titania-supported cobalt catalysts, the formation of high-temperature compounds $CoAl_2O_4$ and $CoTiO_3$, respectively. Moreover, these compounds are not reducible under the applied conditions, the degrees of reduction are only 18-20% (Co/Al_2O_3) and 77% (Co/TiO_2).

Madikizela and Coville (2002) proposed the effect of zinc on the properties and FT behaviour of Co/TiO_2 catalysts. They reported that the physical properties of the catalyst are little affected by Zn loadings of up to 10%. In addition, the TPR data suggests enhanced Co reducibility with increasing Zn content. Improvement in the reducibility of the cobalt could result from an increase in the cobalt dispersion. Besides, the zinc has a positive effect on the activity and the selectivity of the Co/TiO_2 catalysts. This was reflected by increased activity and reduced methane content of the $Co(10\%)/Zn(5\%)/TiO_2$ catalyst. They also suggested that the new $Co(10\%)/Zn(5\%)/TiO_2$ catalysts may be useful in the FT reaction when the reaction was performed in the presence of small amounts of sulfur-containing gases.

Li *et al.* (2002) investigated the effect of carbon monoxide pretreatment on the titania supported cobalt catalyst and compared with these of catalysts pretreated with hydrogen. They reported that the pretreatment gas (reductant) had a remarkable effect on the performance on a ruthenium promoted cobalt catalyst during Fischer-Tropch synthesis. The hydrogen reduced catalyst exhibited a higher initial synthesis gas conversion (72.5%) and reached steady state after 40h on stream. In addition, the carbon monoxide catalyst reached steady state quickly, exhibited lower activity and good stability. Methane selectivity for the carbon monoxide reduced catalyst was 15-20% (carbon basis), higher than that on the hydrogen reduced catalyst (5-10%). Moreover, the effect of carbon monoxide treatment on the used catalyst also proposed. They found that carbon monoxide regeneration increased the activity on the hydrogen reduced catalyst; however, it did not have a significant effect on the carbon monoxide reduced catalyst.

2.3 Effect of noble metal promotion on supported cobalt catalysts

Kogelbauer *et al.* (1996) examined the effect of Ru promotion of Co/Al_2O_3 catalyst characteristic and performance in FT synthesis. They reported the addition of small amount ruthenium to γ-alumina-supported cobalt catalysts facilitated the reduction of Co catalyst. It was suggested that ruthenium acts only as a reduction promoter for Co by increasing the reducibility and dispersion of cobalt. Parallel on this effect, Ru-promoted catalyst showed an increase in CO hydrogenation activity.

Tsubaki *et al.* (2001) and Sun *et al.* (2002) studied the influence of the addition of very small amount of Ru, Pt and Pd to supported cobalt catalysts, which were prepared by mixing cobalt nitrate and cobalt acetate. They found that the Co catalyst prepared by mixing cobalt nitrate and cobalt acetate had a high activity for the CO hydrogenation. The catalytic activity of noble-metal-promoted Co Catalyst followed the order RuCo > PtCo > PdCo. Due to Ru improved Co reducibility greatly but had only a slight effect on Co dispersion. Pt and Pd increased the Co reducibility slightly but significantly influenced Co dispersion. So the addition of small Pt and Pd in catalysts showed higher a methane selectivity, which was attributed to the small metallic cobalt particle and the H_2 spillover effect. They also reported that Pt and Pd formed two distinct phases where Ru was enriched at Co surface. In addition, the Ru-rich sports on the Co surface determined a high reduction degree, as well as a large particle of RuCo and this structure formed during the reduction step of the catalyst preparation. Most of the Pt and Pd was embedded in the bulk phase of Co and CoO_x, not contributing to the reduction of supported cobalt oxide.

Jacobs *et al.* (2002) investigated the effect of support, loading and promoter on the reducibility of cobalt catalysts. They reported that significant support interactions on the reduction of cobalt oxide species were observed in the order $Al_2O_3 > TiO_2 > SiO_2$. Addition of Ru and Pt exhibited a similar catalytic effect by decreasing the reduction temperature of cobalt oxide species, and for Co species where a significant surface interaction with the support was present, while Re impacted mainly the reduction of Co species interaction with the support. They also suggested that, for catalysts prepared with a noble metal promoter and reduced at the same temperature,

the increase in the number of active sites was due mainly to improvements in the percentage reduction rather than the actual dispersion (cluster size). Increasing the cobalt loading, and therefore the average Co cluster size, was found to exhibit improved reducibility by decreasing interactions with the support.

Das *et al.* (2003) studied characterization of Co/Al_2O_3 catalyst with different amount of rhenium loading and catalytic activity for the FT synthesis. They found that the addition of small amounts of rhenium to the cobalt catalyst decreased the reduction temperature of cobalt oxide but did not significantly alter the actual percent dispersion and cluster size, based on the amount of reduced cobalt, to an appreciable amount. Furthermore, addition of Re increases the percent reduction of cobalt and hence increased the initial activity.

CHAPTER III

THEORY

In the previous chapter, reviews of recent research on Co-support compound formation and titania-supported cobalt catalysts for CO hydrogenation have been reviewed. They present knowledge and understanding of influencing parameters on the performance of Co-based catalysts for CO hydrogenation system. This chapter focuses on the fundamental theory of the Fischer-Tropsch Synthesis (FTS) which is well known as one type of carbon monoxide (CO) hydrogenation using Co-based catalysts. The chapter consists of five main sections. Basic deails of Fischer-Tropsch Synthesis (FTS) are discussed in section 3.1. Cobalt properties is explained in section 3.2. Details of Co-based catalysts are described in section 3.3. Cobalt-support compound formation (Co-SCF) is discussed in section 3.4. Titanium dioxide which used as a support is detailed in section 3.5. Details of promoters are discussed in the last section 3.6.

3.1 Fischer-Tropsch Synthesis (FTS)

Fischer-Tropsch synthesis (FTS) is a means to convert synthesis gas obtained from natural gas reforming and coal gasification, into mainly desirable long chain hydrocarbons. During the past decades, FTS has been developed continuously by many researchers, although the rise and fall in research intensity this process has been highly related to the demands for liquid fuels and relative economics. This synthesis is basically the reductive polymerization (oligomerization) of carbon monoxide by hydrogen to form organic products containing mainly hydrocarbons and some oxygenated products in lesser amounts. The main reactions of FTS are:

$$CO + [1+(m/2n)]H_2 \rightarrow (1/n)C_nH_m + H_2O \qquad (3.1)$$

$$CO + 3H_2 \rightarrow CH_4 + H_2O \qquad (3.2)$$

$$CO + H_2O \rightarrow CO_2 + H_2 \qquad (3.3)$$

$$2CO \rightarrow C + CO_2 \qquad (3.4)$$
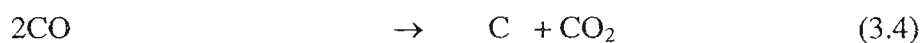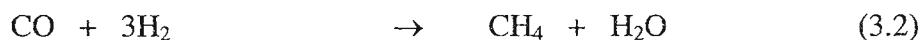
Equations (3.1) is the formation of hydrocarbons higher than C1, and the equation (3.2) is methanation. The water-gas shift reaction, which is undesirable for natural gas conversion, is shown in equation (3.3). The Boudouard reaction, which results in carbon deposition on the catalyst surface, is shown in equation (3.4). Depending upon the type of catalyst used, promoters, reaction conditions (pressures, temperatures and H_2/CO ratios) and type of reactors, the distribution of the molecular weight of the hydrocarbon products can be noticeably varied.

Normally, catalysts used for this synthesis are group VIII metals. By nature, the hydrogenation activity increases in order of $Fe < Co < Ni < Ru$. Ru is the most active. Ni forms predominantly methane, while Co yields much higher ratios of paraffins to olefins and much less oxygenated products such as alcohols and aldehydes than Fe does. With regards to the operating conditions, usually higher pressures will result in higher rates. Entrained bed reactors or slurry bubble column reactors are better than fixed-bed reactors for FTS since they can remove heat from this exothermic synthesis, allowing better temperature control.

The current main goal in using FTS is to obtain high molecular weight, straight chain hydrocarbons. However, methane and other light hydrocarbons are always present as less desirable products from the synthesis. According to the Anderson-Schulz-Flory (ASF) product distribution, typically 10 to 20% of products from the synthesis are usually light hydrocarbon (C_1-C_4) these light alkanes have low boiling points and exist in the gas phase at room temperature, which is inconvenient for transportation. Many attempts have been made to minimize these byproducts and increase the yield of long chain liquid hydrocarbons by improving chain growth probability. It would be more efficient to be able to convert these less desirable products into more useful forms, rather than re-reforming them into syngas and recycling them.

3.2 Cobalt (Young 1960; Othmer, 1991)

3.2.1 General

Cobalt, a transition series metallic element having atomic number 27, is similar to silver in appearance.

Cobalt and cobalt compounds have expended from use colorants in glasses and ground coat frits for pottery to drying agents in paints and lacquers, animal and human nutrients, electroplating materials, high temperature alloys, hard facing alloys, high speed tools, magnetic alloys, alloys used for prosthetics, and used in radiology. Cobalt is also as a catalyst for hydrocarbon refining from crude oil for the synthesis of heating fuel.

3.2.2 Physical Properties

The electronic structure of cobalt is [Ar] $3d^7 4s^2$. At room temperature the crystalline structure of the α (or ε) form, is close-packed hexagonal (cph) and lattice parameters are a = 0.2501 nm and c = 0.4066 nm. Above approximately 417°C, a face-centered cubic (fcc) allotrope, the γ (or β) form, having a lattice parameter a = 0.3544 nm, becomes the stable crystalline form. Physical properties of cobalt are listed in Table 3.1.

The scale formed on unalloyed cobalt during exposure to air or oxygen at high temperature is double-layered. In the range of 300 to 900°C, the scale consists of a thin layer of mixed cobalt oxide, Co_3O_4, on the outside and cobalt (II) oxide, CoO, layer next to metal. Cobalt (III) oxide, Co_2O_3, may be formed at temperatures below 300 °C. Above 900°C, Co_3O_4 decomposes and both layers, although of different appearance, are composed of CoO only. Scales formed below 600°C and above 750°C appear to be stable to cracking on cooling, whereas those produced at 600-750°C crack and flake off the surface.

Cobalt forms numerous compounds and complexes of industrial importance. Cobalt, atomic weight 58.933, is one of the three members of the first transition series of Group 9 (VIIIB). There are thirteen know isotopes, but only three are significant: ^{59}Co is the only stable and naturally occurring isotope; ^{60}Co has a half-life of 5.3 years and is a common source of γ-radioactivity; and ^{57}Co has a 270-d half-life and provides the γ-source for Mössbauer spectroscopy.

Cobalt exists in the +2 or +3 valance states for the major of its compounds and complexes. A multitude of complexes of the cobalt (III) ion exists, but few stable simple salt are known. Octahedral stereochemistries are the most common for cobalt (II) ion as well as for cobalt (III). Cobalt (II) forms numerous simple compounds and complexes, most of which are octahedral or tetrahedral in nature; cobalt (II) forms more tetrahedral complex than other transition-metal ions. Because of the small stability difference between octahedral and tetrahedral complexes of cobalt (II), both can be found equilibrium for a number of complexes. Typically, octahedral cobalt (II) salts and complexes are pink to brownish red; most of the tetrahedral Co (II) species are blue.

Table 3.1 Physical properties of cobalt (Othmer, 1991)

Property	Value
atomic number	27
atomic weight	58.93
transformation temperature, °C	417
heat of transformation, J/g[a]	251
melting point, °C	1493
latent heat of fusion, ΔH_{fus} J/g[a]	395
boiling point, , °C	3100
latent heat of vaporization at bp, ΔH_{vap} kJ/g[a]	6276
specific heat, J/(g·°C)[a]	
15-100°C	0.442
molten metal	0.560
coefficient of thermalexpansion, °C^{-1}	
cph at room temperature	12.5
fcc at 417°C	14.2
thermal conductivity at 25 °C, W/(m·K)	69.16
thermal neutron absorption, Bohr atom	34.8
resistivity, at 20 °C[b], $10^{-8}\Omega\cdot m$	6.24
Curie temperature, °C	1121
saturation induction, $4\pi I_s$, T[c]	1.870
permeability, μ	
initial	68
max	245
residual induction, T[c]	0.490
coercive force, A/m	708
Young's modulus, Gpac	211
Poisson's ratio	0.32

Table 3.1 Physical properties of cobalt (cont.)

Property	Value	
Hardness[f], diamond pyramid, of %Co	99.9	99.98[e]
At 20 °C	225	253
At 300 °C	141	145
At 600 °C	62	43
At 900 °C	22	17
strength of 99.99 %cobalt, MPa[g]	as cast	annealed	sintered
tensile	237	588	679
tensile yield	138	193	302
compressive	841	808	
compressive yield	291	387	

[a] To convert J to cal, divided by 4.184.

[b] conductivity = 27.6 % of International Annealed Copper Standard.

[c] To convert T to gauss, multiply by 10^4.

[d] To convert GPa to psi , multiply by 145,000.

[e] Zone refined.

[f] Vickers.

[g] To convert MPa to psi , multiply by 145.

3.2.3 Cobalt Oxides

Cobalt has three well-known oxides:

Cobalt (II) oxide, CoO, is an olive green, cubic crystalline material. Cobalt (II) oxide is the final product formed when the carbonate or the other oxides are calcined to a sufficiently high temperature, preferably in a neutral or slightly reducing atmosphere. Pure cobalt (II) oxide is a difficult substance to prepare, since it readily takes up oxygen even at room temperature to re-form a higher oxide. Above about 850°C, cobalt (II) oxide form is the stable oxide. The product of commerce is usually dark gray and contains 75-78 wt % cobalt. Cobalt (II) oxide is soluble in

water, ammonia solution, and organic solvents, but dissolves in strong mineral acids. It is used in glass decorating and coloring and is a precursor for the production of cobalt chemical.

Cobalt (III) oxide, Co_2O_3, is form when cobalt compounds are heated at a low temperature in the presence of an excess of air. Some authorities told that cobalt (III) oxide exists only in the hydrate form. The lower hydrate may be made as a black power by oxidizing neutral cobalt solutions with substances like sodium hypochlorite. Co_2O_3 or $Co_2O_3 \cdot H_2O$ is completely converted to Co_3O_4 at temperatures above 265°C. Co_3O_4 will absorb oxygen in a sufficient quantity to correspond to the higher oxide Co_2O_3.

Cobalt oxide, Co_3O_4, is formed when cobalt compounds, such as the cabonate or the hydrated sesquioxide, are heated in air at temperatures above approximately 265°C and not exceeding 800°C.

3.3 Co-based Catalysts

Supported cobalt (CO) catalysts are the preferred catalysts for the synthesis of heavy hydrocarbons from natural gas based syngas (CO and H_2) because of their high Fischer-Tropsch (FT) activity, high selectivity for linear hydrocarbons and low activity for the water-gas shift reaction. It is known that reduced cobalt metal, rather than its oxides or carbides, is the most active phase for CO hydrogenation in such catalysts. Investigations have been done to determine the nature of cobalt species on various supports such as alumina, silica, titania, magnesia, carbon, and zeolites. The influence of various types of cobalt precursors used was also investigated. It was found that the used of organic precursors such as CO (III) acetyl acetate resulting in an increase of CO conversion compared to that of cobalt nitrate.

3.4 Cobalt-Support Compound Formation (Co-SCF)

Compound formation between cobalt metal and the support can occur under pretreatment and/or reaction conditions, leading to catalyst deactivation. The compound formation of cobalt metal with support materials, however, is difficult to

predict because of the lack of sufficient thermodynamic data. Co-support compound formation can be detected evidentially.

3.4.1 Co-Aluminate Formation

Interaction of cobalt with its alumina support has been observed by many authors using various techniques including TPR, XRD, EXAFS, and XPS (ESCA). The migration of cobalt ions into alumina lattice sites of octahedral or tetrahedral symmetry is limited to the first few layers of the support under normal calcination conditions. The reaction of Co with γ-Al_2O_3 can form a surface spinel in Co/γ-Al_2O_3 catalysts. The surface spinel structure can not be observed by X-ray diffraction because it does not have long range, three dimensional order. It has been suggested that cobalt ions occupying surface octahedral site of γ-Al_2O_3 are reducible while cobalt ions occupying tetrahedral sites are non-reducible, at least at temperatures $\leq 900^{\circ}C$. At lower calcination temperatures, filling of the octahedral sites is more favorable. Filling of the tetrahedral site of γ-Al_2O_3 may be enhanced by an increase in calcination temperature.

3.4.2 Co-Silicate Formation

The formation of cobalt silicates on Co/SiO_2 under hydrothermal conditions has been extensively studied by Kogelbauer et al. (1995). Hydrothermal treatment at $200^{\circ}C$ led to a catalyst with lower reducibility due to the formation of both reducible and non-reducible (at temperatures $\leq 900^{\circ}C$) cobalt silicates. It was found that hydrothermal treatment of the reduced catalyst or hydrothermal treatment of the calination catalyst in the presence of hydrogen produces cobalt silicates, while hydrothermal treatment of the calcined catalyst in air does not result in their formation. Hydrothermal treatment of the calcined catalyst in inert gas also has little effect.

3.5 Titanium dioxide (Othmer, 1991; Fujishima *et al.*, 1999)

3.5.1 Physical and Chemical Properties

Titanium dioxide occurs in nature in three crystalline forms: anatase which tends to be more stable at low temperature, brookite, which is usually found only in minerals and rutile, which tends to be more stable at higher temperatures and thus is sometimes found in igneous rock. These crystals are essentially pure titanium dioxide but contain small amounts of impurities, such as iron, chromium or vanadium, which darken them. Crystallographic information on the different forms of titanium dioxide is summarized in Table 3.2.

Table 3.2 Crystallographic information on the different forms of titanium dioxide (Othmer, 1991)

Properties	Anatase	Brookite	Rutile
Crystal structure	Tetragonal	Orthorhombic	Tetragonal
Optical	Uniaxial, negative	Biaxial, positive	Uniaxial, negative
Density, g/cm^3	3.9	4.0	4.23
Harness, Mohs scale	$5^1/_2 - 6$	$5^1/_2 - 6$	$7 - 7^1/_2$
Unit cell	$D_4a^{19}.4TiO_2$	$D_2h^{15}.8TiO_2$	$D_4h^{12}.3TiO_2$
Dimension, nm			
a	0.3758	0.9166	0.4584
b	-	0.5436	-
c	0.9514	0.5135	2.953

Although anatase and rutile are both tetragonal, they are not isomorphous (Figure 3.1). Anatase occurs usually in near-regular octahedral, and rutile forms slender prismatic crystal, which are frequently twinned. Rutile is the thermally stable form and is one of the two most important ores of titanium.

The three allotropic forms of titanium (IV) oxide have been prepared artificially but only rutile, the thermally stable form, has been obtained in the form of transparent large single crystal. The transformation form anatase to rutile is accompanied by the evolution of ca. 12.6 kJ/mol (3.01 kcal/mol), but the rate of transformation is greatly affected by temperature and by the presence of other substance which may either catalyze of inhibit the reaction. The lowest temperature at which conversion of anatase to rutile takes place at a measurable rate is ca. 700°C, but this is not a transition temperature. The change is not reversible; ΔG for the change from anatase to rutile is always negative.

rutile   anatase
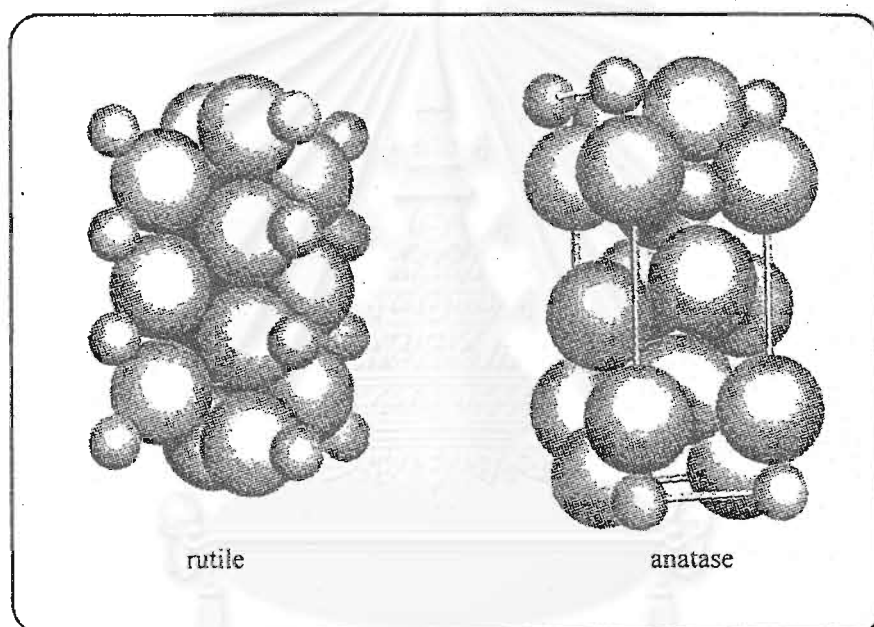
Figure 3.1 Crystal structure of TiO₂. (Fujishima *et al.*,1999)

Brookite has been produced by heating amorphous titanium (IV) oxide, prepared from an alkyl titanates of sodium titanate with sodium or potassium hydroxide in an autoclave at 200 to 600°C for several days. The important commercial forms of titanium (IV) oxide are anatase and rutile, and these can readily be distinguished by X-ray diffraction spectrometry.

Since both anatase and rutile are tetragonal, they are both anisotropic, and their physical properties, e.g. refractive index, vary according to the direction

relative to the crystal axes. In most applications of these substances, the distinction between crystallographic direction is lost because of the random orientation of large numbers of small particles, and it is mean value of the property that is significant.

Measurement of physical properties, in which the crystallographic directions are taken into account, may be made of both natural and synthetic rutile, natural anatase crystals, and natural brookite crystals. Measurements of the refractive index of titanium (IV) oxide must be made by using a crystal that is suitably orientated with respect to the crystallographic axis as a prism in a spectrometer. Crystals of suitable size of all three modifications occur naturally and have been studied. However, rutile is the only form that can be obtained in large artificial crystals from melts. The refractive index of rutile is 2.75. The dielectric constant of rutile varies with direction in the crystal and with any variation from the stoichiometric formula, TiO_2; an average value for rutile in powder from is 114. The dielectric constant of anatase powder is 48.

Titanium (IV) oxide is thermally stable (mp 1855°C) and very resistant to chemical attack. When it is heated strongly under vacuum, there is a slight loss of oxygen corresponding to a change in composition to $TiO_{1.97}$. The product is dark blue but reverts to the original white color when it is heated in air.

Hydrogen and carbon monoxide reduce it only partially at high temperatures, yielding lower oxides or mixtures of carbide and lower oxides. At ca. 2000°C and under vacuum, carbon reduces it to titanium carbide. Reduction by metal, e.g., Na, K, Ca, and Mg, is not complete. Chlorination is only possible if a reducing agent is present; the position of equilibrium in the system is

$$TiO_2 + 2Cl_2 \rightarrow TiCl_4 + O_2 \qquad (3.5)$$
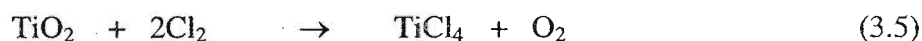
3.6 Promoters (Farrauto and Bartholomew, 1997; Jongsomjit *et al.*, 2001).

There are two kinds of promoters such as textural and chemical promoters. Textural promoters are used to facilitate the dispersion of metal phase during preparation and/or reaction conditions. Chemical promoters are used to enhance the activity and/or selectivity of catalysts. Generally, noble, alkali and alkaline earth metals are considered to be chemical promoters, which play important roles on catalyst performance to date.

The effects of promoters such as Ru, Re, Rh, Pt and Pd on Co catalysts were studied. They reported that these metal promoters can increase the reducibility and dispersion of Co, preserve the activity by preventing the formation of coke, exhibit cluster and ligand effect and act as a source for hydrogen spillover.

CHAPTER IV

EXPERIMENTAL

This chapter consists of experimental systems and procedures used in this work which is divided into three parts including catalyst preparation, catalyst characterization and reaction study in CO hydrogenation.

The first part (section 4.1) is described catalyst preparation such as unpromoted catalyst, Ru-promoted catalyst, reference materials ($CoTiO_3$, CoO and Co_3O_4), catalyst pretreatment and catalyst nomenclature. The second part (section 4.2) is explained catalyst characterization by various techniques including of AAS, BET surface area, TPR, TGA, hydrogen chemisorption, electron microscopy, XRD, electron microscopy and Raman spectroscopy. Finally, the last part (section 4.3) is illustrated catalyst activity measurement in CO hydrogenation.

4.1 Catalyst preparation

4.1.1 Chemicals

The details of chemicals used in this experiment are shown in Table 4.1.

Table 4.1 Chemicals used in the preparation of catalysts.

Chemical	Grade	Supplier
Cobalt (II) nitrate hexahydrate ($Co(NO_3)_2 \cdot 6H_2O$)	Analytical	Aldrich
Ruthenium (III) nitrosyl nitrate ($Ru(NO)(NO_3)_3$)	Analytical	Aldrich
Titania (TiO_2) support JRC-TIO-1 (pure anatase) or T1 JRC-TIO-4 (anatase 82%, rutile 18%)or T2	Japan reference catalyst	Department of Material Science, Shimane University University Catalysts and Chemicals Ind. Co., Ltd.

4.1.2 Preparation of unpromoted catalyst

A Co/TiO_2 catalyst was prepared by incipient wetness impregnation method. Cobalt (II) nitrate hexahydrate was dissolved in deionized water and then impregnated into the support with 20 wt % cobalt by calculating of the required amounts of Co loading (see Appendix A). The catalysts were dried at $110^\circ C$ for 12 hours and calcined in air at $500^\circ C$ for 4 hours.

4.1.3 Preparation of Ru-promoted catalyst

A $CoRu/TiO_2$ catalyst was also prepared by incipient wetness impregnation method. Cobalt (II) nitrate hexahydrate and ruthenium (III) nitrosyl nitrate was dissolved in deionized water and then coimpregnated into the support with 20 wt % cobalt and 0.5 wt % ruthenium by calculating of the required amounts of Co and Ru loading (see Appendix A). The catalysts were dried at $110^\circ C$ for 12 hours and calcined in air at $500^\circ C$ for 4 hours.

4.1.4 Preparation of reference materials

A $CoTiO_3$ material was prepared by mixed cobalt and titania with ratio of Co/Ti = 1 mole and then heat at $1150\ ^\circ C$ for 6 hours in air, then took it out immediately (Brezny and Muan, 1969).

CoO and Co_3O_4 were calcined in air at $500^\circ C$ for 4 hours. Only CoO was reduced with H_2 at $350^\circ C$ for 10 hours and passivated with air at room temperature for 30 min.

4.1.5 Pretreatment procedures

The catalysts were reduced at different conditions with water vapor addition of 0%, 5% and 10% of total pressure during standard reduction using a temperature ramp from ambient to $350^\circ C$ at $5^\circ C/min$ and holding at $350^\circ C$ for 10 h in a gas flow consisting of H_2 or mixtures of H_2 and water vapor (5, 10 vol%). Subsequently, the catalyst was cooled down to room temperature and then passivated

with air at room temperature for 30 min. The pretreatment system was used in this work as shown diagrammatically in Figure 4.1. Calculation details of vapor pressure of water are given in Appendix B.
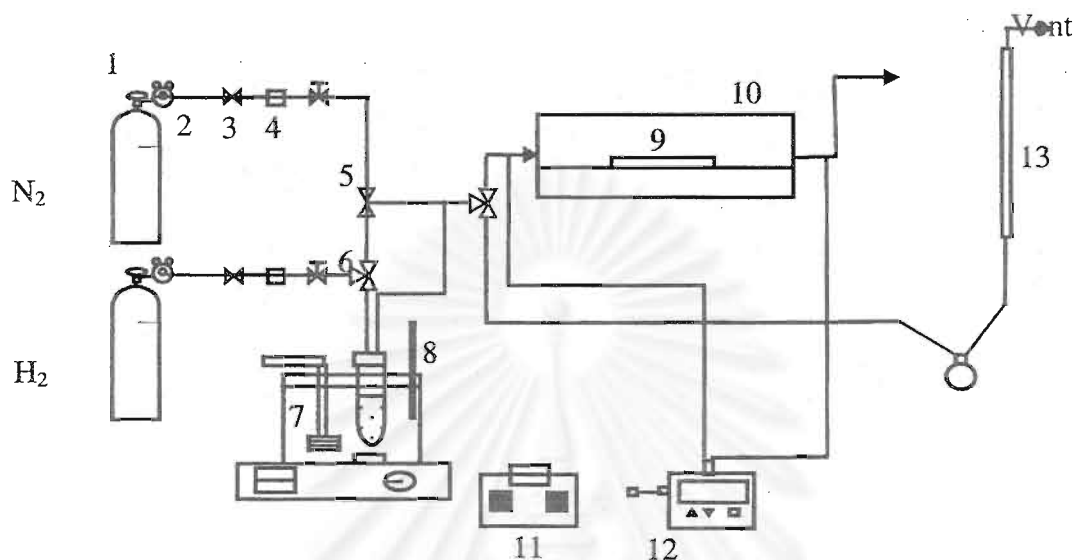
1. Pressure Regulator
2. On-Off Value
3. Gas Filter
4. Metering Valve
5. 2-way Valve
6. 3-way Valve
7. Steam generating system
8. Thermometer
9. Sample Bed
10. Carbolite
11. Variable Voltage Transformer
12 Temperature Controller
13 Bubble Flow Meter

Figure 4.1 Schematic of the apparatus for the pretreatment system.

4.1.6 Catalyst Nomenclature

The nomenclature used for the catalyst samples in this study is following:

Co and CoRu catalysts supported on the titania (anatase form; T1):

- Co/T1-**C**, CoRu/T1-**C**:   the calcined catalyst sample
- Co/T1-**RW0**, CoRu/T1-**RW0**: the calcined catalyst sample reduced in H_2

- Co/T1-**RW5**, CoRu/T1-**RW5**: the calcined catalyst sample reduced in a mixture of H_2 with 5 vol% water vapor added during reduction
- Co/T1-**RW10**, CoRu/T1-**RW10**: the calcined catalyst sample reduced in a mixture of H_2 with 10 vol% water vapor added during reduction

Co and CoRu catalysts supported on the titania (anatase mixed rutile form; T2):

- Co/T2-**C**, CoRu/T2-**C**: the calcined catalyst sample
- Co/T2-**RW0**, CoRu/T2-**RW0**: the calcined catalyst sample reduced in H_2
- Co/T2-**RW5**, CoRu/T2-**RW5**: the calcined catalyst sample reduced in a mixture of H_2 with 5 vol% water vapor added during reduction
- Co/T2-**RW10**, CoRu/T2-**RW10**: the calcined catalyst sample reduced in a mixture of H_2 with 10 vol% water vapor added during reduction

4.2 Catalyst characterization

Various characterization techniques were used in this study in order to clarify the catalyst structure, morphology and surface composition as a result of pretreatment with and without water on the behavior of titania-supported cobalt catalysts.

4.2.1 Atomic absorption spectroscopy (AAS)

AAS was performed to determine the composition of elements in the bulk of catalysts. The composition content of catalysts was collected using Varian, Spectra A8000 at the Department of Science Service Ministry of Science Technology and Environment.

4.2.2 BET surface area

Surface area, pore volume and average pore diameter of catalysts were measured by the BET method, with nitrogen as the adsorbate using a micrometritics model ASAP 2000 at liquid-nitrogen point temperature (77 K) at the Analysis Center

of Department of Chemical Engineering, Faculty of Engineering, Chulalongkorn University.

4.2.3 Temperature programmed reduction (TPR)

TPR was used to determine the reducibilities and reduction behaviors of catalysts. The catalyst sample of 50 mg was used in the operation and temperature ramp from $35^{\circ}C$ to $800^{\circ}C$ at $10^{\circ}C/min$ was applied. The carrier gas was 5 %H_2 in Ar (30 cc/min). During reduction, a cold trap will be placed before the detector to remove water produced. A thermal conductivity detector (TCD) was used to measure the amounts of hydrogen consumption during TPR. The operating condition of the TCD is shown in Table 4.2. The calibration of hydrogen consumption was used cobalt oxide (Co_3O_4) at the same condition. Details of calculation of % reducibility of the calcined catalysts are given in Appendix C.

Table 4.2 Operating condition of the thermal conductivity detector for TPR.

Model	GOW-MAC
Detector type	TCD
Carrier gas	5 %H_2 in Ar
Carrier gas flow rate (cc/min)	30
Detector temperature ($^{\circ}C$)	80
Detector current (mA)	80

4.2.4 Hydrogen chemisorption

Static H_2 chemisoption at 100 $^{\circ}C$ on the reduced catalysts (re-reduced at $350^{\circ}C$ for 10h) was used to determine the number of reduce surface cobalt metal atoms and overall cobalt dispersion. H_2 chemisorption was carried out following the procedure described by Reuel and Bartholomew (1984) using a Micromeritics Pulse Chemisorb 2700 instrument at the Analysis Center of Department of Chemical Engineering, Faculty of Engineering, Chulalongkorn University. Prior to

chemisorption, the catalysts were reduced at 350°C for 10 hours. Details of calculation of the total hydrogen chemisorption and % Co dispersion are given in Appendix D.

4.2.5 Electron microscopy

Scanning electron microscopy (SEM) and Energy dispersive X-ray spectroscopy (EDX) were used to determine the catalyst granule morphology and elemental distribution of the catalyst particles, respectively, using a JEOL JSM-35CF scanning electron microscope. The SEM was operated using the back scattering electron (BSE) mode at 20 kV. After the SEM micrographs were taken, EDX was performed to determine the elemental concentration distribution on the catalyst granules using Link Isis 300 software at the Scientific and Technological Reseach Equipment Centre, Chulalongkorn University (STREC).

4.2.6 X-ray diffraction (XRD)

XRD was performed to determine the bulk phases of catalysts by SIEMENS D 5000 X-ray diffractometer using CuK_α radiation with Ni filter in the 2θ range of 20-80 degrees with resolution $0.04°$.

4.2.7 Raman spectroscopy

Raman spectroscopy was used to determine the surface compositions of catalyst samples. The Raman spectra of the samples were collected by projecting a continuous wave laser of argon ion (Ar^+), 514.5 nm through the samples. A scanning range between 200 and 1000 cm^{-1} was applied. The data were analyzed using Raman microscope (Renishaw Raman Microscope System 2000) with CCD chip detector at National Metal and Materials Technology Center (MTEC), Klong Luang, Pathumthani.

4.3 Reaction study in CO hydrogenation

4.3.1 Materials

The reactant gas used for the reaction study was the carbon monoxide in hydrogen feed stream as supplied by Thai Industrial Gas Limited (TIG). The gas mixture contained 9.73 vol % CO in H_2. The total flow rate was 30 cc/min with the H_2/CO ratio of 10/1. Ultra high purity hydrogen and high purity argon manufactured by Thai Industrial Gas Limited (TIG) were used for reduction and balanced flow rate

4.3.2 Apparatus

Flow diagram of CO hydrogenation system is shown in Figure 4.2. The system consists of a reactor, an automatic temperature controller, an electrical furnace and a gas controlling system.

4.3.2.1 Reactor

The reactor was made from a stainless steel tube (O.D. 3/8"). Two sampling points were provided above and below the catalyst bed. Catalyst was placed between two quartz wool layers.

4.3.2.2 Automation Temperature Controller

This unit consists of a magnetic switch connected to a variable voltage transformer and a solid-state relay temperature controller model no. SS2425DZ connected to a thermocouple. Reactor temperature was measured at the bottom of the catalyst bed in the reactor. The temperature control set point is adjustable within the range of $0\text{-}800^{\circ}C$ at the maximum voltage output of 220 volt.

4.3.2.3 Electrical Furnace

The furnace supplied heat to the reactor for CO hydrogenation. The reactor could be operated from temperature up to $800^{\circ}C$ at the maximum voltage of 220 volt.

4.3.2.4 Gas Controlling System

A reactant for the system was each equipped with a pressure regulator and an on-off valve and the gas flow rates were adjusted by using metering valves.

4.3.2.5 Gas Chromatography

The composition of hydrocarbons in the product stream was analyzed by a Shimadzu GC14B gas chromatograph equipped with a flame ionization detector. A Shimadzu GC8A (molecular sieve 5A) gas chromatography equipped with a thermal conductivity detector was used to analyze CO and H_2 in the feed and product streams. The operating conditions for each instrument are shown in the Table 4.3.

Table 4.3 Operating condition for gas chromatograph

Gas Chromagraph	SHIMADZU GC-8A	SHIMADZU GC-14B
Detector	TCD	FID
Column	Molecular sieve 5A	VZ10
Carrier gas	He (99.999%)	H_2 (99.999%)
Carrier gas flow (ml/min)	30 cc/min	30 cc/min
Column temperature		
- initial (^{o}C)	60	70
- final (^{o}C)	60	70
Injector temperature (^{o}C)	100	100
Detector temperature (^{o}C)	100	150
Current (mA)	80	-
Analysed gas	Ar, CO, H_2	Hydrocarbon C_1-C_4

4.3.3 Procedures

CO hydrogenation was performed using 0.2 g of catalyst. It was packed in the middle of the stainless steel microrector, which located in the electrical furnace. The total flow rate was 30 cc/min with the H_2/CO ratio of 10/1. The catalyst sample was re-reduced *in situ* in flowing H_2 at 350°C for 10 h prior to CO hydrogenation. CO hydrogenation was carried out at 220°C and 1 atm total pressure. The product streams were analyzed by gas chromatography (GC). In all cases, steady state was reached within 5 h.

The effluent gases were sampled to analyse the concentration of hydrocarbon (C1-C4) using GC-14B equipped with a VZ10 column, whereas carbon monoxide concentration was analysed by GC-8A equipped with a Molecular sieve 5A column. Details of the calculation of the catalytic activity to convert carbon monoxide, reaction rate and the selectivity towards hydrocarbon (C1-C4) are given in Appendix F.
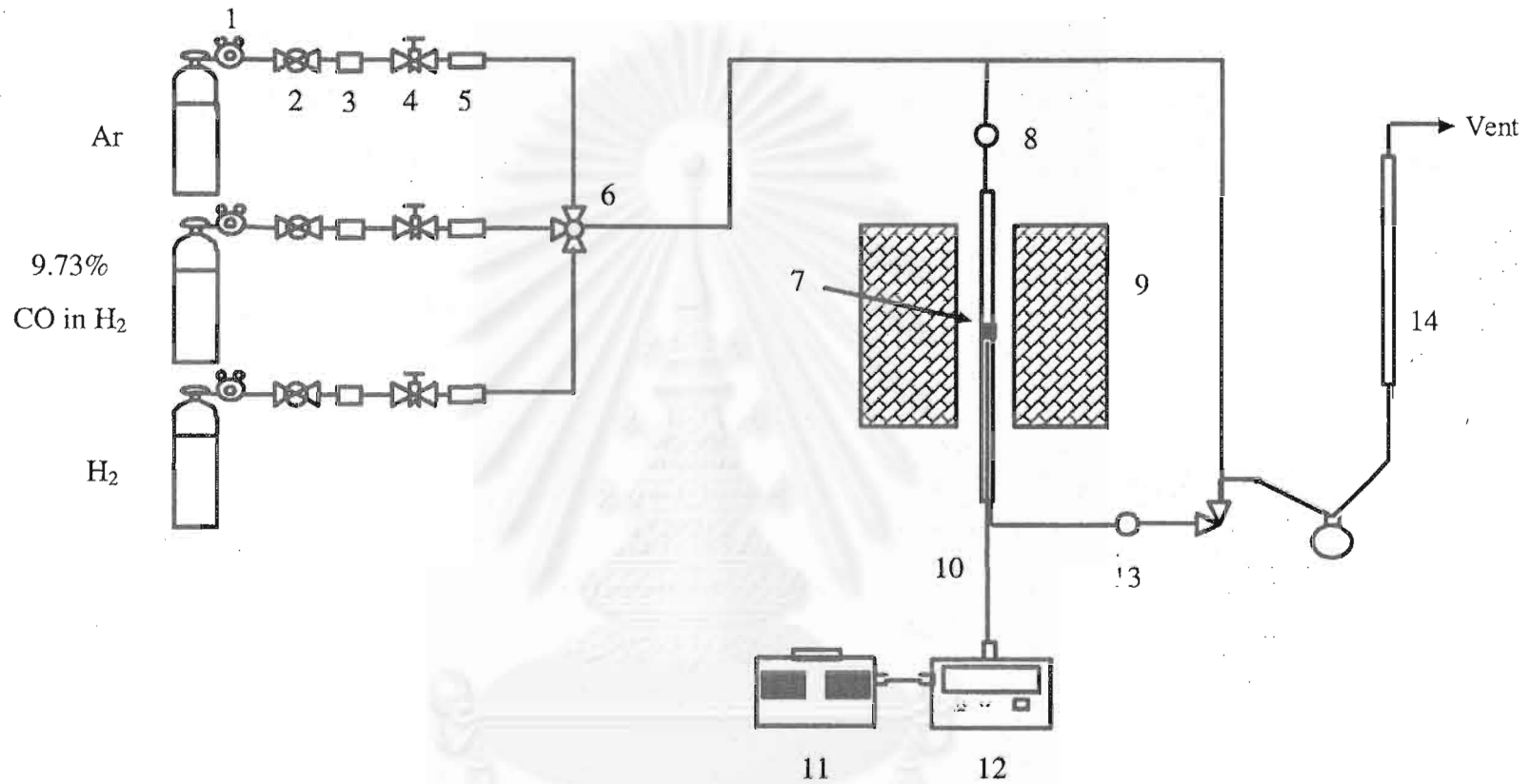
1. Pressure Regulator   2. On-Off Value   3. Gas Filter   4. Metering Valve

5. Back Pressure   6. 3-way Valve   7.Catalyst Bed   8. Sampling point

9. Furnace   10. Thermocouple   11. Variable Voltage Transformer   12. Temperature Controller

13. Heating Line   14. Bubble Flow Meter

Figure 4.2 Flow diagram of CO hydrogenation system

CHAPTER V

RESULTS AND DISCUSSION

This chapter is divided into two parts; results and discussion. The results part contains three sections. Section 5.1.1 is described Co-SCF in T1-supported Co catalysts. Section 5.1.2 is explained Co-SCF in T2-supported Co catalysts. Effect of Ru promotion is illustrated in section 5.1.3. The discussion part consists of three sections; Co-SCF in T1-supported Co catalysts in section 5.2.1, a comparative study of different phases of TiO_2 used in section 5.2.2 and effect of Ru promotion in the last section 5.2.3.

5.1 Results

In order to identify the characteristics of "Co-titanate" formed during reduction, several characterization techniques were conducted. The term "Co-titanate" is used here to refer to the surface compound formed during standard reduction of cobalt and the titania support.

5.1.1 Co-SCF in T1-supported Co catalysts

5.1.1.1 Atomic absorption spectroscopy (AAS)

AAS was performed to determine the composition of elements in the bulk of catalysts. The Co content of T1-supported cobalt catalysts are shown in Table 5.1. It revealed that catalyst samples have 17.8 wt% Co.

5.1.1.2 BET surface area

BET surface areas, pore volumes and average pore diameters of TiO_2, T1 and the catalyst samples after various pretreatments are also shown in Table 5.1. BET surface areas of samples were slightly less than T1 (anatase form) support (70 m^2/g). Since all surface areas of the samples in this study ranged between 46 and 52 m^2/g, there was no significant change in surface areas after the various pretreatments

pretreatments within experimental errors. The pore volume and the average pore diameter of the catalysts also did not change after different pretreatments.

Table 5.1 Content of Co from AAS and BET surface area measurement of T1-supported Co catalysts.

Catalyst samples	Co (wt %)[a]	BET surface area $(m^2/g)^{[b]}$	Pore volume $(cm^3/g)^{[b]}$	Average pore diameter $(Å)^{[b]}$
T1	-	70	0.28	155.9
Co/T1-C	17.8	52	0.18	133.5
Co/T1-RW0	17.8	49	0.18	144.1
Co/T1-RW5	17.8	46	0.16	136.4
Co/T1-RW10	17.8	46	0.17	145.2

[a] Measurement error is ± 2%.

[b] Measurement error is ± 5%.

5.1.1.3 Temperature programmed reduction (TPR)

It can be observed that Co-SCF in Co/T1 essentially occurred during standard reduction resulting in lower reducibilities of the reduced samples during TPR at temperatures 35-800°C as shown in Table 5.2. The reducibilities ranged from 92 to 64% upon the various pretreatments of catalyst samples. Essentially, TPR of the TiO_2, T1 support only was also conducted at the same condition and no hydrogen consumption was detected.

The suggested conceptual diagram of reducibility loss during standard reduction is illustrated in Figure 5.1. First, when performing TPR on a fresh calcined sample, the reducibility gain was 92%. However, when the calcined sample was reduced with and without water vapor addition (5-10 vol%) during reduction, then recalcined it back to the oxide form prior to performing TPR, the reducibilities

obviously decreased. The reducibilities loss during the reduction process were found to be in the range of 22-28%.

Besides the reducibility measurement, TPR also provides information on the reduction behaviors of the catalyst samples pretreated under various conditions. TPR profiles of bulk Co_3O_4 and the catalyst samples after various pretreatment conditions are shown in Figure 5.2. Only one strong reduction peak can be observed for bulk Co_3O_4 and all the samples regardless of various pretreatment conditions used. This peak can be assigned to the overlap of two-step reduction of Co_3O_4 to CoO and then to Co^0 (Kraum and Baern, 1999; Jongsomjit et al., 2001). There was only one reduction peak located at ca. 370-620°C (max. at 520°C) for the calcined sample (Co/T1-C). TPR profiles of all reduced samples were also similar exhibiting only one reduction peak as shown in Figure 5.2. TPR peak located at ca. 400-620°C (max. at 520°C) for Co/T1-RW0 sample was slightly shifted about 10°C higher when the partial pressure of water vapor was increased during reduction.

Table 5.2 TPR and H_2 chemisorption results for T1-supported Co catalyst samples after various pretreatments.

Catalyst samples	Reduction gas mixture (P_{H2}/P_{H2O})	Reducibility (%) during TPR at 35-800°C[a,b]	Total H_2 chemisorption ($\mu mol\ H_2/g_{cat}$)[c]	Overall Co metal dispersion (%)
Co/T1-C	-	92	0.42	0.03
Co/T1-RW0	1/0	70	nil	nil
Co/T1-RW5	0.95/0.05	68	nil	nil
Co/T1-RW10	0.90/0.10	64	nil	nil

[a] The reduced samples were recalcined at the original calcination conditions prior to performing TPR.

[b] Measurement error is ± 5%.

[c] Error = ± 5% of measurement of H_2 chemisorption.

Sample

Reducibility

TPR

Co/T1-C ⟶ ▨▨▨▨▨▨▨ 92%

Reduction with P_{H2}/P_{H2O} = i) [1/0]; ii) [0.95/0.05]; iii) [0.90/0.10]

i) Co/T1-(RW0)   ▨▨ 22% loss

ii) Co/T1-(RW5)   ▨▨ 24% loss

iii)Co/T1-(RW10)   ▨▨ 28% loss

i) Co/T1-(RW0)-C ⎫
                  ⎬ TPR ⟶ ▨▨▨▨▨ 70%
ii) Co/T1-(RW5)-C ⎬   ▨▨▨▨▨ 68%
iii)Co/T1-(RW10)-C⎭   ▨▨▨▨▨ 64%

▨▨ Reducibility gain during TPR

▨▨ Reducibility loss during reduction*
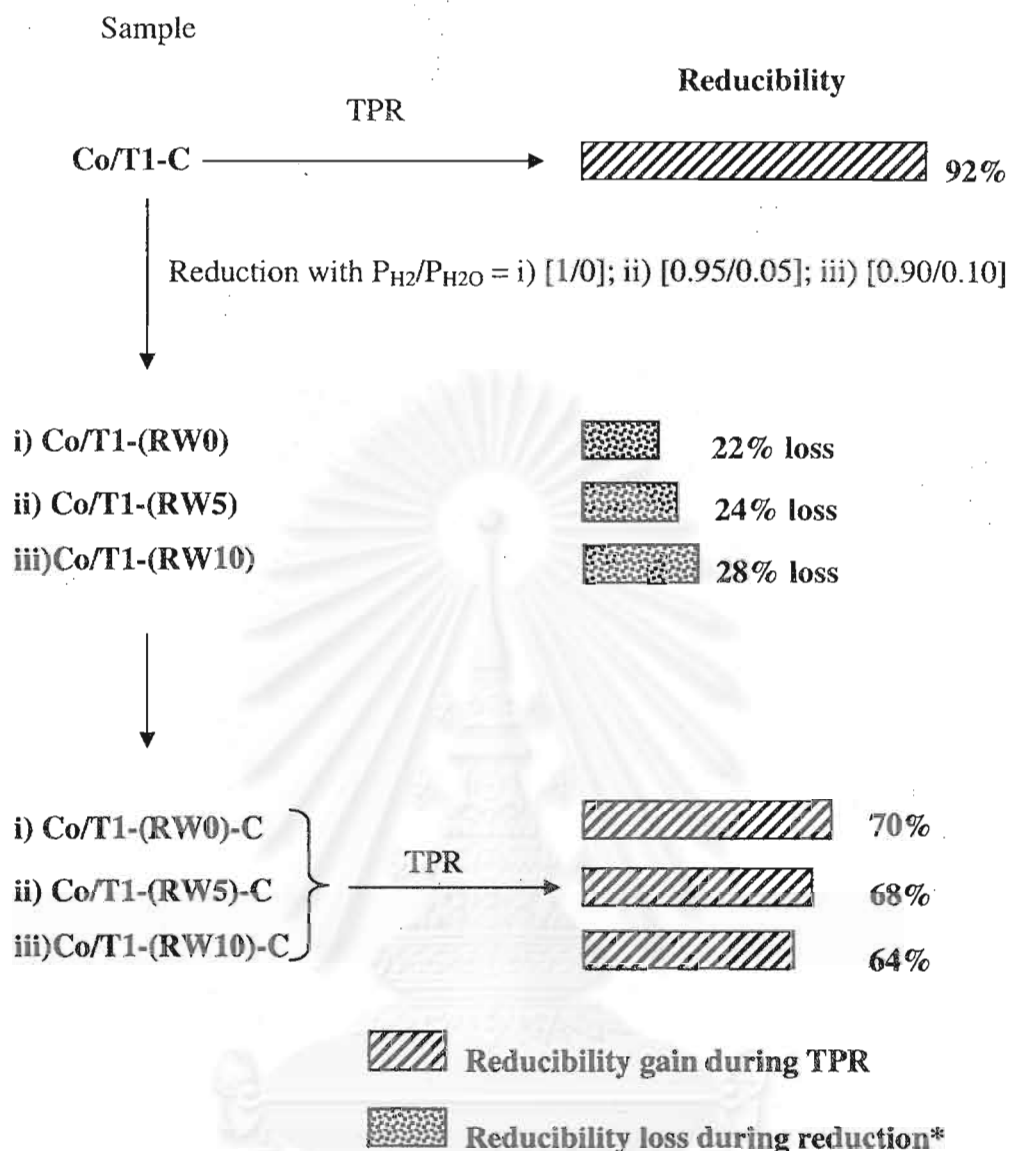
* The difference in reducibility gain from a fresh calcined sample and the reducibility gain from a reduced and recalcined sample.

Figure 5.1 Suggested conceptual diagram for the reducibility loss during reduction process of T1-supported Co catalysts.
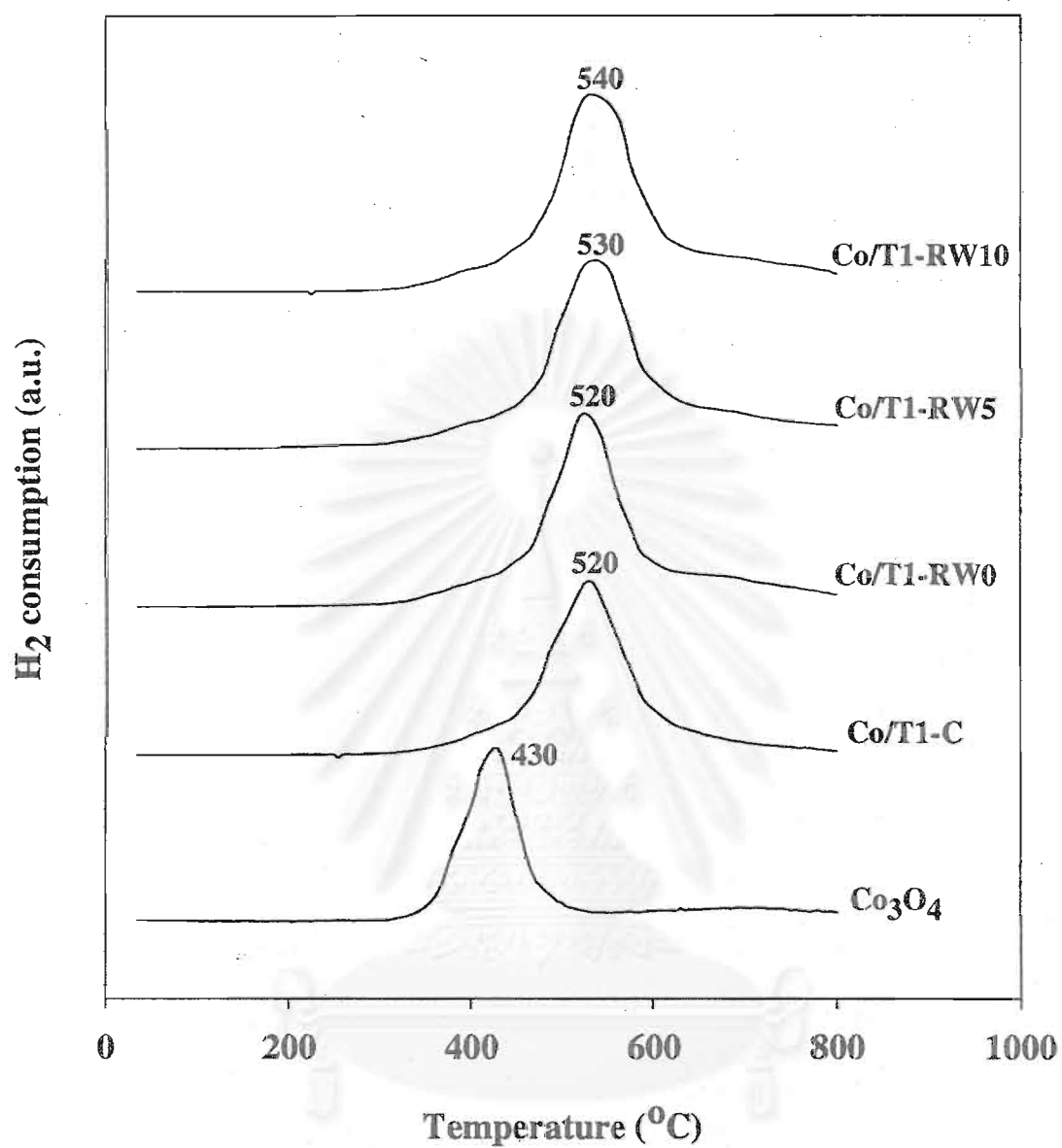
Figure 5.2 TPR profiles of bulk Co_3O_4 and the T1-supported Co catalysts after various pretreatment conditions.

5.1.1.4 H₂ chemisorption

H_2 chemisorption was used to determine the number of reduce surface cobalt metal atoms and percentage overall cobalt dispersion. The results of H_2 chemisorption for Co/T1 catalysts after different pretreatments are given in Table 5.2. Moreover, the overall Co metal dispersion in the catalyst samples are also shown. The Co metal dispersion of the samples likely decreased with increasing amount of water vapor during reduction.

5.1.1.5 Electron microscopy

SEM and EDX were performed to study the morphologies of the catalyst samples and elemental distributions of the catalyst samples, respectively. There was no significant change in morphologies of catalyst samples. By observation on the external surface of the catalyst granules, cobalt patches (the term "patches" is used to refer the entities rich in cobalt supported on the catalyst granules) can be seen all over the external surface of samples. In general, all of them were similar regardless the pretreatment conditions used. The typical morphology in an external area of catalyst granules with different magnification for Co/T1-C and Co/T1-RW10 are shown in Figure 5.3.and Figure 5.4. It can be observed that cobalt patches (white spots) were well distributed all over the external surface of catalyst granules. The elemental distributions can be clearly seen by EDX. Figure 5.5 and Figure 5.6 show the typical elemental distribution for a cross section of a granule of Co/T1-C and Co/T1-RW10, respectively. The distribution of cobalt was well dispersed throughout the catalyst granule as also seen by SEM.
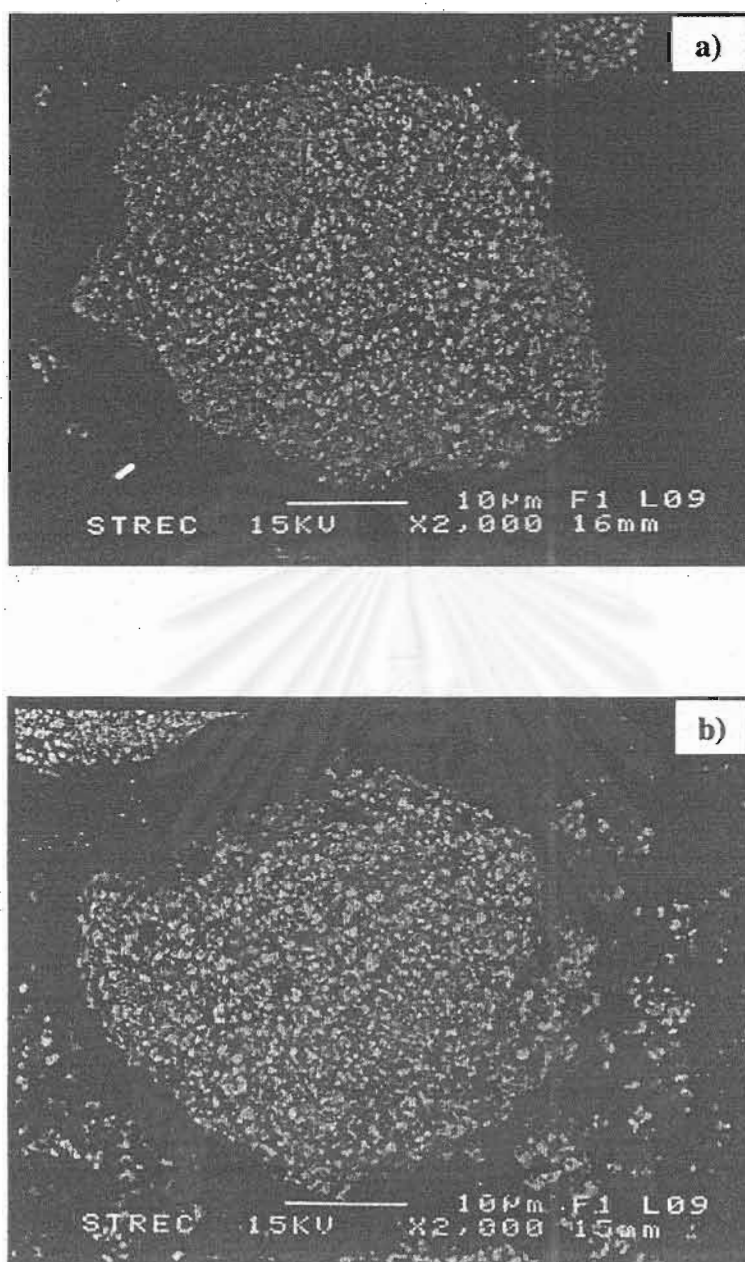
Figure 5.3 SEM micrographs of catalyst granule at the external surface at 2000x magnification; a) Co/T1-C, and b) Co/T1-RW10.
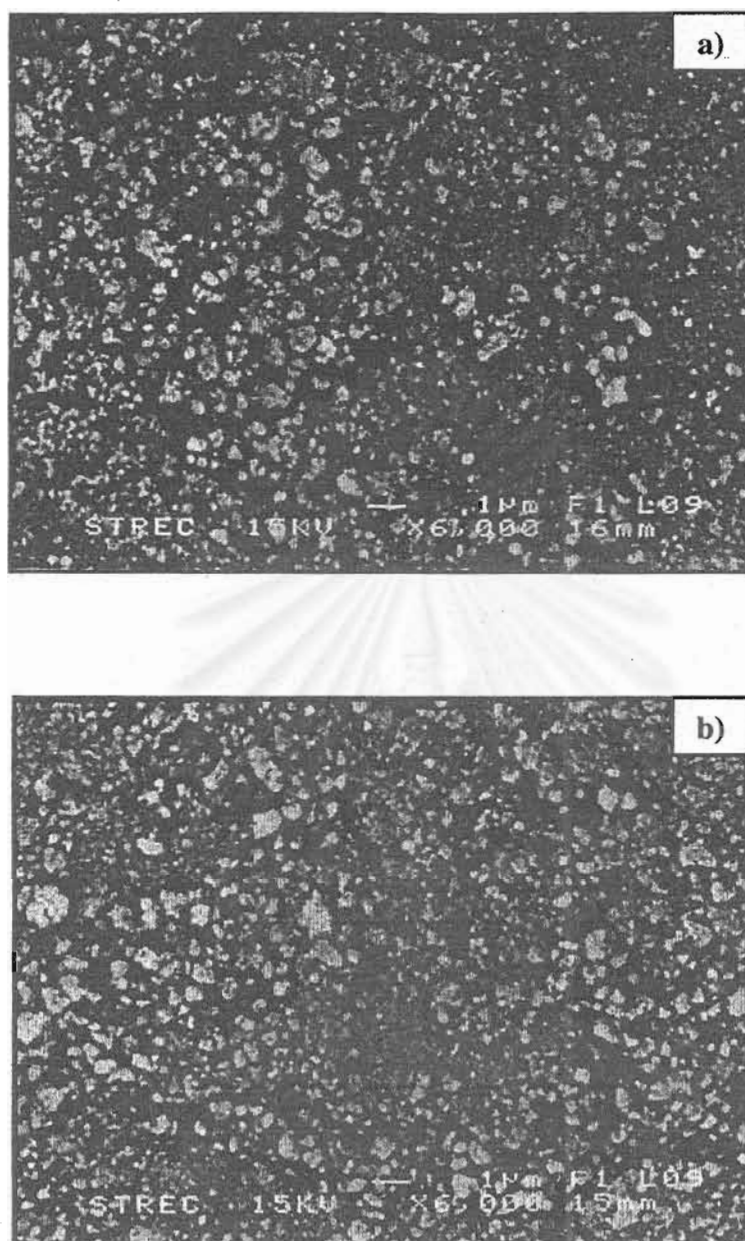
Figure 5.4 SEM micrographs of catalyst granule at the external surface at 6000x magnification; a) Co/T1-C, and b) Co/T1-RW10.
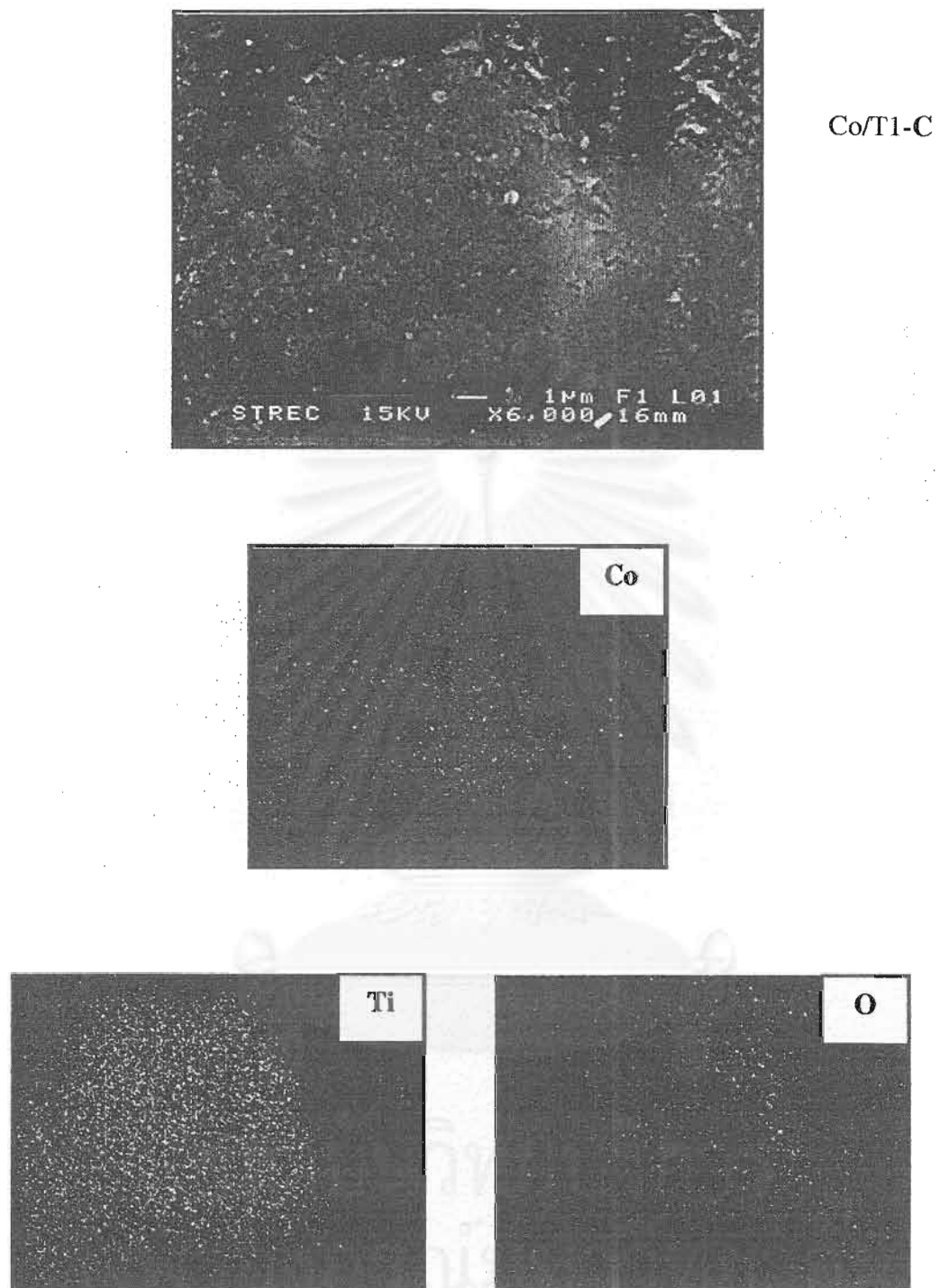
Co/T1-C

Figure 5.5 SEM micrograph and EDX mapping of Co/T1-C catalyst granule (cross section).

Co/T1-RW10
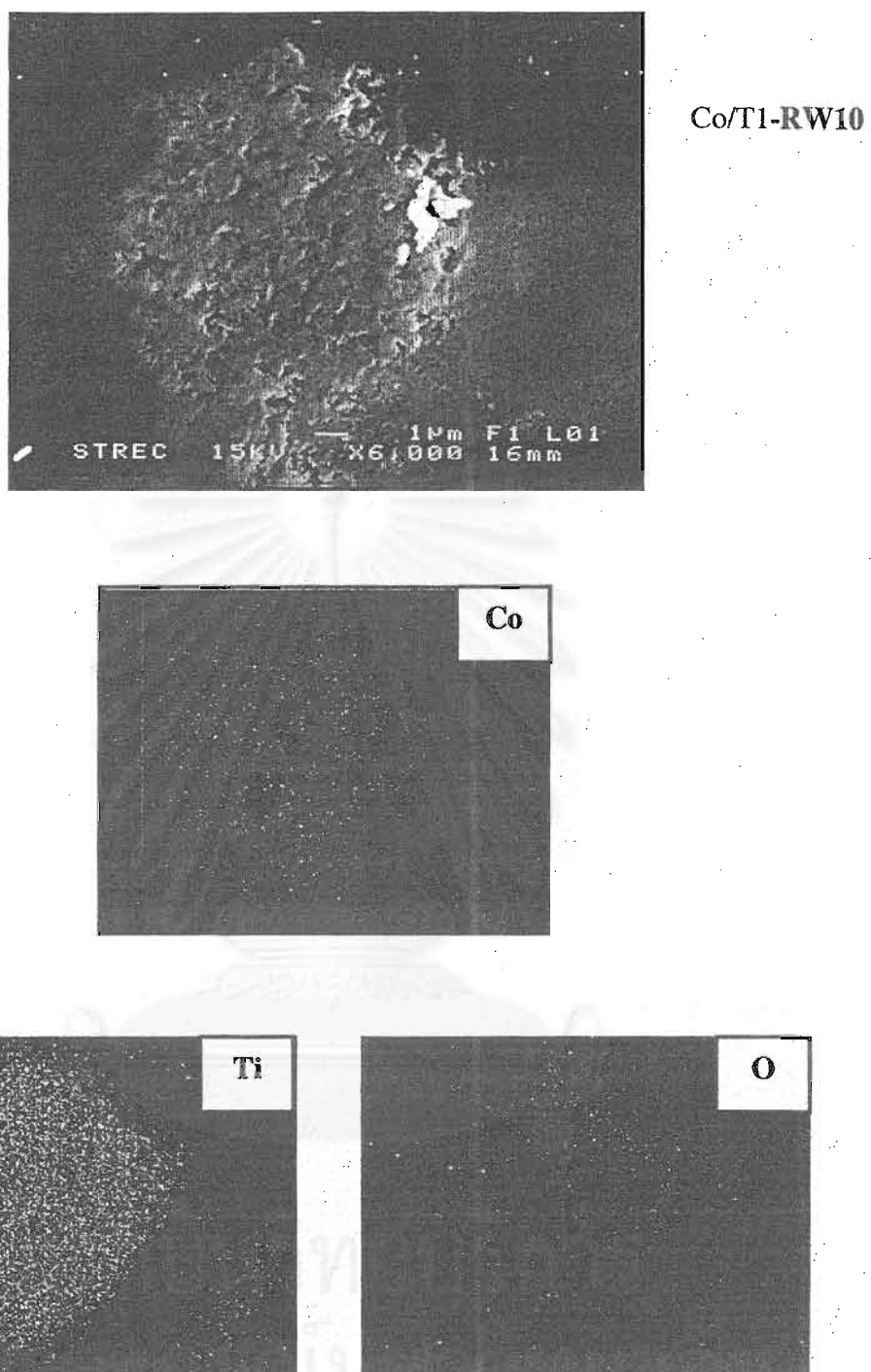
Figure 5.6 SEM micrograph and EDX mapping of Co/T1-RW10 catalyst granule (cross section).

5.1.1.6 X-ray diffraction (XRD)

The bulk crystalline phases of samples were determined using XRD. XRD patterns of T1, $CoTiO_3$ and catalyst samples after various pretreatments are shown in Figure 5.7. XRD patterns of T1 showed strong diffraction peaks at $26°$, $37°$, $48°$, $55°$, $56°$, $62°$, $69°$, $71°$ and $75°$ indicating the TiO_2 in the anatase form. After calcination, the diffraction peaks of Co_3O_4 at $36°$, $46°$, and $65°$ can be observed. Apparently, the relative intensity of those peaks is much lower compared to the T1 peaks. To identify the XRD peaks of samples, XRD peaks of $CoTiO_3$ were also collected and it showed the diffraction peaks at $23°$, $32°$, $35°$, $49°$, $52°$, $62°$ and $64°$ as also shown in Figure 5.7. After reduction at various conditions and passivation, the diffraction peaks of CoO were present at $37°$ and $63°$.

XRD patterns of samples after TPR measurement up to $800°C$ are shown in Figure 5.8. The similar trend as shown in Figure 5.7 was found except for the observation of cobalt metal peaks at $44°$ and $52°$ due to sintering. No phase change, i.e from anatase to rutile form of TiO_2 was observed.
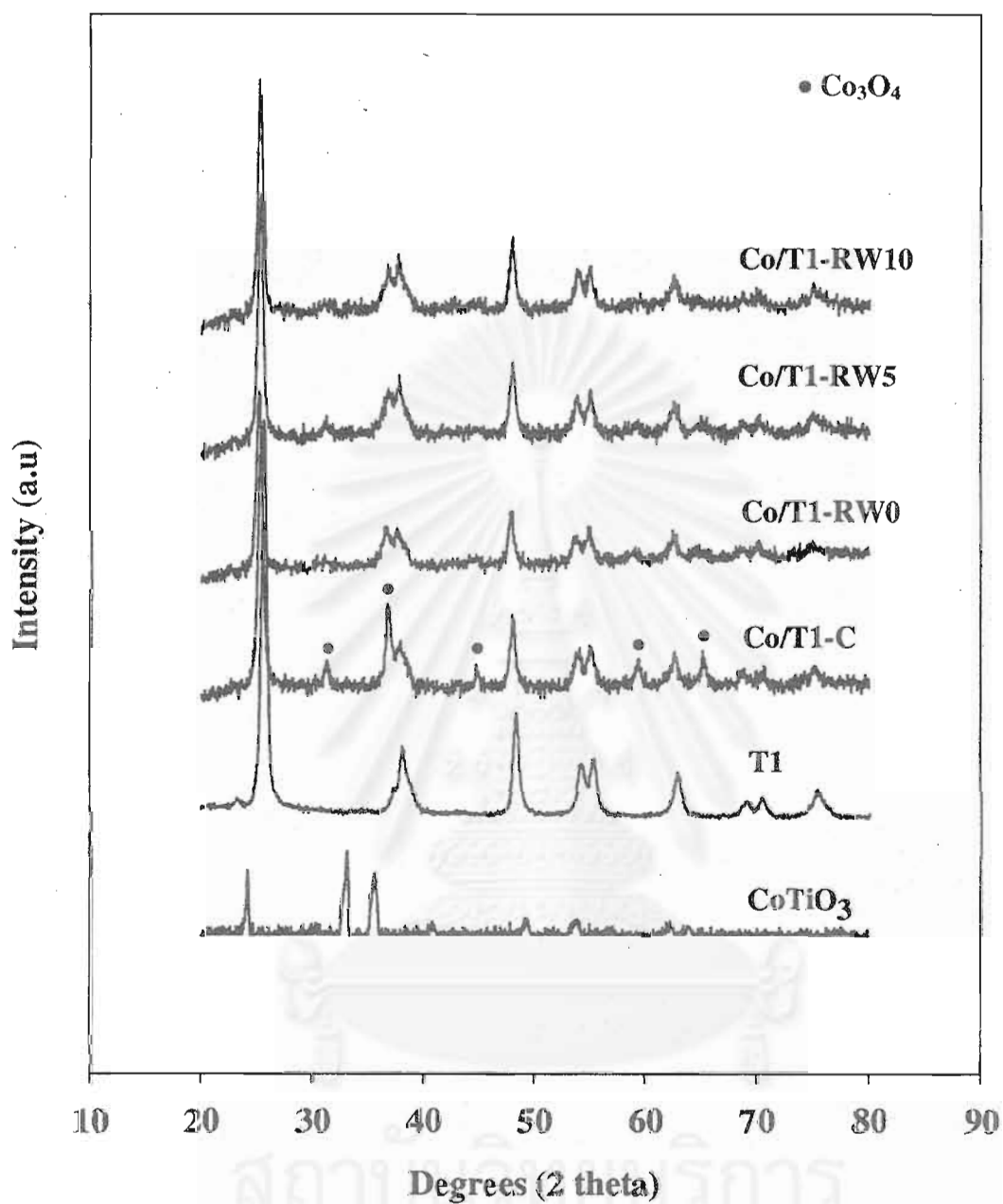
Figure 5.7 XRD patterns of $CoTiO_3$, T1 and the T1-supported Co catalysts after various pretreatment conditions.
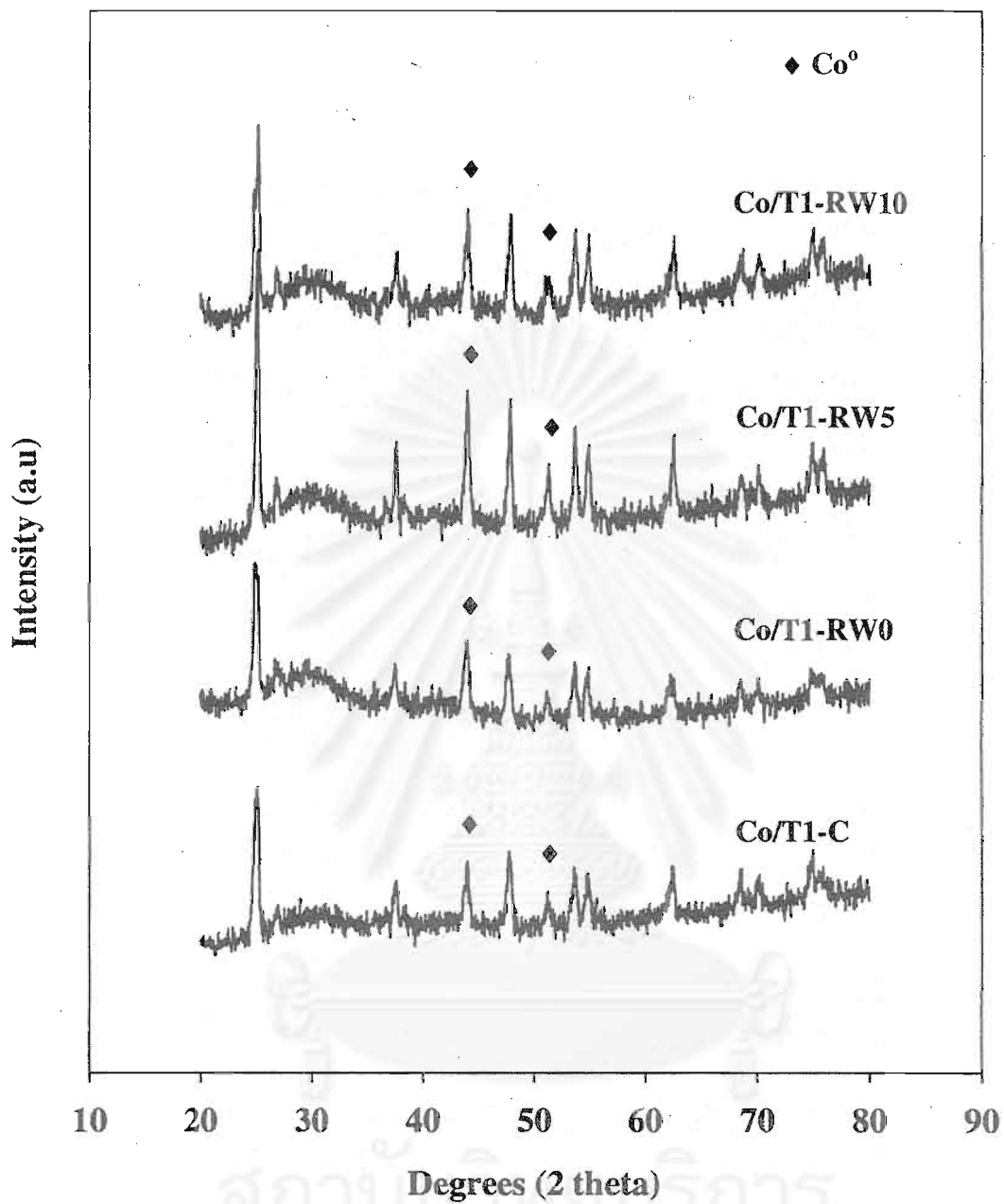
Figure 5.8 XRD patterns of the Co/T1 catalysts after TPR measurement up to 800°C.

5.1.1.7 Raman spectroscopy

Raman spectra of T1, CoO, Co_3O_4, $CoTiO_3$ and the catalyst samples after various pretreatments are shown in Figure 5.9. To identify Raman bands of samples, the Raman spectra of Co_3O_4, CoO and $CoTiO_3$ were collected. The Raman bands of $CoTiO_3$ exhibited bands at 695, 604, 455, 382, 336 and 266 cm^{-1} which are similar to the ones reported by Brik *et al.* (2001). The strong Raman bands for TiO_2 were observed at 640, 514, and 397 cm^{-1} indicating the TiO_2 in its anatase form (Brik *et al.*, 2002). The Raman spectrum of the calcined sample exhibited Raman bands at 640, 514, and 397 cm^{-1} as seen in those for T1 support including two shoulders at 690 and 480 cm^{-1}, assigned to Co_3O_4 (Jongsomjit *et al.*, 2001, 2002, 2003). Raman spectra of all reduced samples showed the Raman bands of TiO_2 support and the shoulders at 690 and 480 cm^{-1}. These can be assigned to Co_3O_4 present on catalyst surface rather than CoO (detected in the bulk by XRD) since Raman spectroscopy is more of surface technique (Jongsomjit *et al.*, 2002).

Besides the strong signal of TiO_2, the signal of CoO and Co_3O_4 is likely to hinder the observation of surface "Co-titanate" as well. In order to eliminate that interference, we also conducted Raman spectroscopy on the reduced samples with a lesser degree of passivation and the Raman spectra of samples are shown in Figure 5.10. It can be observed that the characteristic peaks of the reduced samples were similar to each other, but deviated from the characteristic peaks of Co_3O_4 as seen in Figure 5.9. The Raman band of the reduced samples at 397 cm^{-1} of the TiO_2 became broader. This perhaps resulted from the overlap between the peaks of 397 cm^{-1} of the TiO_2 and 382 cm^{-1} of $CoTiO_3$ due to the formation of surface "Co-titanate".

Figure 5.9 Raman spectra of Co_3O_4, CoO, $CoTiO_3$, T1 and the Co/T1 catalysts after various pretreatment conditions.
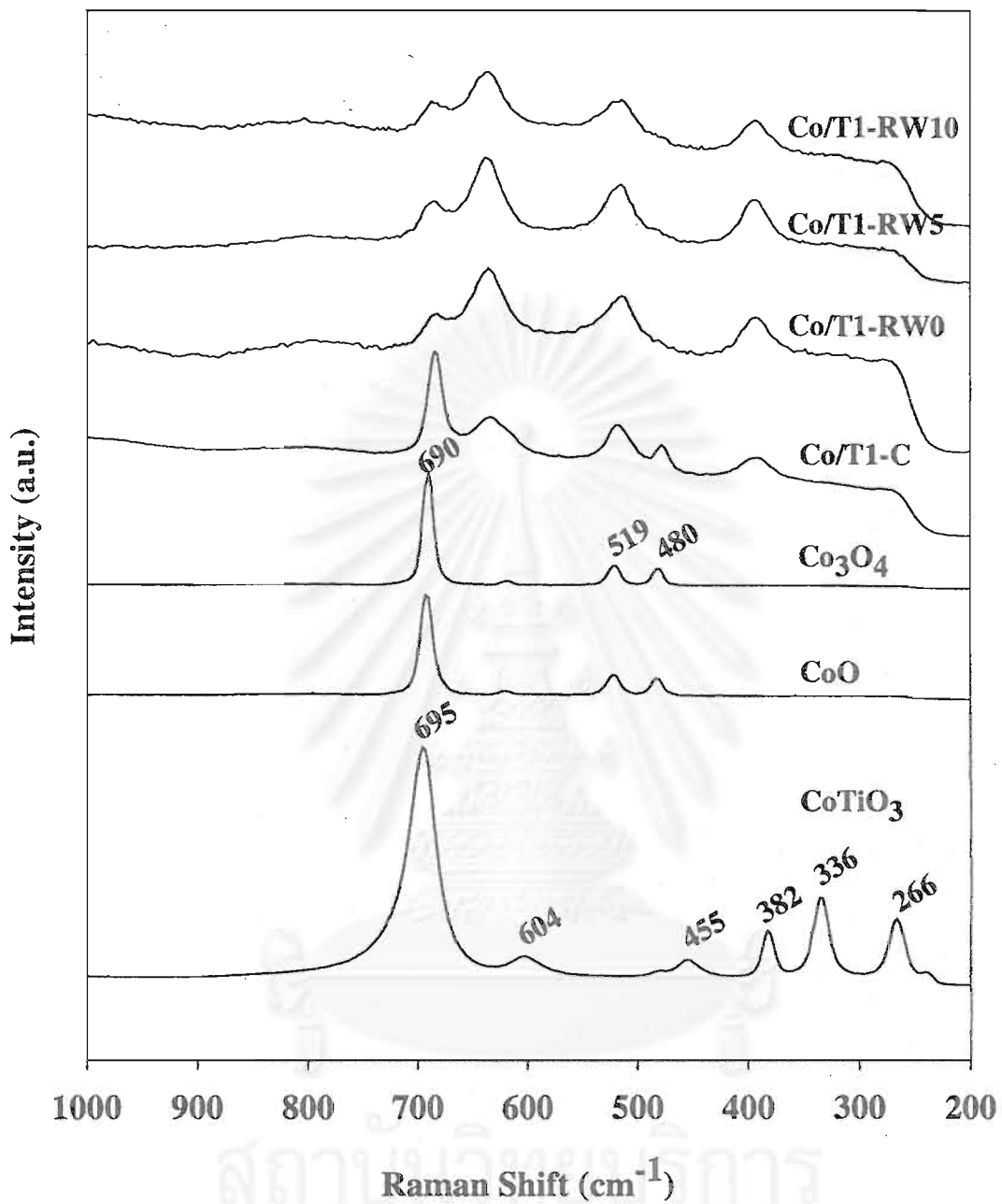
Figure 5.10 Raman spectra of Co_3O_4, CoO, $CoTiO_3$, the calcined sample and the reduced with a lesser degree of passivation samples.

5.1.1.8 Reaction study in CO hydrogenation

CO hydrogenation was performed to determine the overall activity of the catalyst samples reduced at various conditions. The results are shown in Table 5.3. It indicated that the CO conversion ranged between 3.71 to 0.34% (initial) and 2.09 to 0.08% (steady state). The reaction rate ranged between 0.0139 to 0.0013 $gCH_2/g_{cat}h^{-1}$ (initial) and 0.079 to 0.0003 $gCH_2/g_{cat}h^{-1}$ (steady state). However, there was no any significant difference in selectivity for any of samples based on reaction conditions used in this study.

Table 5.3 Reaction rate for CO hydrogenation on the Co/T1 catalyst samples reduced at various conditions.

Sample	CO conversion(%)[a]		Rate($\times 10^2 gCH_2/g_{cat}h^{-1}$)[b]		CH_4 selectivity(%)	
	Initial[c]	SS[d]	Initial	SS	Initial	SS
Co/T1-C	3.71	2.09	1.39	0.79	71	68
Co/T1-RW0	1.53	0.73	0.58	0.27	68	65
Co/T1-RW5	0.83	0.46	0.31	0.17	71	70
Co/T1-RW10	0.34	0.08	0.13	0.03	73	69

[a] CO hydrogenation was carried out at 220°C, 1 atm, and $H_2/CO/Ar = 20/2/8$ cc/min.

[b] Error ±5%

[c] After 5 min of reaction

[d] After 5 h of reaction

5.1.2 Co-SCF in T2-supported Co catalysts

5.1.2.1 Atomic absorption spectroscopy (AAS)

The content of Co in T2-supported Co catalysts are shown in Table5.4. The final Co loading of the catalyst samples are 16.3 wt% Co.

5.1.2.2 BET surface area

BET surface areas, pore volumes and average pore diameters of T2 support and the catalyst samples after various pretreatments are shown in Table 5.4. BET surface areas of the T2 support is 49 m^2/g since the BET surface areas of the Co catalysts after various pretreatments is less than the T2 support and ranged between 30-34 m^2/g. No significant change of surface area after the various pretreatments. The pore volume and the average pore diameter of the catalysts also did not change after different pretreatments.

Table 5.4 Content of Co from AAS and BET surface area measurement of T2-supported Co catalysts.

Catalyst samples	Co (wt %)[a]	BET surface area (m^2/g)[b]	Pore volume (cm^3/g)[b]	Average pore diameter (Å)[b]
T2	-	49[c]	-	-
Co/T2-C	16.3	34	0.19	221.8
Co/T2-RW0	16.3	32	0.19	231.9
Co/T2-RW5	16.3	32	0.15	192.6
Co/T2-RW10	16.3	30	0.19	248.8

[a] Measurement error is ± 2%.

[b] Measurement error is ± 5%.

[c] From single point measurement.

5.1.2.3 Temperature programmed reduction (TPR)

The reducibilities during TPR at temperature 35-800°C of the catalyst samples after various pretreatments are shown in Table 5.5. The reducibilities were ranged between 68 to 78% depending on the amount of water added during reduction. The more amount of water added, the less reducibility of the catalyst sample was as shown in Table 5.5. Besides, TPR of the T2 support only was also conducted at the same condition and no hydrogen consumption was detected.

The suggested conceptual diagram of reducibility loss during standard reduction is illustrated in Figure 5.11. First, the fresh calcined sample has reducibility gain 78% after that it was reduced with the amount of water add (0, 5 and 10 vol%) during reduction. Before testing used TPR, these catalyst samples were recalcined back to the oxide form. It was found that the reducibilities were decreased. The losses of reducibilities during reduction were ranged in 4-10%.

In addition, TPR was performed information on the reduction behaviors of the catalyst samples pretreated under various conditions. Figure 5.12 was illustrated TPR profiles of bulk Co_3O_4 and the Co/T2 catalyst samples after various pretreatment conditions. It can be perceived that bulk Co_3O_4 and all the samples after various pretreatment conditions indicated only one strong reduction peak. This peak can be assigned to the overlap of two-step reduction of Co_3O_4 (Kraum and Baern, 1999; Voβ et al., 2003).

$$Co_3O_4 + H_2 \rightarrow 3Co + H_2O \qquad (5.1)$$
$$CoO + H_2 \rightarrow Co^o + H_2O \qquad (5.2)$$
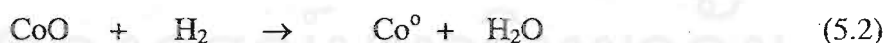
There was only one reduction peak located at ca. 315-640°C (max. at 510°C) for the calcined sample (Co/T2-C). TPR profiles of all reduced samples were also similar exhibiting only one reduction peak as shown in Figure 5.12. TPR peak located at ca. 330-640°C (max. at 510°C) for Co/T2-**RW0** sample was not shifted when the more amount of water vapor added during reduction.

5.1.2.4 H₂ chemisorption

Total H_2 chemisorption and the overall Co metal dispersion for T2-supported Co catalyst samples after different pretreatments are given in Table 5.5. The addition of water vapor during reduction manifested the lower Co metal dispersion of the samples (0.35 to 0.21%).

Table 5.5 TPR and H_2 chemisorption results for T2-supported Co catalyst samples after various pretreatments.

Catalyst samples	Reduction gas mixture (P_{H2}/P_{H2O})	Reducibility (%) during TPR at 35-800°C[a,b]	Total H_2 chemisorption (μmol H_2/g_{cat})[c]	Overall Co metal dispersion (%)
Co/T2-**C**	-	78	4.81	0.35
Co/T2-**RW0**	1/0	74	3.27	0.24
Co/T2-**RW5**	0.95/0.05	72	3.21	0.23
Co/T2-**RW10**	0.90/0.10	68	2.97	0.21

[a] The reduced samples were recalcined at the original calcination conditions prior to performing TPR.

[b] Measurement error is ± 5%.

[c] Error = ± 5% of measurement of H_2 chemisorption.

Sample

Reducibility

TPR

Co/T2-C $\longrightarrow$ 78%

Reduction with P_{H2}/P_{H2O} = i) [1/0]; ii) [0.95/0.05]; iii) [0.90/0.10]

i) Co/T2-(RW0)   4% loss

ii) Co/T2-(RW5)   6% loss

iii)Co/T2-(RW10)   10% loss

i) Co/T2-(RW0)-C ⎫
                 ⎬   TPR   74%
ii) Co/T2-(RW5)-C⎟   72%
iii)Co/T2-(RW10)-C⎭   68%

Reducibility gain during TPR

Reducibility loss during reduction*
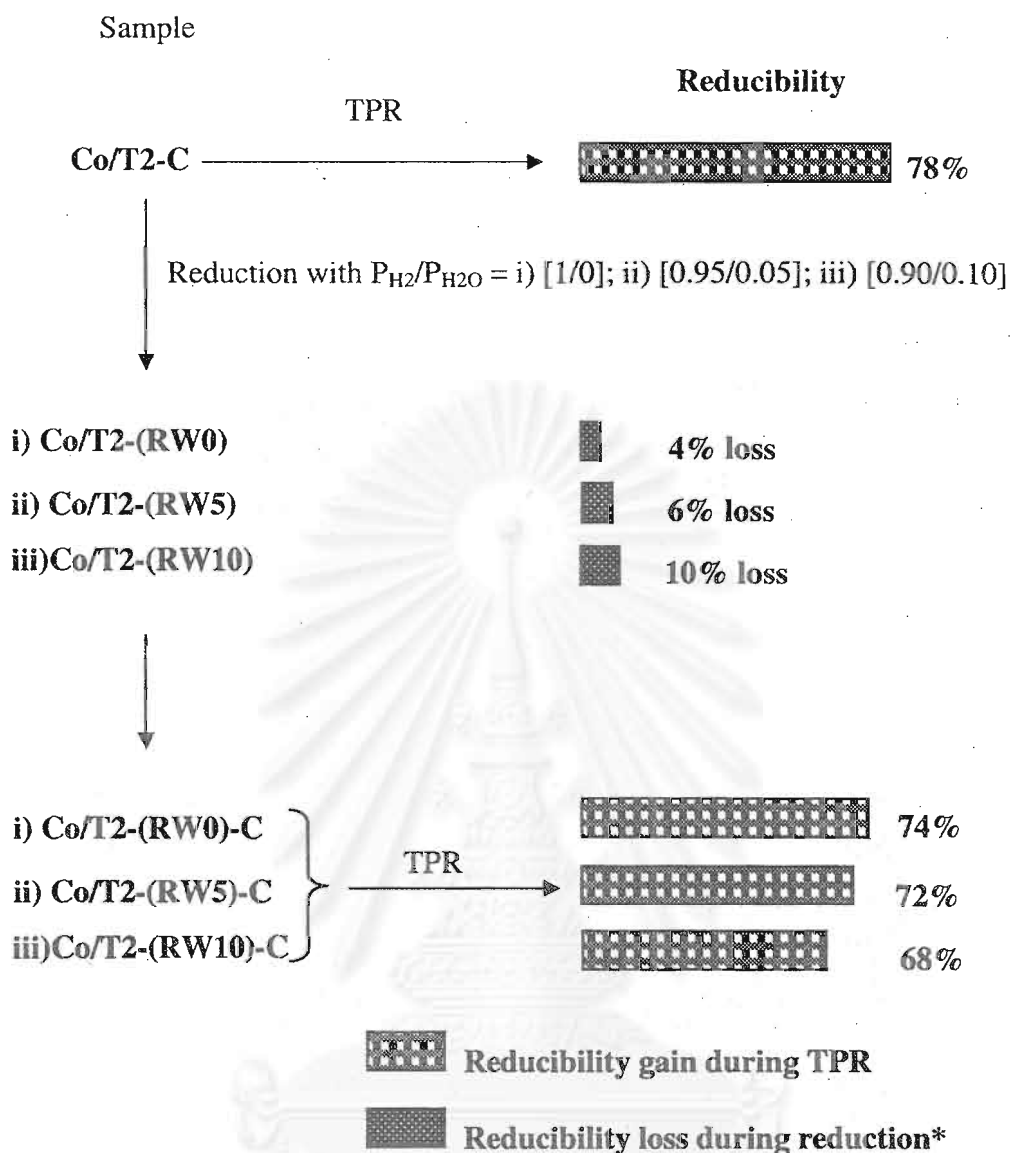
* The difference in reducibility gain from a fresh calcined sample and the reducibility gain from a reduced and recalcined sample.

Figure 5.11 Suggested conceptual diagram for the reducibility loss during reduction process of T2-supported Co catalysts.
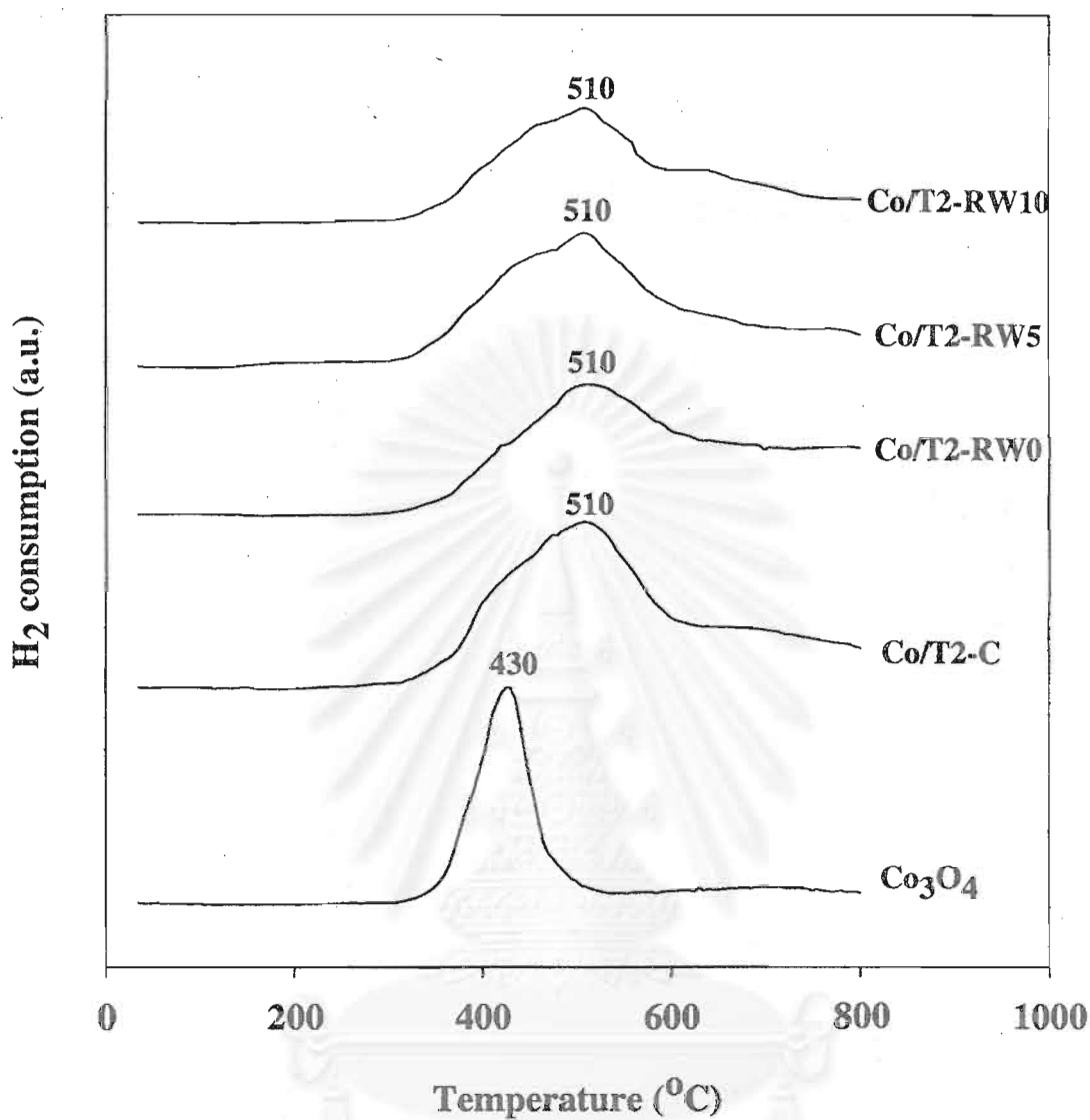
Figure 5.12 TPR profiles of bulk Co_3O_4 and the Co/T2 catalysts after various pretreatment conditions.

5.1.2.5 Electron microscopy

The morphologies of the catalyst samples and elemental distributions of the catalyst samples were determined using SEM and EDX, respectively. The typical morphology in an external area of catalyst granules with different magnification for Co/T2-C and Co/T2-RW10 are performed in Figure 5.13 and Figure 5.14. It found that the morphologies of the catalyst samples after different pretreatment conditions were no significant change and cobalt patches (white spots) were well distributed all over the external surface of catalyst granules. The typical elemental distribution for a cross section of a granule of Co/T2-RW5 and Co/T2-RW10 were illustrated in Figure 5.15 and Figure 5.16, respectively. The distribution of cobalt was well dispersed throughout the catalyst granule as also seen by SEM.
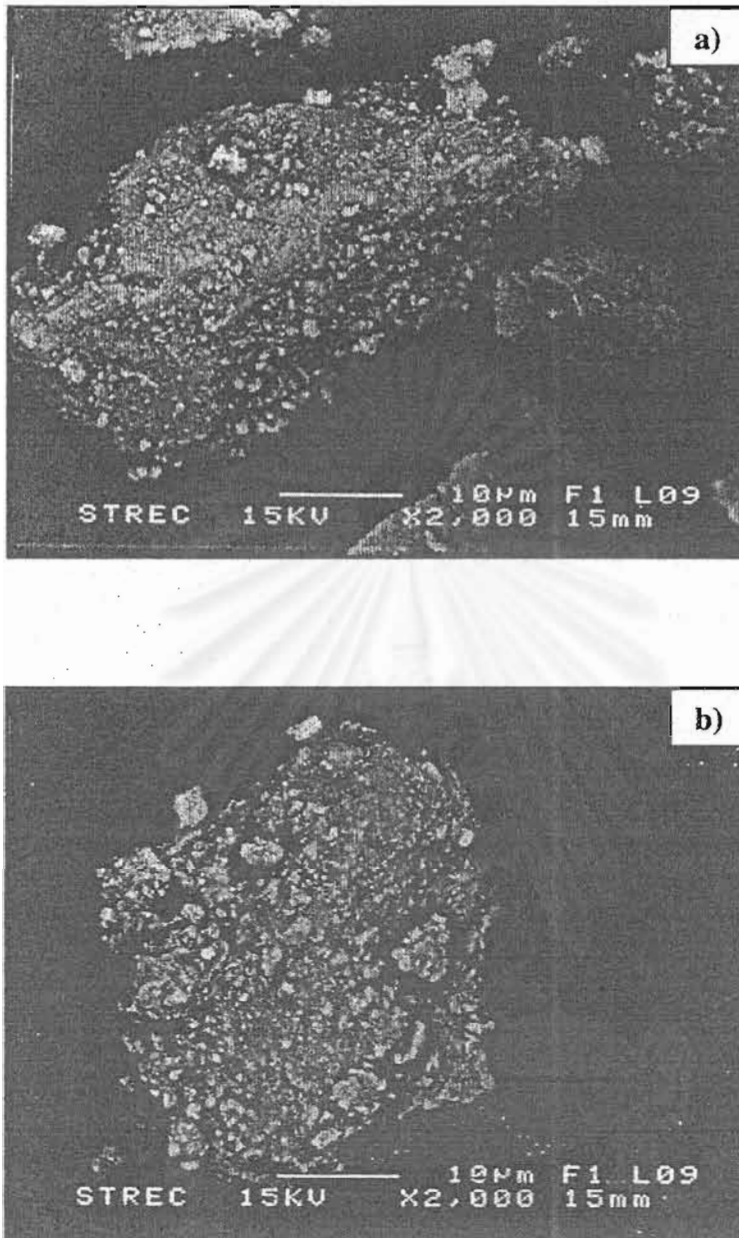
Figure 5.13 SEM micrographs of catalyst granule at the external surface at 2000x

magnification; a) Co/T2-**C**, and b) Co/T2-**RW10**.
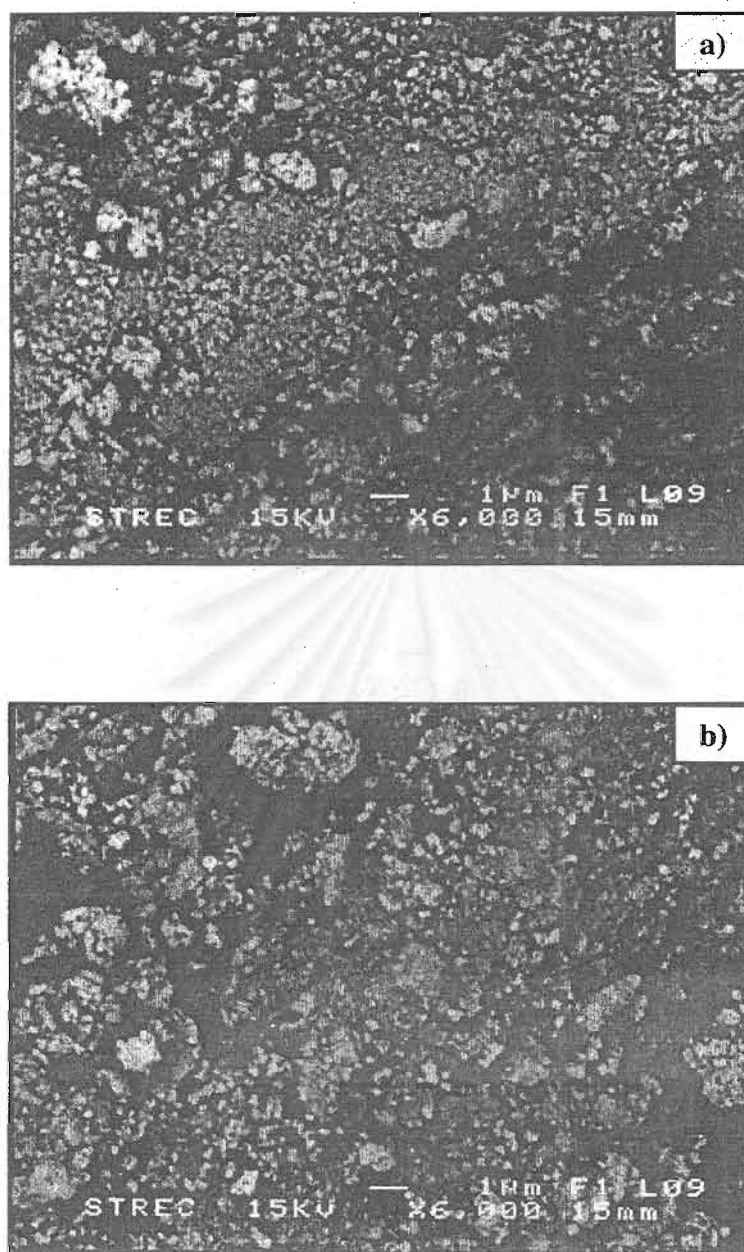
Figure 5.14 SEM micrographs of catalyst granule at the external surface at 6000x

magnification; a) Co/T2-C, and b) Co/T2-RW10.
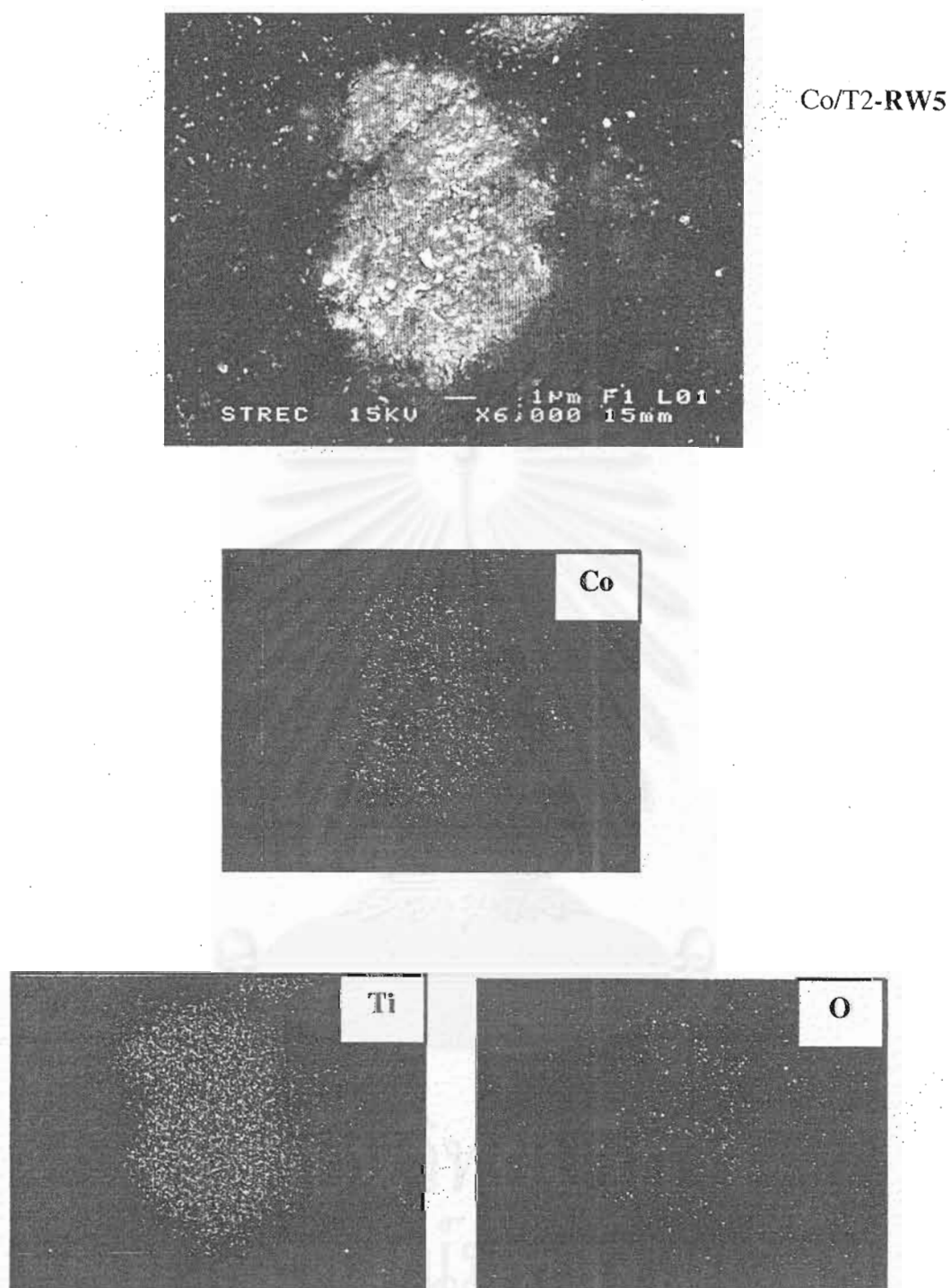
Co/T2-**RW5**

Figure 5.15 SEM micrograph and EDX mapping of Co/T2-**RW5** catalyst granule (cross section).
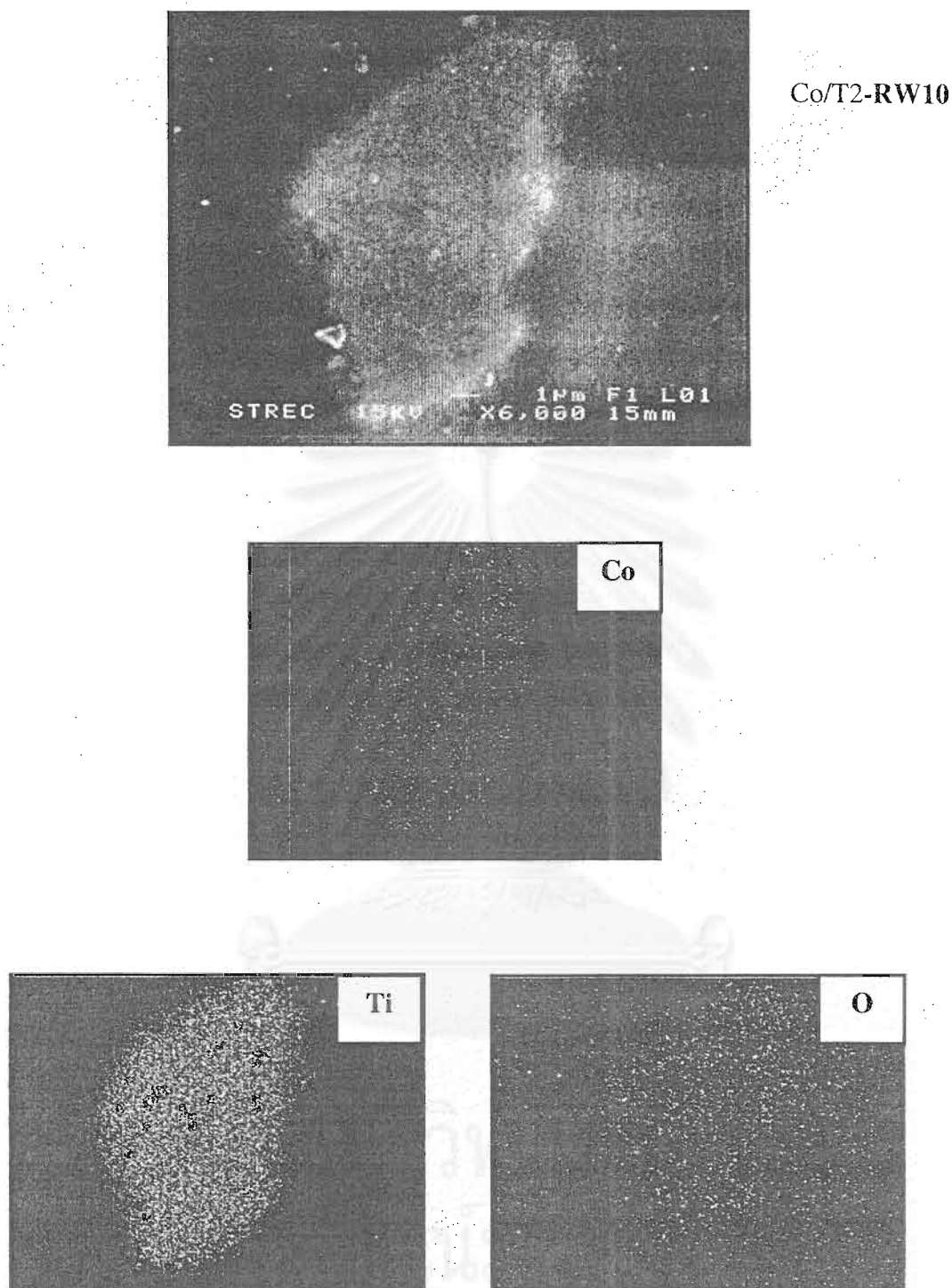
Co/T2-**RW10**

Figure 5.16 SEM micrograph and EDX mapping of Co/T2-**RW10** catalyst granule (cross section).

5.1.2.6 X-ray diffraction (XRD)

XRD patterns of $CoTiO_3$, T2 and the Co/T2 catalyst samples after various pretreatments and reference XRD spectra of $CoTiO_3$, Co_3O_4 and titania are shown in Figure 5.17 and Figure 5.18, respectively. XRD patterns of T2 support showed strong diffraction peaks at 26°, 37°, 48°, 55°, 56°, 62°, 69°, 71° and 75° indicating the TiO_2 in the anatase form and the diffraction peaks at 27°, 36°, 42° and 57° exhibiting the TiO_2 in the rutile form. Both crystalline form of titania at different diffraction are shown in Figure 5.18. After calcination, the diffraction peaks of Co_3O_4 at 36°, 46°, and 65° can be observed. Apparently, the relative intensity of those peaks is much lower compared to the T2 peaks. To identify the XRD peaks of samples, XRD peaks of $CoTiO_3$ were also collected and it showed the diffraction peaks at 23°, 32°, 35°, 49°, 52°, 62° and 64° as also shown in Figure 5.17. After reduction at various conditions and passivation, the diffraction peaks of CoO were present at 37° and 63°.

XRD patterns of samples after TPR measurement up to 800°C are shown in Figure 5.19. The similar trend as shown in Figure 5.17 was found except for the observation of cobalt metal peaks at 44° and 52° due to sintering.
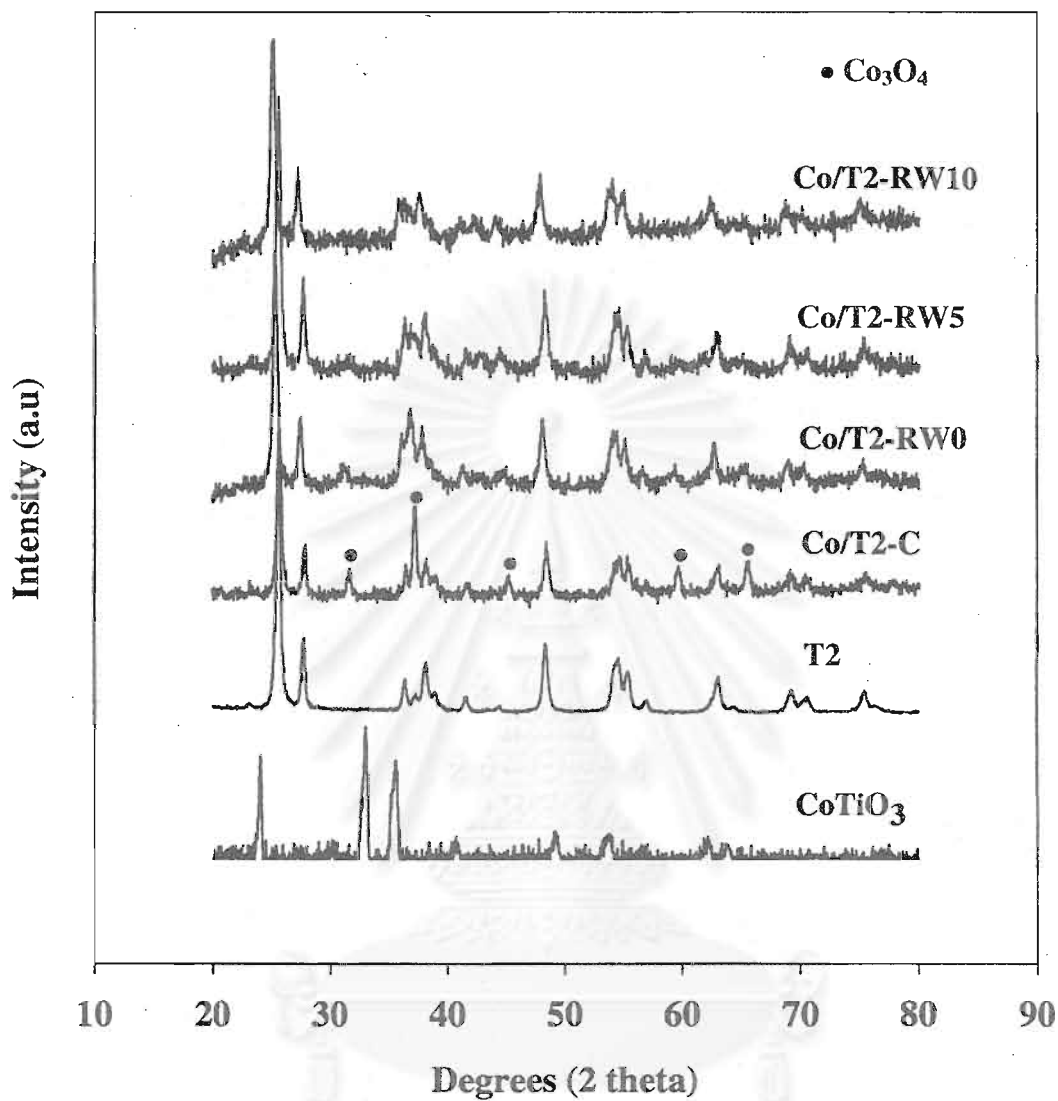
Figure 5.17 XRD patterns of CoTiO$_3$, T2 and the Co/T2 catalysts after various pretreatment conditions.
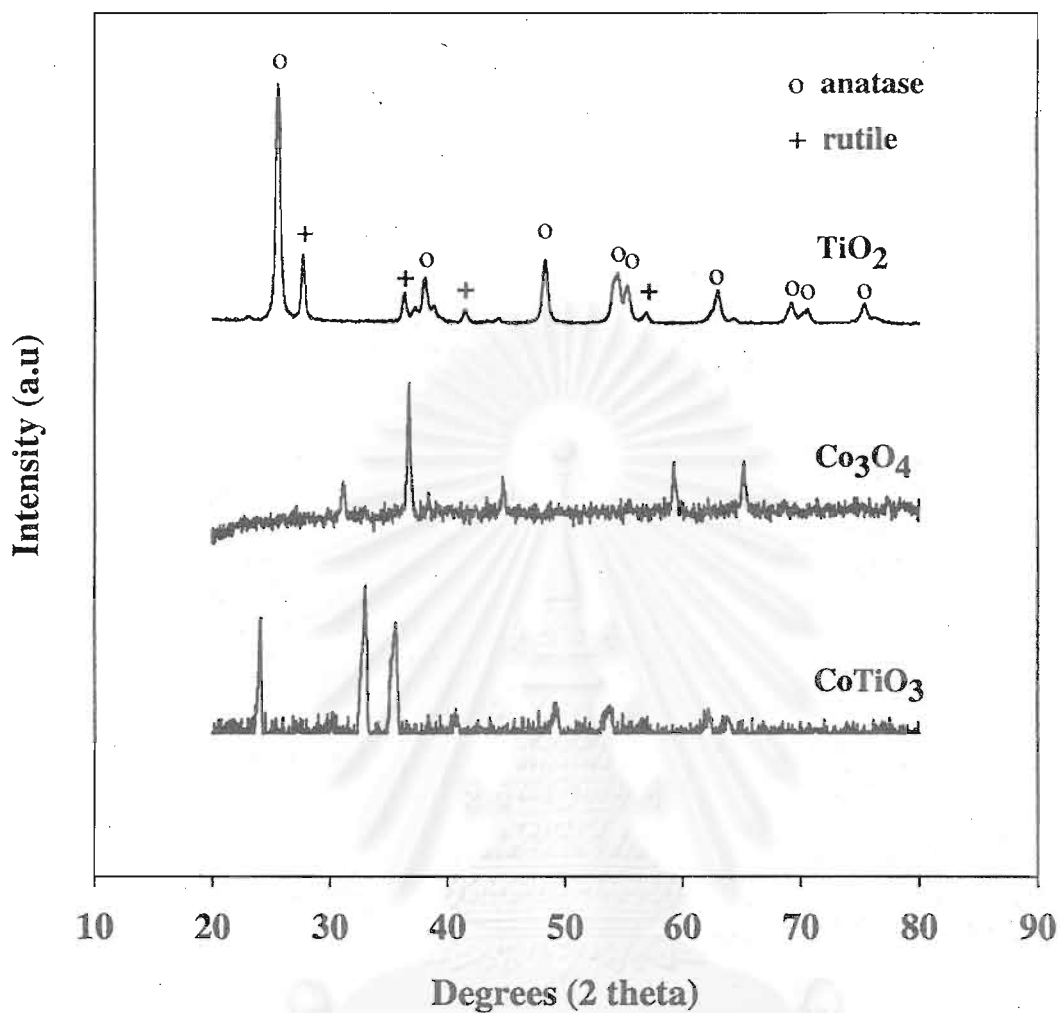
Figure 5.18 Reference XRD spectra of CoTiO₃, Co₃O₄ and titania.
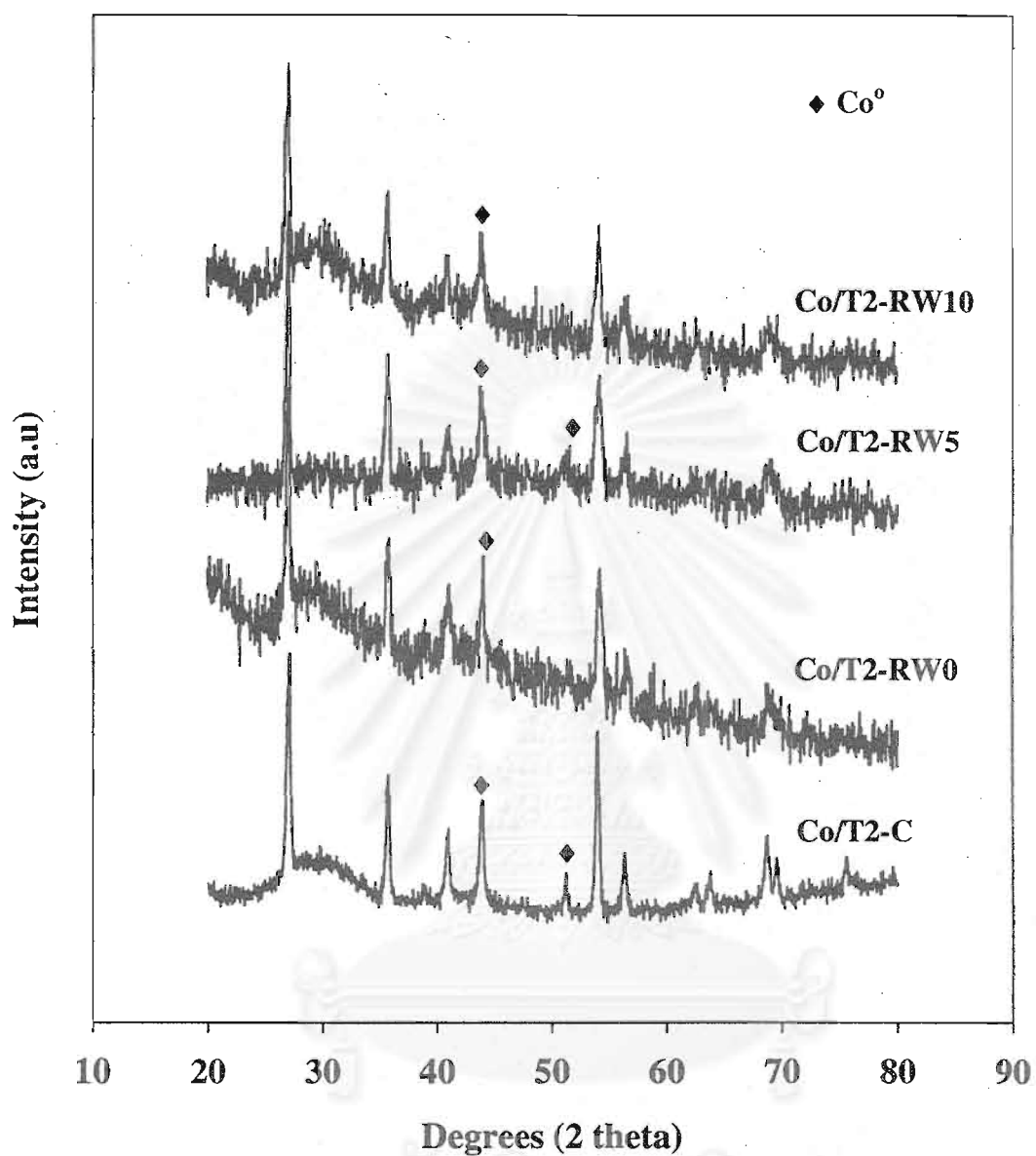
Figure 5.19 XRD patterns of the T2 supported Co catalysts after TPR measurement up to 800°C.

5.1.2.7 Raman spectroscopy

Raman spectra of CoO, Co_3O_4, $CoTiO_3$, T2 and the Co/T2 catalysts reduced at various pretreatments are shown in Figure 5.20. $CoTiO_3$ performed the Raman bands at 695, 604, 455, 382, 336 and 266 cm^{-1} which are similar to the ones reported by Brik et $al.$ (2001). For the T2 support, the strong Raman bands were observed at 640, 514, and 397 cm^{-1} indicating the TiO_2 in its anatase form (Zhang et $al.$ 2001) while Broad Raman bands at .445 cm^{-1} exhibiting the titania in rutile form (Zhang et $al.$ 2001). The Raman spectrum of the calcined sample exhibited Raman bands at 640 and 514 cm^{-1} as seen in those for T2 support including two shoulders at 690 and 480 cm^{-1}, assigned to Co_3O_4 (Jongsomjit et $al.$, 2001, 2002, 2003). Raman spectra of all reduced samples showed the Raman bands of TiO_2 support and the shoulders at 690 and 480 cm^{-1}. These can be assigned to Co_3O_4 present on catalyst surface rather than CoO (detected in the bulk by XRD) since Raman spectroscopy is more of surface technique (Jongsomjit et $al.$, 2002).

Besides the strong signal of TiO_2, the signal of CoO and Co_3O_4 is likely to hinder the observation of surface "Co-titanate" as well. In order to eliminate that interference, Raman spectroscopy were conducted on the reduced samples with a lesser degree of passivation and the Raman spectra of samples are shown in Figure 5.21. It can be observed that the characteristic peaks of the reduced samples were similar to each other, but deviated from the characteristic peaks of Co_3O_4 as seen in Figure 5.20. The Raman band of the reduced samples at 397 cm^{-1} of the TiO_2 became broader. This perhaps resulted from the overlap between the peaks of 397 cm^{-1} of the TiO_2 and 382 cm^{-1} of $CoTiO_3$ due to the formation of surface "Co-titanate".
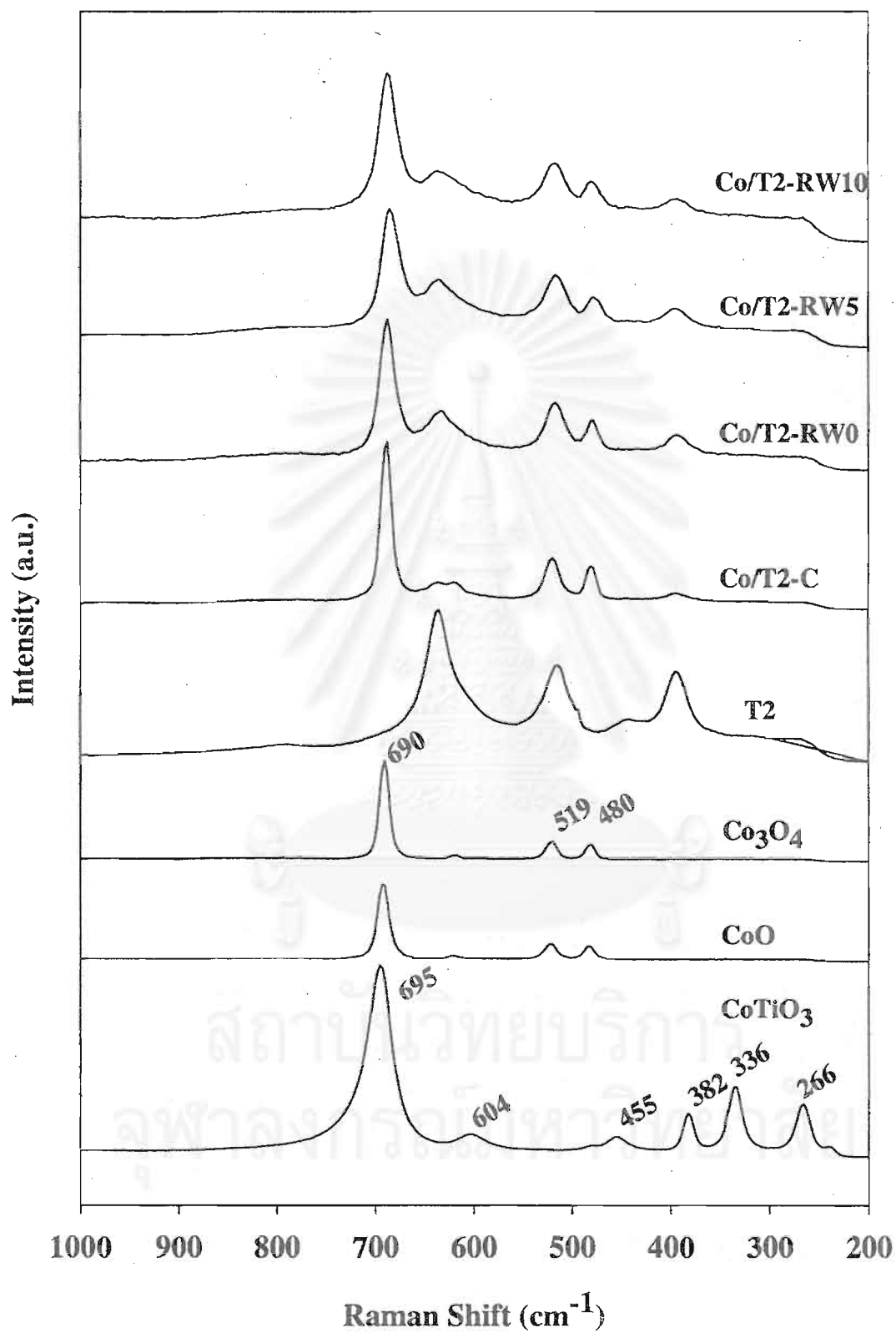
Figure 5.20 Raman spectra of Co_3O_4, CoO, $CoTiO_3$, T2 and the Co/T2 catalysts after various pretreatment conditions.
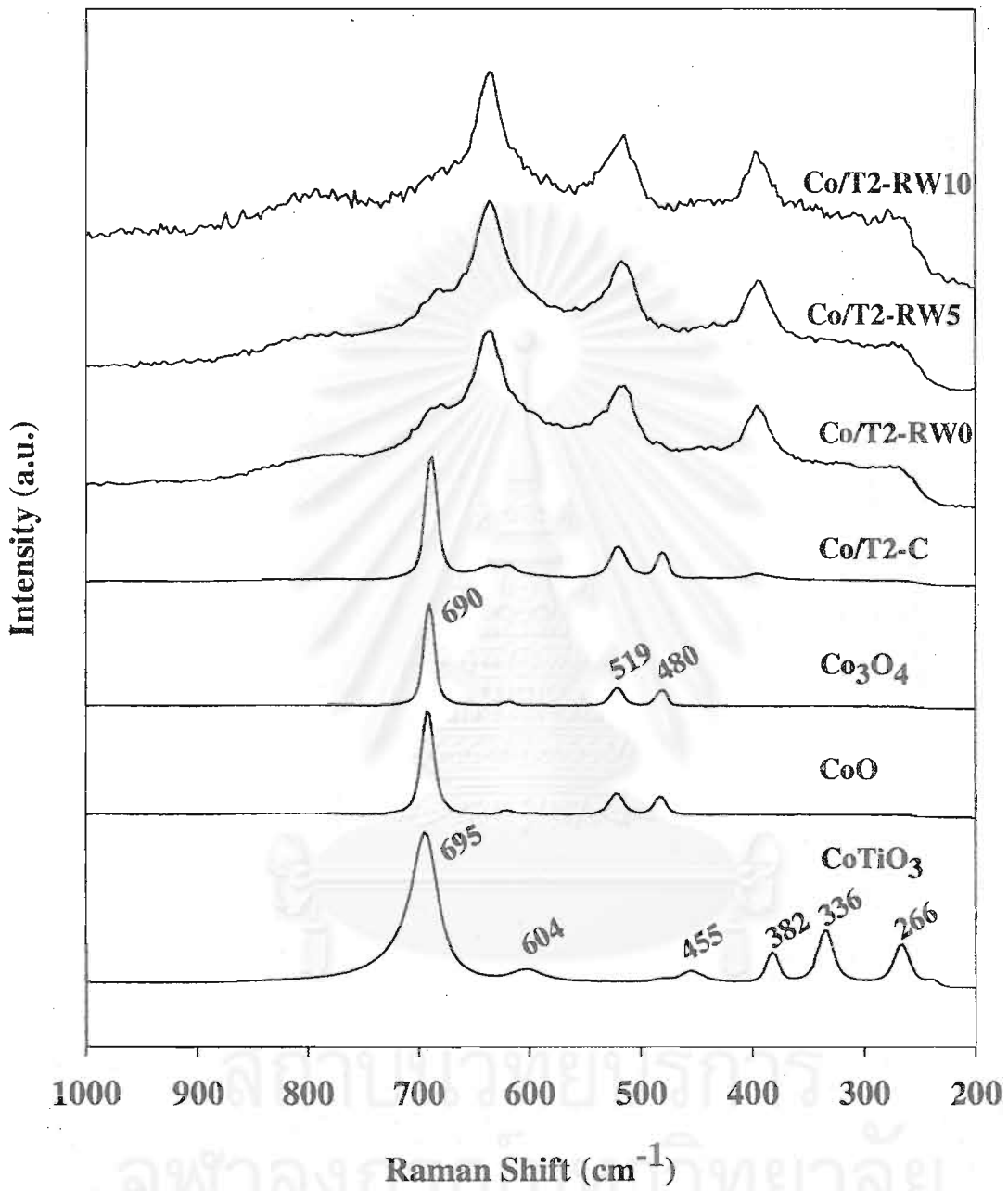
Figure 5.21 Raman spectra of Co_3O_4, CoO, $CoTiO_3$, the calcined sample and the reduced with a lesser degree of passivation samples.

5.1.2.8 Reaction study in CO hydrogenation

The overall activity of the Co/T2 catalyst samples were tested in CO hydrogenation. The results are shown in Table 5.6. It can be perceived that the CO conversion ranged between 67.44 to 60.25% (initial) and 54.94 to 52.56% (steady state). The reaction rate ranged between 0.25 to 0.23 $gCH_2/g_{cat}h^{-1}$ (initial) and 0.21 to 0.19 $gCH_2/g_{cat}h^{-1}$ (steady state). However, there was no any significant difference in selectivity for any of samples based on reaction conditions used in this study.

Table 5.6 Reaction rate for CO hydrogenation on the T2 supported Co catalyst samples reduced at various conditions.

Sample	CO conversion(%)[a]		Rate ($gCH_2/g_{cat}h^{-1}$)[b]		CH_4 selectivity(%)	
	Initial[c]	SS[d]	Initial	SS	Initial	SS
Co/T2-C	67.44	54.94	0.25	0.21	94	96
Co/T2-RW0	60.77	53.12	0.23	0.20	94	94
Co/T2-RW5	60.56	52.80	0.23	0.20	98	98
Co/T2-RW10	60.25	52.56	0.23	0.19	95	96

[a] CO hydrogenation was carried out at 220°C, 1 atm, and $H_2/CO/Ar = 20/2/8$ cc/min.

[b] Error ±5%

[c] After 5 min of reaction

[d] After 5 h of reaction

5.1.3 Effect of Ru promotion

5.1.3.1 Atomic absorption spectroscopy (AAS)

The final Co loading of the catalyst samples were determined using atomic absorption spectroscopy (AAS). The amount of Co in T2-supported CoRu catalysts are shown in Table 5.7. The CoRu/T2 catalysts after various pretreatments have 15.1 wt% Co.

5.1.3.2 BET surface area

BET surface areas, pore volumes and average pore diameters of titania support, T2, and the catalyst samples after various pretreatment conditions are also shown in Table 5.7. The BET surface areas of the T2 support were determined to be 49 m^2/g. While the CoRu/T2 catalyst samples had BET surface areas less than the T2 support. The BET surface areas of the CoRu/T2 catalysts after different pretreatment conditions ranged between 30-34 m^2/g. There was no significant change in surface areas after the various pretreatments within experimental errors.

Table 5.7 Content of Co from AAS and BET surface area measurement of T2-supported CoRu catalysts.

Catalyst samples	Co (wt %)[a]	BET surface area (m^2/g)[b]	Pore volume (cm^3/g)[b]	Average pore diameter (Å)[b]
T2	-	49[c]	-	-
CoRu/T2-C	15.1	37	0.17	182.4
CoRu/T2-RW0	15.1	37[c]	-	-
CoRu/T2-RW5	15.1	37[c]	-	-
CoRu/T2-RW10	15.1	36[c]	-	-

[a] Measurement error is ± 2%.

[b] Measurement error is ± 5%.

[c] From single point measurement.

5.1.3.3 Temperature programmed reduction (TPR)

The results of TPR at temperature 35-800°C of the Ru-promoted Co/T2 catalyst samples at various conditions are shown in Table 5.8. When water vapor was added during standard reduction resulting in a decrease in reducibility which also indicated in Table 5.8. The reducibilities of the CoRu/T2 catalyst samples were ranged from 75 to 87% upon the partial pressure of water vapor increased during reduction.

The suggested conceptual diagram of reducibility loss during standard reduction of the CoRu/T2 is exhibited in Figure 5.22. First, the reducibility of the fresh calcined catalyst sample was 78%. When it was reduced with added water vapor (0, 5 and 10 vol%) during reduction then recalcined it back to the oxide form prior to performing TPR. It can be noticed that the reducibilities were decreased. The reducibilities loss during reduction were ranged in 4-12%.

In addition, TPR was also explained information on the reduction behaviors of the catalyst samples pretreated under various conditions. TPR profiles of bulk Co_3O_4 and the CoRu/T2 catalyst samples after various pretreatment conditions are illustrated in Figure 5.22. It found that bulk Co_3O_4 and all the CoRu/T2 samples after various pretreatment conditions indicated only one strong reduction peak. This peak can be assigned to the stepwised reduction of Ru_2O_3 and Co_3O_4 (Jongsomjit *et al.*, 2001; Panpranot *et al.*, 2002).

For the calcined sample (CoRu/T2-C), there was only one reduction peak located at ca. 285-580°C (max. at 435°C) while the all reduced samples were also similar exhibiting only one reduction peak as shown in Figure 5.23. When the more of water vapor was added, TPR peak located at ca. 325-585°C (max. at 455°C) for CoRu/T2-RW0 sample was not shifted when the amount of water vapor increased.

5.1.3.4 H₂ chemisorption

The results of H_2 chemisorption for CoRu/T2 catalysts after different pretreatments are given in Table 5.8. Furthermore, the overall Co metal dispersion in the catalyst samples are also shown. The result indicated that the overall dispersion of the samples decreases with increasing amount of water vapor during reduction. The overall dispersion of the CoRu/T2 catalysts ranged between 0.40 and 0.58% upon the more amount of water vapor added.

Table 5.8 TPR and H_2 chemisorption results for the T2-supported CoRu catalyst samples after various pretreatments.

Catalyst samples	Reduction gas mixture (P_{H2}/P_{H2O})	Reducibility (%) during TPR at 35-800°C[a,b]	Total H_2 chemisorption (μmol H_2/g_{cat})[c]	Overall Co metal dispersion (%)
CoRu/T2-C	-	87	7.47	0.58
CoRu/T2-RW0	1/0	83	6.69	0.52
CoRu/T2-RW5	0.95/0.05	77	5.86	0.46
CoRu/T2-RW10	0.90/0.10	75	5.16	0.40

[a] The reduced samples were recalcined at the original calcination conditions prior to performing TPR.

[b] Measurement error is ± 5%.

[c] Error = ± 5% of measurement of H_2 chemisorption.

Sample

Reducibility

TPR

CoRu/T2-C $\longrightarrow$ ❖❖❖❖❖❖❖❖❖❖ 87%

Reduction with P_{H2}/P_{H2O} = i) [1/0]; ii) [0.95/0.05]; iii) [0.90/0.10]

i) **CoRu/T2-(RW0)**   ▨ 4% loss

ii) **CoRu/T2-(RW5)**   ▨ 10% loss

iii)**CoRu/T2-(RW10)**   ▨ 12% loss

i) **CoRu/T2-(RW0)-C** ⎫
                        ⎪ TPR
ii) **CoRu/T2-(RW5)-C** ⎬ $\longrightarrow$
                        ⎪
iii)**CoRu/T2-(RW10)-C** ⎭

❖❖❖❖❖❖❖❖❖❖ 83%

❖❖❖❖❖❖❖❖ 77%

❖❖❖❖❖❖❖❖ 75%

▨ **Reducibility gain during TPR**

▨ **Reducibility loss during reduction***
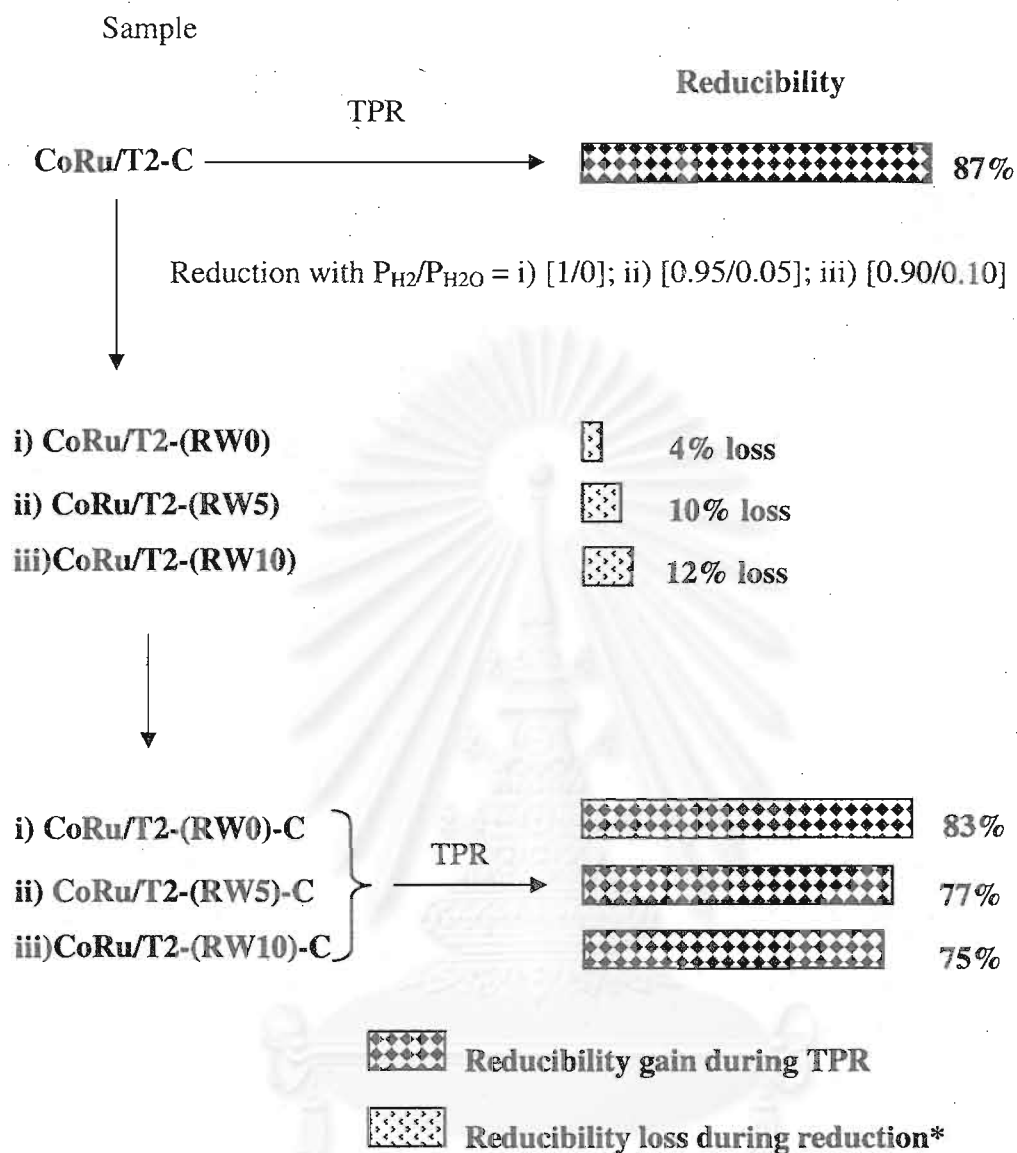
* The difference in reducibility gain from a fresh calcined sample and the
reducibility gain from a reduced and recalcined sample.

Figure 5.22 Suggested conceptual diagram for the reducibility loss during reduction
process of T2-supported CoRu catalysts.
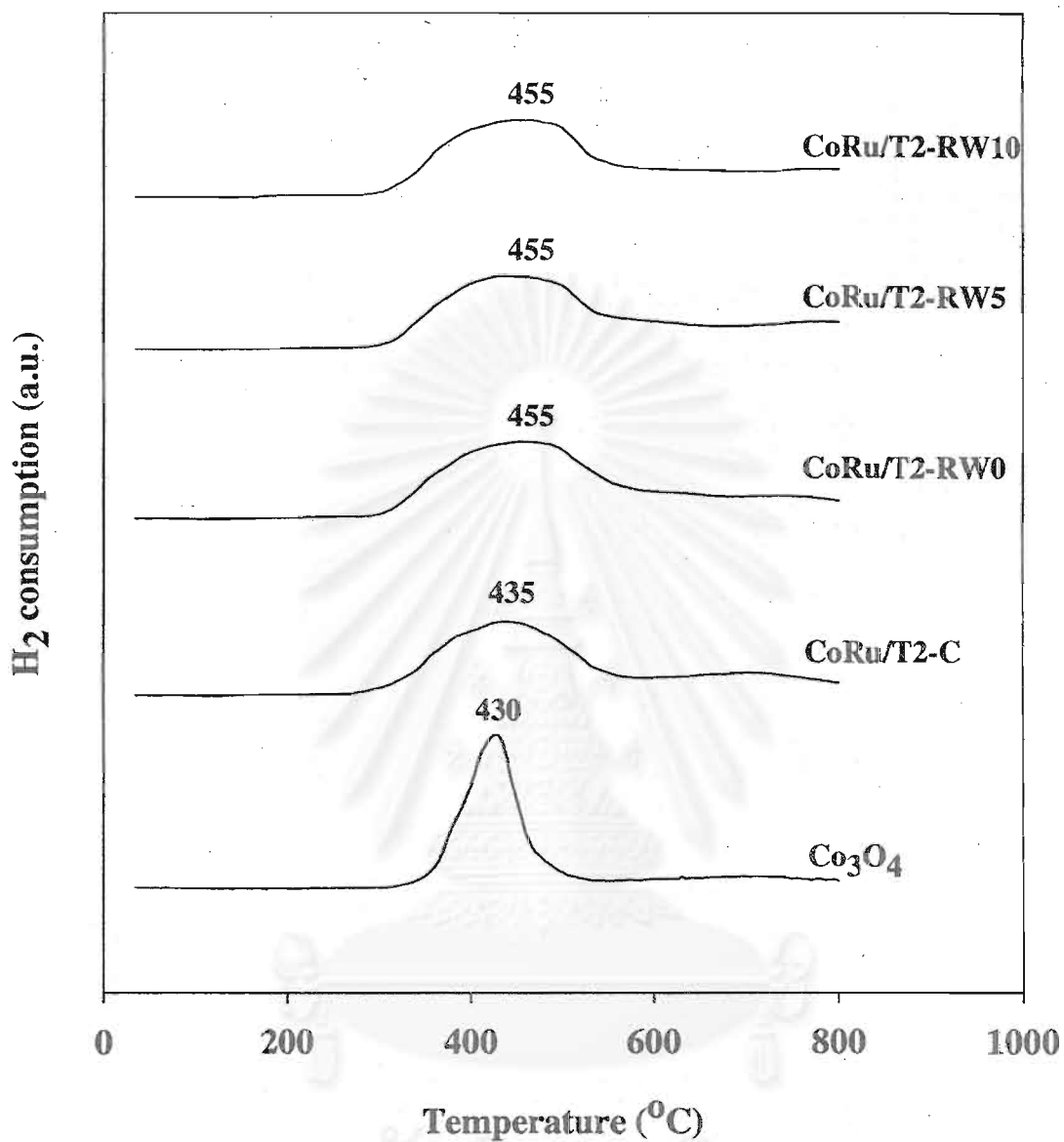
Figure 5.23 TPR profiles of bulk Co_3O_4 and the CoRu/T2 catalysts after various pretreatment conditions.

5.1.3.5 Electron microscopy

SEM and EDX were used to determine the catalyst granule morphology and elemental distribution of the catalyst particles, consecutively. The typical morphology in an external area of catalyst granules with different magnification for CoRu/T2-C and CoRu/T2-RW10 are illustrated in Figure 5.24 and Figure 5.25. It can be perceived that cobalt patches (white spots) were well distributed all over the external surface of catalyst granules. The elemental distributions can be clearly seen by EDX. Figure 5.26 and Figure 5.27 show the typical elemental distribution for a cross section of a granule of CoRu/T2-C and CoRu/T2-RW5, respectively. The distribution of cobalt was well dispersed throughout the catalyst granule as also seen by SEM.
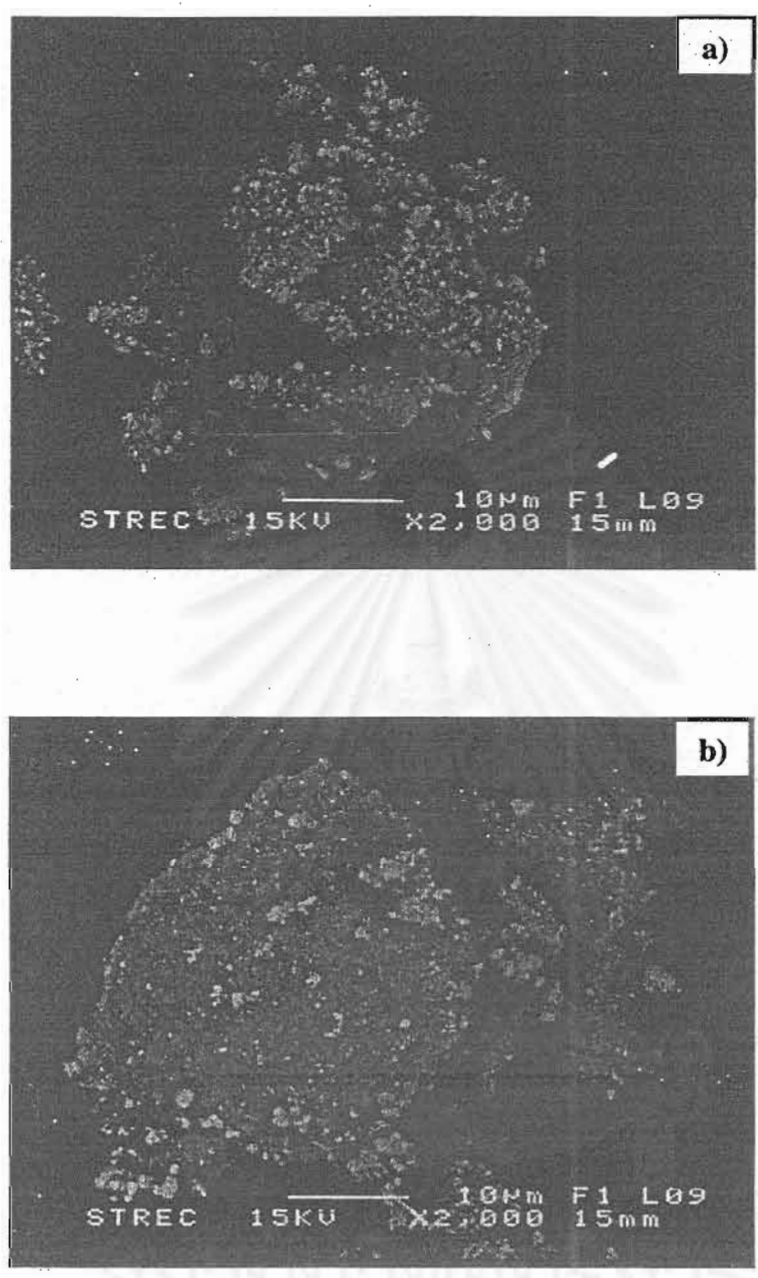
Figure 5.24 SEM micrographs of catalyst granule at the external surface at 2000x magnification; a) CoRu/T2-C, and b) CoRu/T2-RW10.
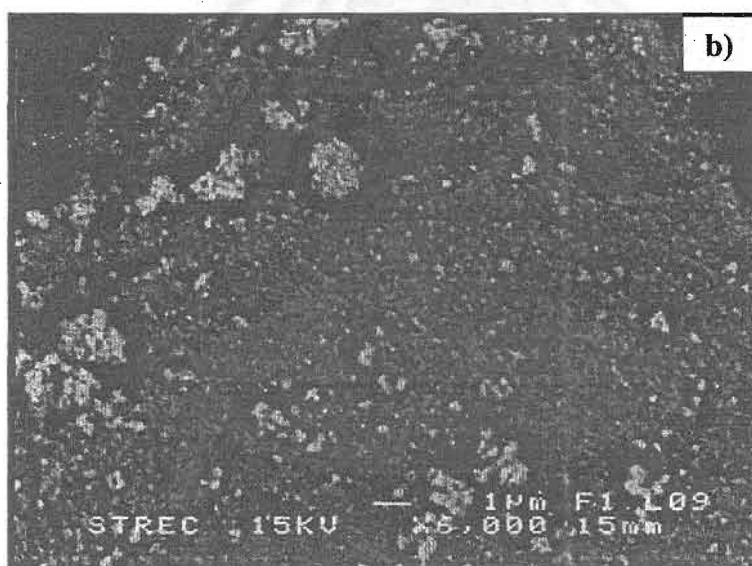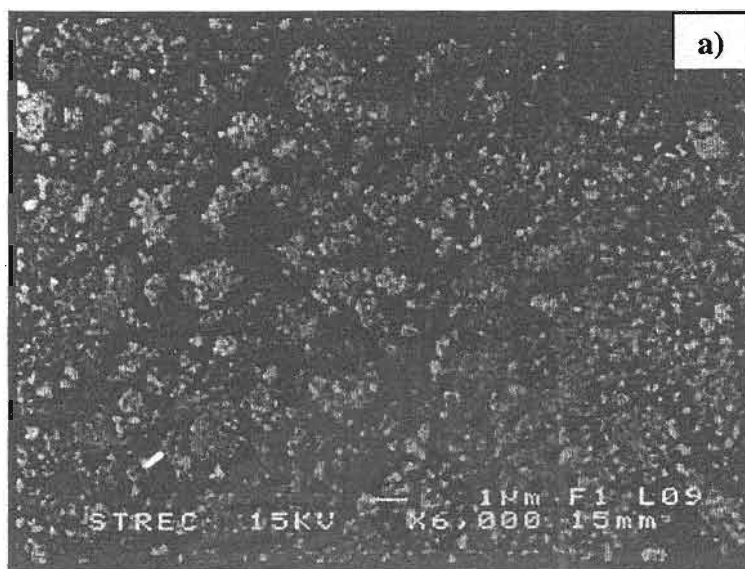
Figure 5.25 SEM micrographs of catalyst granule at the external surface at 6000x
magnification; a) CoRu/T2-**C**, and b) CoRu/T2-**RW**10.
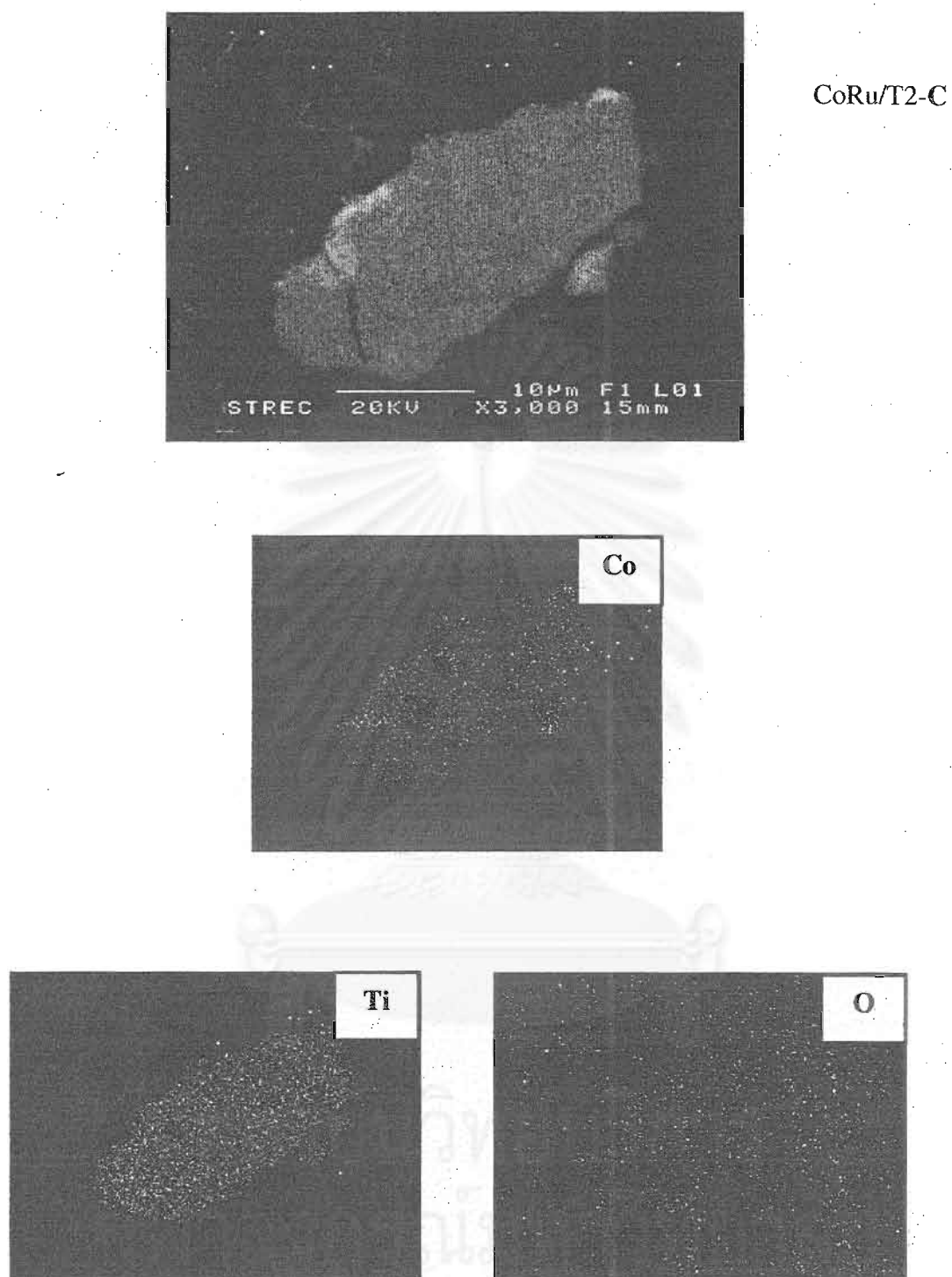
CoRu/T2-C

Figure 5.26 SEM micrograph and EDX mapping of CoRu/T2-C catalyst granule (cross section).
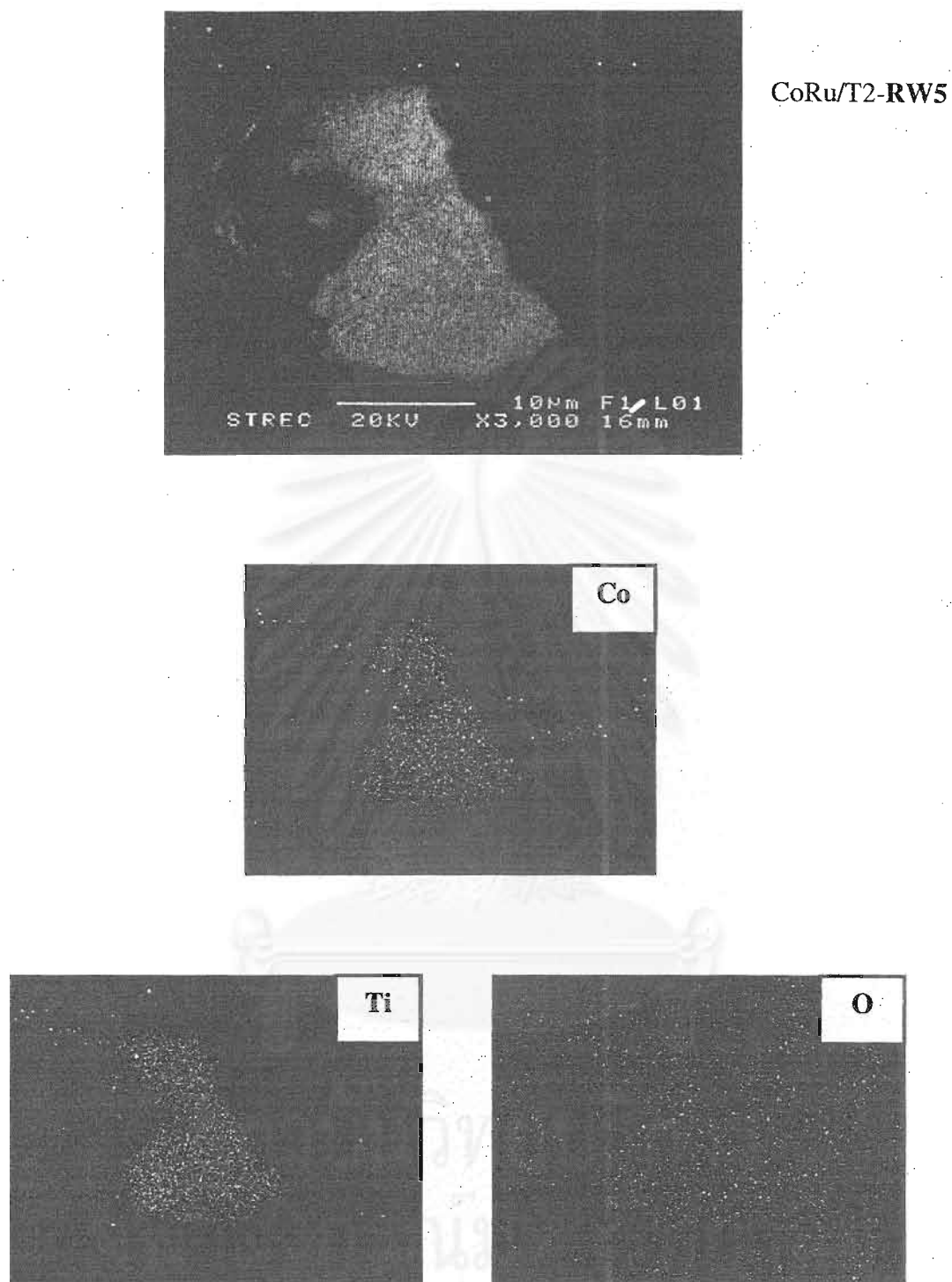
CoRu/T2-**RW5**

Figure 5.27 SEM micrograph and EDX mapping of CoRu/T2-**RW5** catalyst granule (cross section).

5.1.3.6 X-ray diffraction (XRD)

XRD patterns of the Ru-promoted Co/T2-supported catalysts after various pretreatment conditions are shown in Figure 5.28. XRD patterns of the T2-supported CoRu catalysts showed diffraction peaks at 26°, 37°, 48°, 55°, 56°, 62°, 69°, 71° and 75° indicating the TiO_2 in the anatase form and the diffraction peaks at 27°, 36°, 42° and 57° explaining the TiO_2 in the rutile form. After calcination, the diffraction peaks of Co_3O_4 at 36°, 46°, and 65° can be observed. After reduction at various conditions and passivation, the diffraction peaks of CoO were present at 37° and 63°.

XRD patterns of the T2-supported CoRu catalysts samples after TPR measurement up to 800°C are shown in Figure 5.29. The similar trend as shown in Figure 5.28 was found except for the observation of cobalt metal peaks at 44° and 52° due to sintering.
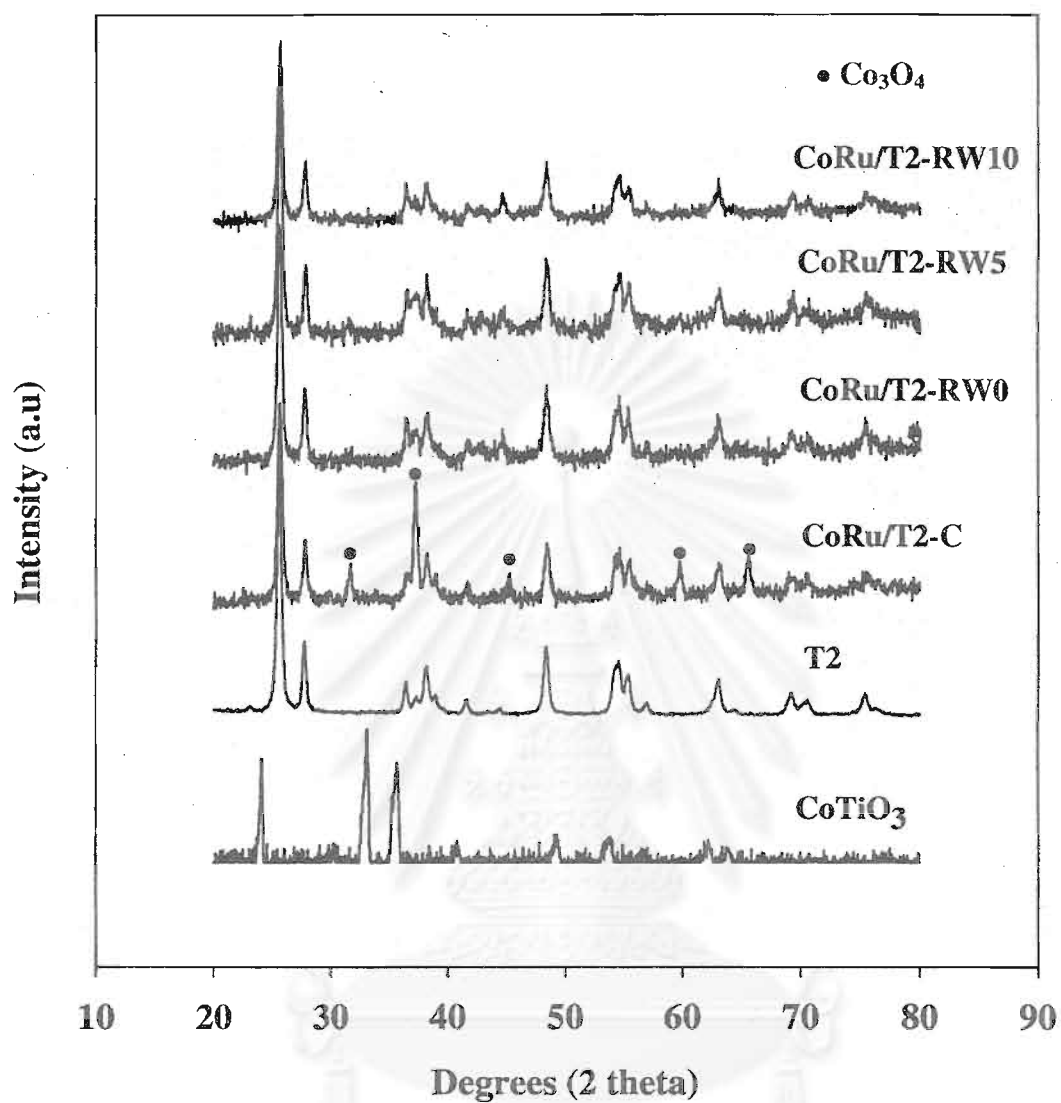
Figure 5.28 XRD patterns of the T2-supported CoRu catalysts after various pretreatment conditions.
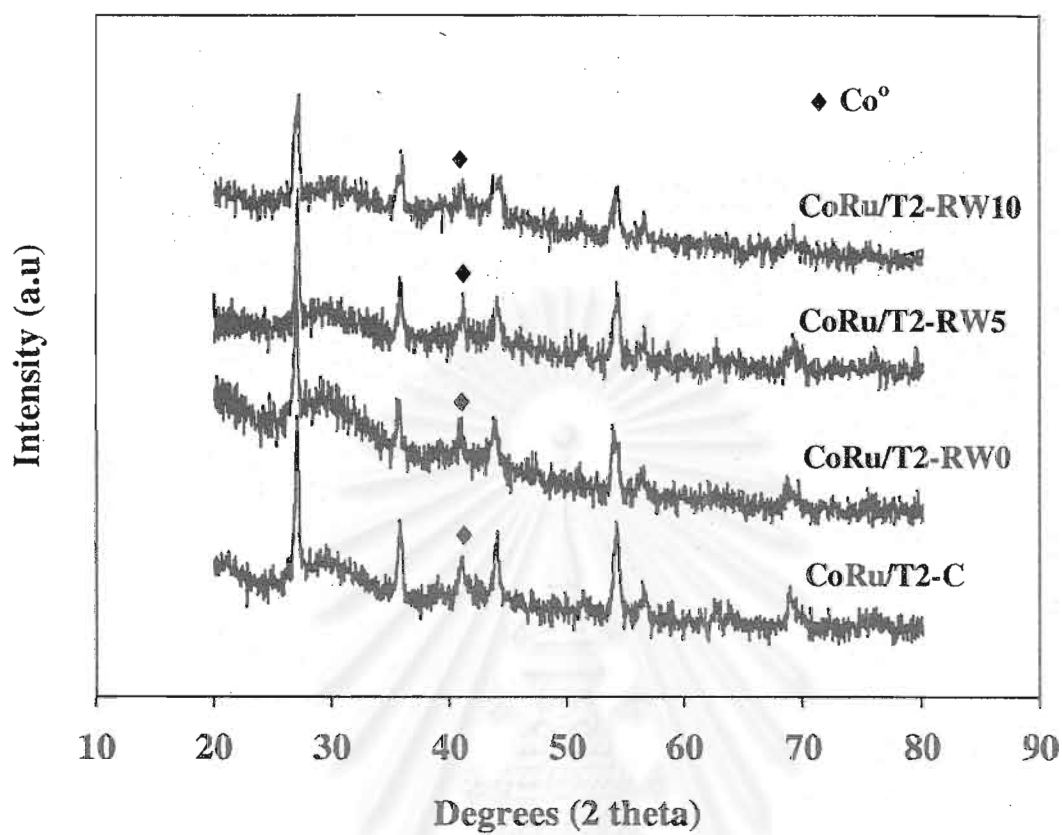
Figure 5.29 XRD patterns of the CoRu/T2 catalysts after TPR measurement up to 800°C.

5.1.3.7 Raman spectroscopy

Raman spectra of the T2-supported CoRu catalysts after various pretreatments are shown in Figure 5.30. For the T1- and T2-supported CoRu catalysts, Raman bands at 640, 514, and 397 cm^{-1} exhibited the TiO_2 in its anatase form (Brik *et al.*, 2002) but the CoRu/T2 catalysts also showed broad Raman bands at .445 cm^{-1} exhibiting the titania in rutile form (Zhang *et al.*, 2001). Both of the CoRu/T1 and CoRu/T2 calcined samples indicated Raman bands at 690 and 480 cm^{-1}, assigned to Co_3O_4 (Jongsomjit *et al.*, 2001, 2002, 2003). Raman spectra of all reduced samples showed the Raman bands of TiO_2 support and the shoulders at 690 and 480 cm^{-1}. These can be assigned to Co_3O_4 present on catalyst surface rather than CoO (detected in the bulk by XRD) since Raman spectroscopy is more of surface technique (Jongsomjit *et al.*, 2002).
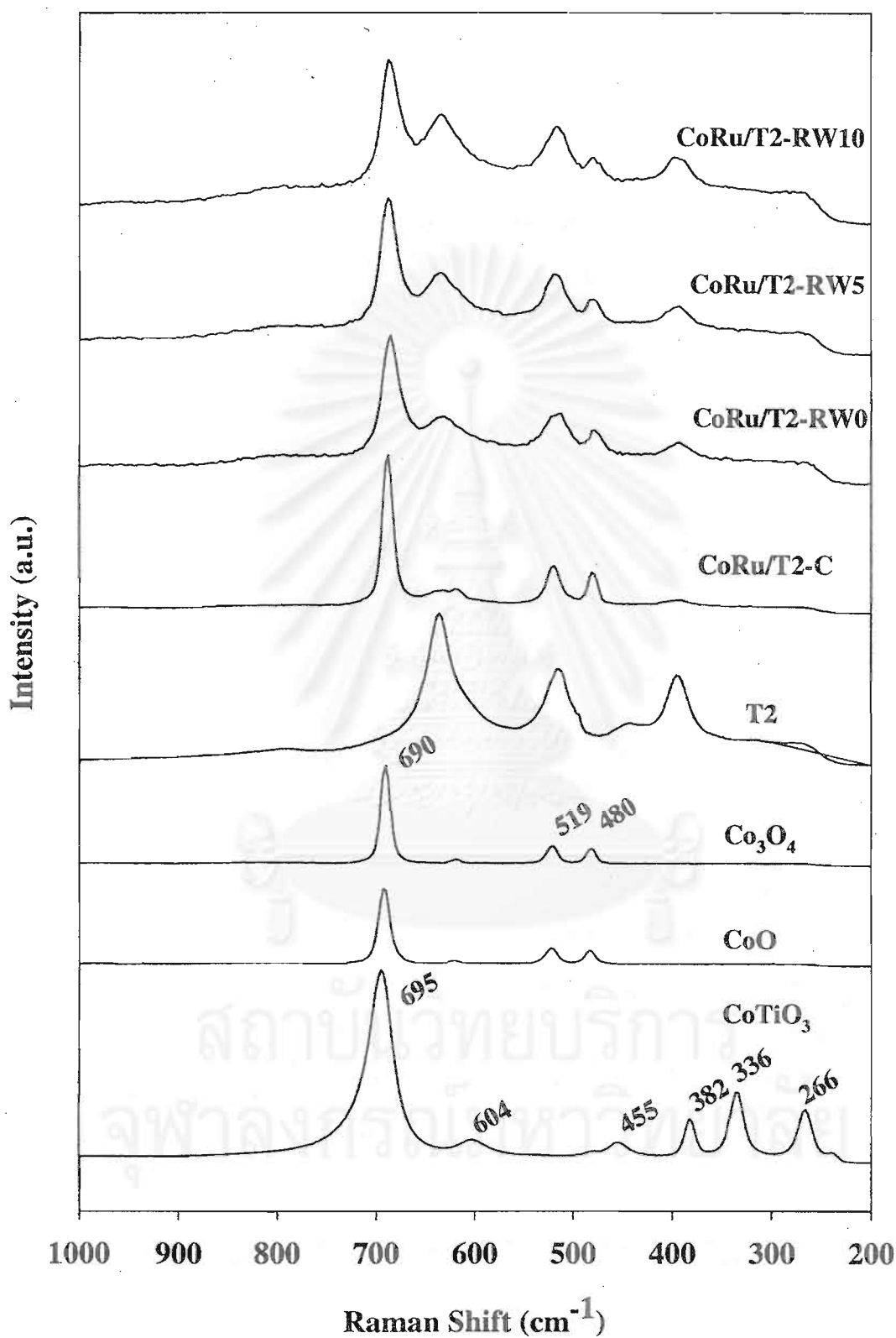
Figure 5.30 Raman spectra of Co_3O_4, CoO, $CoTiO_3$, and the T2-supported CoRu catalysts after various pretreatment conditions.

5.1.3.8 Reaction study in CO hydrogenation

The CoRu/T2 catalyst samples were tested in the CO hydrogenation system to determine the overall activity. The results are shown in Table 5.9. It indicated that the CO conversion ranged between 98.89 to 95.98% (initial) and 97.23 to 92.73% (steady state). The reaction rate ranged between 0.37 to 0.36 $gCH_2/g_{cat}h^{-1}$ (initial) and 0.36 to 0.34 $gCH_2/g_{cat}h^{-1}$ (steady state). However, there was no any significant difference in selectivity for any of samples based on reaction conditions used in this study.

Table 5.9 Reaction rate for CO hydrogenation on the T2-supported CoRu catalyst samples reduced at various conditions.

Sample	CO conversion(%)[a]		Rate ($gCH_2/g_{cat}h^{-1}$)[b]		CH$_4$ selectivity(%)	
	Initial[c]	SS[d]	Initial	SS	Initial	SS
CoRu/T2-C	98.89	97.23	0.37	0.36	99	98
CoRu/T2-RW0	97.32	96.62	0.36	0.36	98	98
CoRu/T2-RW5	96.21	93.86	0.36	0.35	97	97
CoRu/T2-RW10	95.98	92.73	0.36	0.34	99	99

[a] CO hydrogenation was carried out at 220°C, 1 atm, and $H_2/CO/Ar = 20/2/8$ cc/min.

[b] Error ±5%

[c] After 5 min of reaction

[d] After 5 h of reaction

5.2 Discussion

The first portion of this thesis focused on investigation of the Co-support compound formation (Co-SCF) in titania-supported cobalt catalysts. The titania support used in this study was in the form of pure anatase (T1) phase only. The discussion of this part is shown in section 5.2.1.

A comparative study of different phase of titania supports on activity and selectivity during CO hydrogenation of Co/TiO_2 catalysts was the focus of second portion of this thesis. After the nature of Co-SCF in titania-supported (pure anatase) Co catalyst was identified, the extensive study of how differences in titania support phases can affect the catalyst performance was investigated. By a comparative of titania supports used between the pure anatase phase (T1) and mixed phase; anatase and rutile (T2), the discussion based on the results was made in section 5.2.2.

An effort of the last portion of this thesis was to determine effects of ruthenium (Ru) promotion on such a compound formed. Based on the results obtained, the discussion was made in section 5.2.3.

All discussion are as follows:

5.2.1 Co-SCF in T1-supported Co catalysts

The overall activity of the Co/T1 catalysts were decreased depending on the partial pressure of the water vapor added during standard reduction. It was related to the results of TPR. It can be observed that Co-SCF in Co/T1 essentially occurred during standard reduction resulting in lower reducibilities of the reduced samples during TPR at temperatures 35-800°C. The reducibilities ranged between 64 and 92% upon the addition of water vapor. It should be noted that the loss in the degree of reduction was attributed to the compound formation of cobalt and the titania support. The loss of reducibilities during reduction were ranged 22 to 28% indicating the non-reducible (at temperatures < 800°C) "Co-titanate" compound formed. It should be mentioned that a decrease in the degree of reduction of reduced samples slightly changed upon increasing the partial pressures of water vapor during the reduction

process. In the reviews, Zhang *et al.* (1999) investigated the reducibilities of CoRu/γ-Al_2O_3 during standard reduction and TPR in the present of added water vapor. They reported that water has a significant effect on the reduction behavior of CoRu/γ-Al_2O_3. It was suggested that water vapor present during reduction leads to a decrease in the degree of reduction of the cobalt perhaps in two ways: (i) inhibition of the reduction of well-dispersed CoO interacting with the alumina support, possibly by increasing the cobalt-alumina interaction, and (ii) facilitation of the migration of cobalt ions into probable tetrahedral sites of γ-Al_2O_3 to form a non-reducible (at temperatures < 900°C) spinel. However, considering the Co-SCF in Co/TiO_2, the effect of water vapor added during standard reduction was essentially less pronounced compared to that on the alumina support. The only slight effect of water vapor on Co-SCF in Co/TiO_2 is also listed in Table 5.2 indicating that the reducibilities of the reduced samples only slightly decreased within experimental error when water vapor (5-10 vol%) was added during standard reduction.

The bulk of Co_3O_4 and all of the Co/T1 catalyst samples were showed only one strong reduction peak. This can be assigned to the overlap of two-step reduction of Co_3O_4 to CoO and then Co^o (Kraum and Baern, 1999; Jongsomjit *et al.*, 2001; Voβ *et al.*, 2003). The bulk Co_3O_4 indicated the maximum temperature of peak at ca. 430°C. The calcined sample, Co/T1-C showed only one reduction peak maximum at 520°C explained that no residual cobalt nitrates remain on the calcined sample of Co/TiO_2 upon the calcination condition used in this study. In some cases, the peak of the decomposition of cobalt nitrates during TPR of supported cobalt catalysts can be observed at temperatures between 200-300°C, especially with silica and alumina supports (Kogelbauer *et al.*, 1996; Hilmen *et al.*, 1996; Jongsomjit *et al.*, 2001, 2002, 2003). However, prolonged calcination or reduction and recalcination results in complete decomposition of any cobalt nitrates present (Kogelbauer *et al.*, 1996). Moreover, the reduced Co/T1 catalysts were also similar exhibiting only one reduction peak which located maximum temperature at 520°C for Co/T1-RW0 sample was slightly shifted about 10-20°C higher when the increase of partial pressure of water vapor during reduction indicating slightly stronger interaction between cobalt and titania.

The much stronger interaction between cobalt and the supports such as silica and alumina can be usually observed leading to an observation of two separated peaks during TPR of the reduced and recalcined samples (Kogelbauer *et al.*, 1995; Kogelbauer *et al.*, 1996; Jongsomjit *et al.*, 2001, 2002, 2003). The higher temperature reduction peak can be assigned to the reduction of cobalt strongly interacting with the supports, i.e. $Co_XO_Y-Al_2O_3$ and $Co_XO_Y-SiO_2$, which cannot be observed in the reduced and recalcined Co/TiO_2 catalyst. Based on the TPR results, it should be noted that a degree of reduction of the reduced Co/TiO_2 catalyst was found to decrease during standard reduction due to "Co-titanate" formed. However, the reduction behaviors of samples reduced in various conditions were similar upon the TPR measurement conditions used in this study. This can be concluded that "Co-titanate" formed in a Co/TiO_2 catalyst resulted in only a decrease in the reducibility without changing the reduction behaviors of it. The effect of partial pressures of water vapor during reduction on the formation of "Co-titanate" seemed to be less pronounced.

The results of H_2 chemisorption can be confirmed that Co-SCF was occurred in the Co/T1 catalyst. It was explained the Co metal dispersion of the catalyst sample decreased with increasing amount of water vapor during reduction. This may be related to the loss of reducibilities, as seen by TPR.

Several characterization techniques were also used to identify the characteristics of "Co-titanate" formed during reduction. From the BET surface area results, the decrease in surface area, pore volume and average pore diameters of the titania support as 17.8 wt% Co loading suggested that Co particles were deposited in the pores of the TiO_2 which can confirm by EDX mapping. Furthermore, the BET surface area, pore volume and average pore diameters of the Co/T1 catalyst samples did not change significantly after various pretreatments. This indicated that "Co-titanate" formed did not cause any change in surface areas of the catalysts. The morphologies and elemental distribution were basically not significant change upon the formation of "Co-titanate".

The bulk crystalline phases of samples were determined using XRD. To identify the XRD peaks of samples, XRD peaks of $CoTiO_3$ were collected. Kraum *et*

al. (1999) reported the observation for XRD peaks of $CoTiO_3$ phase along with Co_3O_4 on the calcined Co/TiO_2 catalyst using cobalt (III) acetyl acetonate as a precursor for cobalt. They suggested that the formation of $CoTiO_3$ by the use of cobalt (III) acetyl acetonate as a precursor can be attributed to the migration of cobalt ions into the support lattice, with the consecutive formation of titanate. However, based on differences in the cobalt precursor, the amounts of cobalt loading and the calcination condition used in the present study, the formation of $CoTiO_3$ was not observed in the calcined Co/TiO_2 catalyst. After reduction at various conditions and passivation, it can perceive the diffraction peaks of CoO. This indicated that Co_3O_4 in the calcined samples was reduced to highly dispersed cobalt metal and CoO during standard reduction at $350^{\circ}C$. Any Co_3O_4 formed during passivation was present in only very thin surface layers and was consequently XRD invisible. This indicated that XRD results revealed that the "Co-titanate" formed was in a highly dispersed form, thus, it is invisible in XRD after either standard reduction or TPR.

Raman spectroscopy was performed the compound formation between Co and the TiO_2 support occurring reduction. The calcined sample exhibited Raman bands at 640, 514, and 397 cm^{-1} as seen in those for TiO_2 including two shoulders at 690 and 480 cm^{-1}, assigned to Co_3O_4 (Jongsomjit *et al.*, 2001, 2002, 2003). Raman spectra of all reduced samples showed the Raman bands of TiO_2 support and the shoulders at 690 and 480 cm^{-1}. These can be assigned to Co_3O_4 present on catalyst surface rather than CoO (detected in the bulk by XRD) since Raman spectroscopy is more of surface technique (Jongsomjit *et al.*, 2002). This can be suggested that "Co-titanate" form during reduction was different from $CoTiO_3$ and invisible in Raman spectroscopy. The invisible of "Co-titanate" bands was probably caused by (i) its highly dispersed form and (ii) the Raman signals were hindered due to the highly strong Raman intensities of TiO_2 support.

It was reported that reduced samples of $Co/\gamma-Al_2O_3$ at high partial pressure of water vapor during reduction exhibited the broad Raman bands between 400-700 cm^{-1} (Jongsomjit *et al.*, 2001). This was suggested that these broad Raman bands represent a surface cobalt compound related to cobalt strongly interacting with the alumina support as a "Co-aluminate". The identified "Co-alumiante" was

suggested to be different from $CoAl_2O_4$ (spinel) due to being a non-stoichiometric surface "Co-aluminate" compound. This highly dispersed "Co-aluminate" may be formed, possibly by cobalt migration into the alumina matrix and was detectable using Raman spectroscopy, but not XRD. In addition, the alumina support itself does not exhibit any of Raman bands between 100-1000 cm^{-1}, thus, the Raman bands of "Co-aluminate" can be clearly detected. However, in the present study, the highly strong Raman intensities of the titania support may result in a hindrance of the Raman bands, if present, of the highly dispersed "Co-titanate" formed. Besides the strong signal of TiO_2, the signal of CoO and Co_3O_4 is likely to hinder the observation of surface "Co-titanate" as well. In order to eliminate that interference, the reduced samples were also conducted Raman spectroscopy with a lesser degree of passivation and the Raman spectra of samples are shown in Figure 5.10. It can be observed that the characteristic peaks of the reduced samples were similar to each other, but deviated from the characteristic peaks of Co_3O_4 as seen in Figure 5.9. The Raman band of the reduced samples at 397 cm^{-1} of the TiO_2 became broader. This perhaps resulted from the overlap between the peaks of 397 cm^{-1} of the TiO_2 and 382 cm^{-1} of $CoTiO_3$ due to the formation of surface "Co-titanate". However, to elucidate all kinds of hindrances, rigorous surface techniques may be needed for further investigation. Nevertheless, Raman spectroscopy revealed that the "Co-titanate" formed was different from $CoTiO_3$ probably due to its also being nonstoichiometric (cobalt deficiency) surface "Co-titanate" compound.

5.2.2 A comparative study of different phases of TiO_2 used

In this section, the main focus was to compare the results of Co catalysts in the T1 (pure anatase) and T2 (anatase mixed rutile phase; anatase 82%, rutile 18%) supports.

In general, characteristics results of Co/T2 catalysts reduced at different conditions, exhibited similar trends compared to those of Co/T1 catalysts. For example, the reducibilities of the Co/T2 catalyst samples decreased when water vapor was added during standard reduction indicating the presence of Co-SCF in Co/T2 catalysts. No significant changes in surface area, morphologies and elemental distribution were observed. XRD revealed that the "Co-titanate" is in a highly

dispersed form thus, it cannot be detected by XRD. Raman spectroscopy indicated that the "Co-titanate" formed was different from $CoTiO_3$ probably due to it also being nonstoichiometric (cobalt deficiency) surface "Co-titanate" compound.

However, the most significant discovery of this study was overall activities during CO hydrogenation increased for Co/T2 due to two reasons. First, TPR profile of Co/T2 catalysts performed reduction peak which located lower temperature at ca. 315-640°C (max at 510°C) for the calcined sample, Co/T2-C. All reduced samples indicated TPR peak located at ca. 330-640°C (max at 510°C) which were not shifted when the more amount of water vapor added during reduction. Secondly, the loss of reducibilities during TPR for Co/T2 catalysts were lower (4-10%) than those for Co/T1 catalysts (22-28%).

One might think that different surface area for both T1 (70 m^2/g) and T2 (49 m^2/g) can be the cause of changes in activities of both catalysts. In order to elucidate this confusion, effect of various surface areas for titania used was also investigated as shown in Table 5.10. It was found that higher surface areas resulted in higher overall activities. Based on the result as mentioned, Co/T2 (lower surface areas) would have had lower activities compared to those of Co/T1 (higher surface areas). Nevertheless, it was not what it has been found. Based on the result, the Co/T2 had higher activities, thus it can be concluded that increases in activities should have been due to the presence of rutile phase in T2 (not because of the change in surface area). It is suggesting that rutile phase may be helpful due to possibly two reasons: (i) rutile phase may increase stability of the support, thus Co-SCF can be inhibited to form and (ii) rutile phase may change reduction behavior resulting in the lower reduction temperature during standard reduction.

Table 5.10 Reaction rate for CO hydrogenation on the titania-supported CoRu catalyst samples.

Sample[a]	BET surface area of the support (m^2/g)	CO conversion(%)[b]		Rate ($gCH_2/g_{cat}h^{-1}$)[c]	
		Initial[d]	SS[e]	Initial	SS
Co/T1-C	70	3.71	2.09	0.014	0.008
Co/T3-C	145	42.70	9.35	0.16	0.04
Co/T4-C	170	59.58	12.24	0.22	0.04

[a] T1, T3, T4 = anatase form

[b] CO hydrogenation was carried out at 220°C, 1 atm, and $H_2/CO/Ar$ = 20/2/8 cc/min.

[c] Error ±5%

[d] After 5 min of reaction

[e] After 5 h of reaction

5.2.3 Effect of Ru promotion

The addition of Ru promoter on the catalysts exhibited increasing of the overall activity of the Co catalysts and it can probably prevent the formation of "Co-titanate" occurring during reduction which related to the TPR measurement and H_2 chemisorption.

From TPR measurement at temperature 35-800°C, it was found that the reducibilities of the CoRu/T2 catalysts ranged between 75 and 87% depending on the more amounts of water vapor added. The loss of reducibilities were ranged 4 to 12% that indicating that the non-reducible (at temperature < 800°C) "Co-titanate" compound form. The TPR profile of the Ru-promoted Co/T2 catalysts were illustrated only one strong reduction peak. This peak can be assigned to the stepwised reduction of Ru_2O_3 and Co_3O_4 (Jongsomjit et al.,2001);

$$Ru_2O_3 \quad + \quad 3H_2 \quad \rightarrow \quad 2Ru \quad + \; 3H_2O \qquad (5.3)$$

$$Co_3O_4 \quad + \quad H_2 \quad \rightarrow \quad 3Co \quad + \; H_2O \qquad (5.1)$$

$$CoO \quad + \quad H_2 \quad \rightarrow \quad Co^o \quad + \; H_2O \qquad (5.2)$$
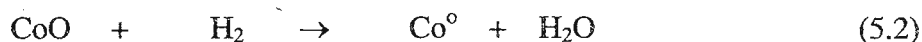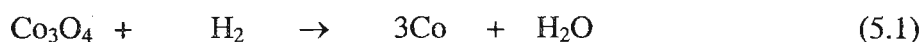
The reduction behavior can be affected by a wide range of variables including particle size, support interaction and reduction gas composition in the different of location of TPR peak (Farrauto and Bartholomew, 1997). The reduction of Ru_2O_3 to Ru^o which usually takes place at lower temperatures ca. 160°C and the reduction of Co_3O_4 occurred at ca. 200-300°C especially with silica and alumina support (Jongsomjit et al.,2001; Panpranot et al., 2002). The step of two reductions were separated peaks. It also observed that in this study, the CoRu/T2-C sample located maximum temperature at ca. 435°C while the Co/T2-C sample indicated maximum temperature at ca. 510°C. The maximum reduction temperature decreased suggesting that the addition of Ru promoter resulted in an increase in reducibility of the catalyst and reduction lower temperature. This is probably due to two causes: (i) hydrogen spillover effect as seen from other supports such as silica and alumina or/and (ii) Ru promoter can block the formation of Co-SCF by minimizing the impact of water vapor on the formation of compound. Kogelbauer et al. (1996) studied Ru promotion in Co/Al_2O_3. They reported that ruthenium appeared to inhibited formation of highly irreducible Co species (Co oxide strongly interacting with the support or Co aluminate) or to promote their reduction, indicated by the absence of the board high temperature TPR feature observed with Co/Al_2O_3 and the greater degree of reduction.

The results of H_2 chemisorption indicated Ru promotion also resulted in an increase in the overall dispersion of the Co on the catalyst sample. Moreover, the overall dispersion was decreased with the more amounts of water added during reduction. Dispersion from H_2 chemisorption should increase with Ru promotion, but BET surface area should not change since only a small amount of Ru was added. On the other hand, the effect of various pretreatments did not change significantly. This also explained that "Co-titanate" form did not cause any change in surface area of the catalysts.

The morphologies of the CoRu/T2 catalysts were also no significant change while the dispersion of Co patches in both of an external area and cross section of a granule were more dispersed with the addition of Ru promoter, as performed by SEM and EDX. When the more amount of water vapor added, cobalt patches were form small groups. This may caused the addition of Ru, Co is more dispersed, thus after pretreatments, the "Co-titanate" compound can be detected. By the ways, in some cases such as alumina support. Jongsomjit *et al.* (2001) described the Co metal and compounds can be detected. They reported that after reduction with and without added water vapor, significant differences were observed using SEM. The disappearance of large numbers of smaller Co patches particles can be seen after the introduction of additional water vapor during reduction. They suggested that there were two possibilities: (i) water vapor can facilitate the migration of small Co particles, resulting in particle agglomeration (sintering), or (ii) it increased the diffusion of Co atoms from the smaller Co particles into almina.

XRD resulted that XRD peaks of Ru promoter were not detected because Ru was present in small amount and well dispersed on the catalyst surface. In addition, it can be observed that Co-SCF formed in the titania support is in a highly dispersed form which cannot be detected by XRD. Raman spectroscopy was also used to identify the "Co-titanate" formed. It was found that the "Co-titanate" formed was different from $CoTiO_3$ probably due to its also being nonstoichiometric (cobalt deficiency) surface "Co-titanate" compound.

CHAPTER VI

CONCLUSIONS AND RECOMMENDATION

This chapter is focused upon the conclusions of the experimental details of the Co-SCF in titania-supported cobalt catalysts and the effect of Ru on the Co-SCF in titania-supported cobalt catalysts which was described in section 6.1. In addition, Recommendations for further study are given in section 6.2.

6.1 Conclusions

Co-support compound formation (Co-SCF) in titania-supported cobalt catalyst can occur during standard reduction resulting in a lower reducibility of catalyst. The compound of cobalt and titania formed referred as "Co-titanate" was considered to be non-reducible at temperatures < 800°C. The "Co-titanate" formed resulted in a decrease in the degree of reduction without any significant change in the reduction behaviors. It was found that the partial pressures of water vapor during reduction probably had only a slight effect on an increase in the "Co-titanate" formation. Due to its highly dispersed form, it cannot be detected by XRD. However, Raman spectroscopy revealed that this highly dispersed "Co-titanate" formed was likely different from $CoTiO_3$ and present as a nonstoichiometric surface "Co-titanate" compound.

The "Co-titanate" formed also resulted in decreased activities of catalyst without any changes in selectivity. In addition, the existing of rutile form in titania can enhance the overall activity and the stability of the titania-supported cobalt catalysts. This is probably due to rutile may help promoting the activity of the Co/TiO_2 catalysts and inhibiting Co-SCF. The addition of Ru promoter to the Co/TiO_2 catalysts was found to enhance both reducibilities and the overall activities. Furthermore, the Ru promoter also decreased significantly the formation of more difficult to reduced Co-support species (Co_XO_Y-TiO_2). This is probably two causes due to (i) hydrogen spillover effect as seen from other supports such as silica and alumina or/and (ii) Ru promoter may block the formation of Co-SCF by minimizing the impact of water vapor on the formation of compound.

6.2 Recommendations

1. Effect of anatase: rutile ratio in titania supports should be further investigated in order to determine which the optimum anatase: rutile ratio should result in high activities and high selectivities for diesel fuel production.

2. Effect of various titania supports prepared from different methods should be further studied in order to discover the best titania support for cobalt catalysts.

REFERENCES

Brezny, B., and Muan, A. Phase relations and stabilities of compounds in the system CoO-TiO$_2$*. J. inorg. nucl. Chem. 31 (1969): 649-655.

Brik, Y., Kacimi, M., Ziyad, M., and Bozon-Verduraz, F. Titania-supported cobalt and cobalt-phosphorus catalysts: Characterization and performances in ethane oxidative dehydrogenation. J. Catal. 202 (2001): 118-128.

Brik, Y., Kacimi, M., Ziyad, M., Bozon-Verduraz, F., and Ziyad, M. Characterization and comparison of the activity of boron-modified Co/TiO$_2$ catalysts in butan-2-ol conversion and oxidative dehydrogenation of ethane. J. Catal. 211 (2002): 470-481.

Choi, J.G. Reduction of supporte cobalt catalysts by hydrogen. Catal Lett. 35 (1995): 291-296.

Curtis, V., Nicolaides, C.P., and Coville, N.J., Hildebrandt, D., Glasser, D. The effect of sulfur on supported cobalt Fischer-Tropsch catalysts. Catal.Today 49 (1999): 33-40.

Das, T.K., Jacobs, G., Patterson, P.M., Conner, W.A., Li, J., and Davis, B.H. Fischer-Tropsch synthesis: characterization and catalytic properties of rhenium promoted cobalt alumina catalysts. Fuel 82 (2003): 805-815.

Duvenhage, D.J., and Coville, N.J. Fe:Co/TiO$_2$ bimellic catalysts for the Fischer-Tropsch reaction I. Characterization and reactor studies. Appl. Catal. A 153 (1997): 43-67.

Duvenhage, D.J., Coville, and N.J. Fe:Co/TiO$_2$ bimellic catalysts for the Fischer-Tropsch reaction Part 2. The effect of calcination and reduction temperature. Appl. Catal. A 233(2002): 63-75.

Farrauto, R.J. and Bartholomew, C.H. Fundamentals of industrial catalytic processes. 1 st ed. London: Chapman & Hall, 1997.

Fujishima, A., Hashimoto, K., and Watanabe, T., TiO2 photocatalysis: fundamental and applications. 1 st ed. Tokyo: BKC, 1999.

Hilmen, A.M., Schanke, D., and Holmen. A. TPR study of the mechanism of rhenium of almina-supported cobalt Fischer-Tropsch catalysts. Catal Lett. 38 (1996): 143-147.

Hilmen, A.M., Schanke, D., Hanssen, K.F., and Holmen. A. Study of the effect of water on almina supported cobalt Fischer-Tropsch catalysts. Appl. Catal A. 186 (1999): 169-188.

Ho, S.W., Cruz, J.M., Houalla, M., and Hercules, D.M. The structure and activity of titania supportd cobalt catalysts. J. Catal. 135 (1992): 173-185.

Ho, S.W. Surface hydroxyls and chemisorbed hydrogen on titania and titania supported cobalt. J. Chin Chem Soc. 43 (1996): 155-163.

Jacobs, G., Das, T.K., Zhang, Y., Li, J., Racoillet, G., and Davis, B.H. Fischer-Tropsch synthesis: support, loading, and promoter effects on the reducibility of cobalt catalysts. Appl. Catal. A 233 (2002):263-281.

Jongsomjit, B., Panpranot, J., and Goodwin, J.G., Jr. Co-support compound formation in alumina-supported cobalt catalysts. J. Catal. 204 (2001): 98-109.

Jongsomjit, B., and Goodwin, J.G., Jr. Co-support compound formation in Co/Al$_2$O$_3$ catalysts: effect of reduction gas containing CO. Catal. Today 77 (2002): 191-204.

Jongsomjit, B., Panpranot, J., and Goodwin, J.G., Jr. Effect of zirconia-modified alumina on the properties of Co/γ-Al$_2$O$_3$ catalysts. J. Catal. 215 (2003): 66-77.

Kogelbauer, A., Weber, J.C., and Goodwin, J.G., Jr. The formation of cobalt silicates on Co/SiO$_2$ under hydrothermal conditions. Catal Lett. 34 (1995): 259-267.

Kogelbauer, A., Goodwin, J.G., Jr., and Oukaci, R. Ruthenium promotion of Co/Al$_2$O$_3$ Fischer-Tropsch catalysts. J. Catal. 160 (1996): 125-133.

Kraum, M., and Baerns, M. Fischer-Tropsch synthesis: the influence of various cobalt compounds applied in the preparation of supported cobalt catalysts on their performance. Appl. Catal. A 186(2002): 189-200.

Madikizela, N.N., and Coville, N.J.A study of Co/Zn/TiO2 catalysts in the fischer-Tropsch reaction. J. Mol. Catal. A 181 (2002): 129-136.

Othmer, K. Encyclopedia of chemical technology. Vol. 6. 4 th ed. New York: A Wiley-Interscience Publication, John Wiley&Son, 1991.

Panpranot, J., Goodwin, J.G., Jr., and Sayari, A. CO hydrogenation on Ru-promoted Co/MCM-41 catalysts. J. Catal. 211 (2002): 530-539.

Li, J., and Coville, N.J.The effect of boron on the catalyst reducibility and activity of Co/TiO$_2$ Fischer-Tropsch catalysts. Appl. Catal. A 181(1999): 201-208.

Li, J., and Coville, N.J. Effect of boron on the sulfur poisoning of Co/TiO2 Fischer-Tropsch catalysts. Appl. Catal. A 208(2002): 177-184.

Li, J., and Coville, N.J. Effect of boron source on the catalyst reducibility and Fischer-Tropsch synthesis activity of Co/TiO$_2$ catalysts. Catal. Today 71 (2002): 403-410.

Li, J., Xu, L., Keogh, R., and Davis, B.Fischer-Tropsch synthesis. Effect of CO pretreatment on a ruthenium promoted Co/TiO$_2$. Catal Lett. 70 (2002)127-130.

Reid, R.C., Prausnitz, J.M., and Sherwood, T.K. The properties of gases and liquids. 3 rd ed. New York: McGraw-Hill Book company, (1977).

Reuel, R.C., and Bartholomew, C.H. The stoichiometries of H$_2$ and CO adsorption on cobalt: effects of support and preparation. J. Catal. 85 (1984): 63-77.

Reuel, R.C., and Bartholomew, C.H. Effects of support and dispersion on the CO hydrogenation activity/selectivity properties of cobalt. J. Catal. 85 (1984): 78-88.

Riva, R., Miessner, H., and Piero, G.D.Metal-support interaction in Co/SiO$_2$ and Co/TiO$_2$. Appl. Catal. A 196(2000): 111-123.

Schanke, D., Hilmen, A.M., Bergene, E., Kinnari, K., Rytter, E.,Adnanes, E., and Holmen, A. Study of the deactivation mechanism of Al$_2$O$_3$-supported cobalt Fischer-Tropsch catalysts. Catal Lett. 34 (1995): 269-284.

Sun, S., Fujimoto, K. Yoneyama, Y., and Tsubaki, N. Fischer-Tropsch synthesis using Co/SiO$_2$ catalysts prepared from mixed precursors and addition effect of noble metals. Fuel 81 (2002): 1583-1591.

Tsubaki, N., Sun, S., and Fujimoto, K. Different function of the noble metals added to cobalt catalysts for Fischer-Tropsch synthesis. J. Catal. 199 (2001): 236-246.

Voβ, M., Borgmann, D., and Wedler, G. Characterization of alumina, silica, and titania supported cobalt catalysts. J. Catal. 212 (2002): 10-21.

Young, R.S. COBALT: Its Chemistry, Metallurgy, and Uses. New York: Reinhpld Publishing Corporation, 1960.

Zennaro, R., Tagliabue, M., and Bartholomew, C.H. Kinetics of Fischer-Tropsch synthesis on titania-supported cobalt. Catal. Today 58 (2000): 309-319.

Zhang, Y., Wei, D., Hammache, S., and Goodwin, J.G., Jr. Effect of water vapor on the reduction of Ru-promoted Co/Al$_2$O$_3$. J. Catal. 188 (1999): 281-290.

Zhang, J., Ayusawa, T., Minagawa, M., Kinugawa, K., Yamashita, H., Matsuoka, M., and Anpo, M. Investigations of TiO$_2$ Photocatalysts for the decomposition of NO in the flow system. J. Catal. 198 (2001): 1-8.

APPENDICES

APPENDIX A

CALCULATION FOR CATALYST PREPARATION

Preparation of 20%Co/TiO$_2$ with and with promoted Ru catalysts by the incipient wetness impregnation method are shown as follows:

Reagent: - Cobalt (II) nitrate hexahydrate (Co(NO$_3$)$_2$ · 6H$_2$O)

Molecular weight   =   290.93

- Ruthenium (III) nitrosyl nitrate (Ru(NO) (NO$_3$)$_3$)

Molecular weight   =   193.07

- Support: - Titania [TiO$_2$]

Calculation for the preparation of unpromoted catalyst (20%Co/TiO$_2$)

Based on 100 g of catalyst used, the composition of the catalyst will be as follows:

Cobalt   =   20 g

Titania   =   100-20   =   80 g

For 5 g of titania

Cobalt required   =   5×(20/80)   =   1.25 g

Cobalt 1.25 g was prepared from Co(NO$_3$)$_2$ · 6H$_2$O and molecular weight of Co is 58.93

$$\text{Co(NO}_3)_2 \cdot 6\text{H}_2\text{O required} = \frac{\text{MW of Co(NO}_3)_2 \cdot 6\text{H}_2\text{O} \times \text{cobalt required}}{\text{MW of Co}}$$

$$= (290.93/58.93) \times 1.25 = 6.17 \text{ g}$$

Since the pore volume of the titania support is 0.8 ml/g and 1 ml/g for JRC-TIO1, JRC-TIO4, respectively. Thus, the total volume of impregnation solution which must be used is 4 ml for JRC-TIO1 and 5 ml for JRC-TIO4 by the requirement of incipient wetness impregnation method, the de-ionized water is added until equal pore volume for dissolve Cobalt (II) nitrate hexahydrate.

Calculation for the preparation of Ru-promoted catalyst (0.5% Ru-20% Co/TiO$_2$)

Based on 100 g of catalyst used, the composition of the catalyst will be as follows:

Cobalt	=	20 g		
Ruthenium	=	0.5 g		
Titania	=	100-(20+0.5)	=	79.5 g

For 5 g of titania

Cobalt required	=	5×(20/79.5)	=	1.26 g
Ruthenium required	=	5×(0.5/79.5)	=	0.03 g

Cobalt 1.26 g was prepared from Co(NO$_3$)$_2$ · 6H$_2$O and molecular weight of Co is 58.93.

$$Co(NO_3)_2 \cdot 6H_2O \text{ required} = \frac{MW \text{ of } Co(NO_3)_2 \cdot 6H_2O \times \text{cobalt required}}{MW \text{ of Co}}$$

$$= (290.93/58.93) \times 1.26 = 6.22 \text{ g}$$

Ruthenium 0.03 g was prepared from (Ru(NO) (NO$_3$)$_3$) and molecular weight of Ru is 101.07.

$$(Ru(NO) \cdot (NO_3)_3) \text{ required} = \frac{MW \text{ of } (Ru(NO) (NO_3)_3) \times \text{ruthenium required}}{MW \text{ of Ru}}$$

$$= (193.07/101.07) \times 0.03 = 0.06 \text{ g}$$

Dissolve of cobalt Cobalt (II) nitrate hexahydrate, ruthenium (III) nitrosyl nitrate and volume of de-ionized water like preparation of unpromoted catalyst.

APPENDIX B

VAPOR PRESSURE OF WATER

The partial vapor pressure of water to the requirement was set by adjusting the temperature of saturator following Antoine equation (Reid *et al.*, 1977).

$$\ln P = A - \frac{B}{(t+C)}$$

When P = vapor pressure of reactant, mm Hg

t = temperature, K

A, B, and C are constants shown in Table B.1

Range of temperature that applied ability 284-441 K

Table B.1 The values of constants.

| Constant	Value of constant
A	18.3036
B	3816.44
C	-46.13

APPENDIX C

CALCULATION FOR REDUCIBILITY

For supported cobalt catalyst, it can be assumed that the major species of calcined Co catalysts is Co_3O_4. H_2 consumption of Co_3O_4 is calculated as follows:

$$\text{Molecular weight of Co} \quad = \quad 58.93$$
$$\text{Molecular weight of } Co_3O_4 \quad = \quad 240.79$$

Calculation of the calibration of H_2 consumption using cobalt oxide (Co_3O_4)

Let the weight of Co_3O_4 used $\quad = \quad 0.01$ g

$\quad = \quad 4.153 \times 10^{-5}$ mole

From equation of Co_3O_4 reduction;

$$Co_3O_4 \quad + \quad 4H_2 \quad \rightarrow \quad 3Co \quad + \quad 4H_2O \qquad \text{(D.1)}$$
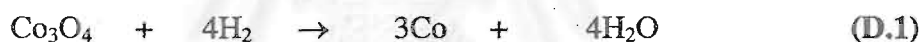
$$H_2 \quad = \quad 4 \, Co_3O_4$$
$$= \quad 4 \times 4.153 \times 10^{-5} \quad = \quad 1.661 \times 10^{-4} \text{ mole}$$

Integral area of Co_3O_4 after reduction $\quad = \quad 396572.5 \quad$ unit

Thus, the amount of H_2 that can be consumed at 100 % reducibility is 1.661×10^{-4} mole which related to the integral area of Co_3O_4 after reduction 396572.5 unit.

Calculation of reducibility of supported cobalt catalyst

Integral area of the calcined catalyst	$=$ X	unit
The amount of H_2 consumption $\quad =$	$[1.661 \times 10^{-4} \times (X)/396572.5]$	mole
Let the weight of calcined catalyst used	$=$ W	g
Concentration of Co (by AAS)	$=$ Y	% wt
Mole of Co	$=$ $[(W \times Y)/58.93]$	mole
Mole of Co_3O_4	$=$ $[(W \times Y)/3 \times 58.93]$	mole

Mole of H_2 can be consumed $= [(W \times Y) \times 4/3 \times 58.93]$ mole

Reducibility (%) of supported Co catalyst $= \dfrac{[1.661 \times 10^{-4} \times (X)/396572.5] \times 100}{[(W \times Y) \times 4/3 \times 58.93]}$

APPENDIX D

CALCULATION FOR TOTAL H_2 CHEMISORPTION AND DISPERSION

Calculation of the total H_2 chemisorption and metal dispersion of the catalyst, a stoichiometry of H/Co = 1, measured by H_2 chemisorption is as follows:

Let the weight of catalyst used	=	W	g
Integral area of H_2 peak after adsorption	=	A	unit
Integral area of 45 μl of standard H_2 peak	=	B	unit
Amounts of H_2 adsorbed on catalyst	=	B-A	unit
Concentration of Co (by AAS)	=	C	% wt
Volume of H_2 adsorbed on catalyst	=	45×[(B-A)/B]	μl
Volume of 1 mole of H_2 at 100°C	=	28.038	μl
Mole of H_2 adsorbed on catalyst	=	[(B-A)/B]×[45/28.038]	μmole

Total hydrogen chemisorption = [(B-A)/B]×[45/28.038]×[1/W] μmole /g of catalyst

= N μmole /g of catalyst

Molecular weight of cobalt = 58.93

Metal dispersion (%) = $\dfrac{2 \times H_{2\ tot}/g\ of\ catalyst \times 100}{No\ \mu mole\ Co_{tot}/g\ of\ catalyst}$

= $\dfrac{2 \times N \times 100}{No\ \mu mole\ Co_{tot}}$

= $\dfrac{2 \times N \times 58.93 \times 100}{C \times 10^6}$

= $\dfrac{1.179 \times N}{C}$

APPENDIX E

CALIBRATION CURVES

This appendix showed the calibration curves for calculation of composition of reactant and products in CO hydrogenation reaction. The reactant is CO and the main product is methane. The other products are linear hydrocarbons of heavier molecular weight that are C_2-C_4 such as ethane, ethylene, propane, propylene and butane.

The thermal conductivity detector, gas chromatography Shimadzu model 8Awas used to analyze the concentration of CO by using Molecular sieve 5A column.

The VZ10 column are used with a gas chromatography equipped with a flame ionization detector, Shimadzu modal 14B, to analyze the concentration of products including of methane, ethane, ethylene, propane, propylene and butane.

Mole of reagent in y-axis and area reported by gas chromatography in x-axis are exhibited in the curves. The calibration curves of CO, methane, ethane, ethylene, propane, propylene and butane are illustrated in the following figures.

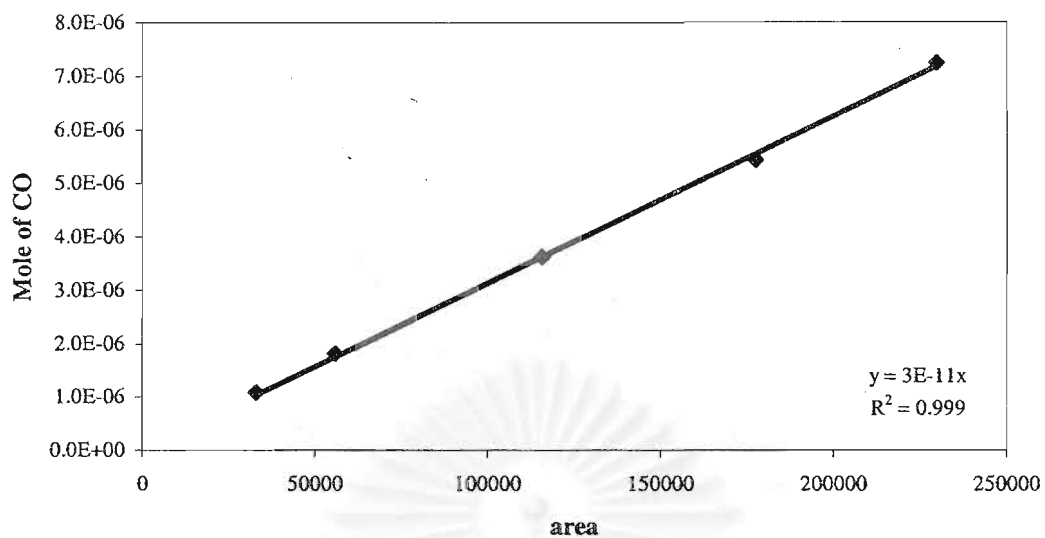**Figure E.1** The calibration curve of CO.

$y = 3E\text{-}11x$
$R^2 = 0.999$

Figure E.2 The calibration curve of methane.

$y = 6E\text{-}13x$
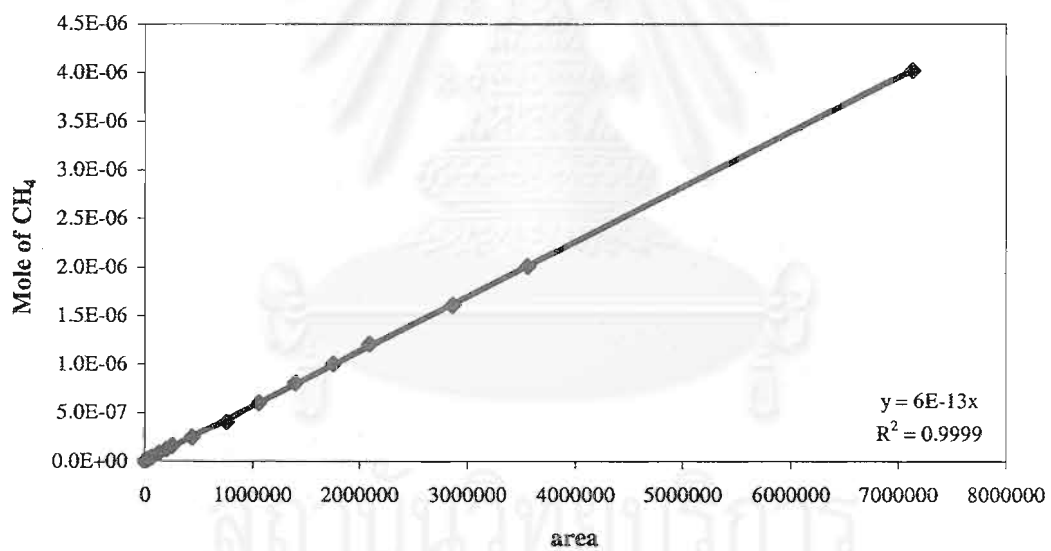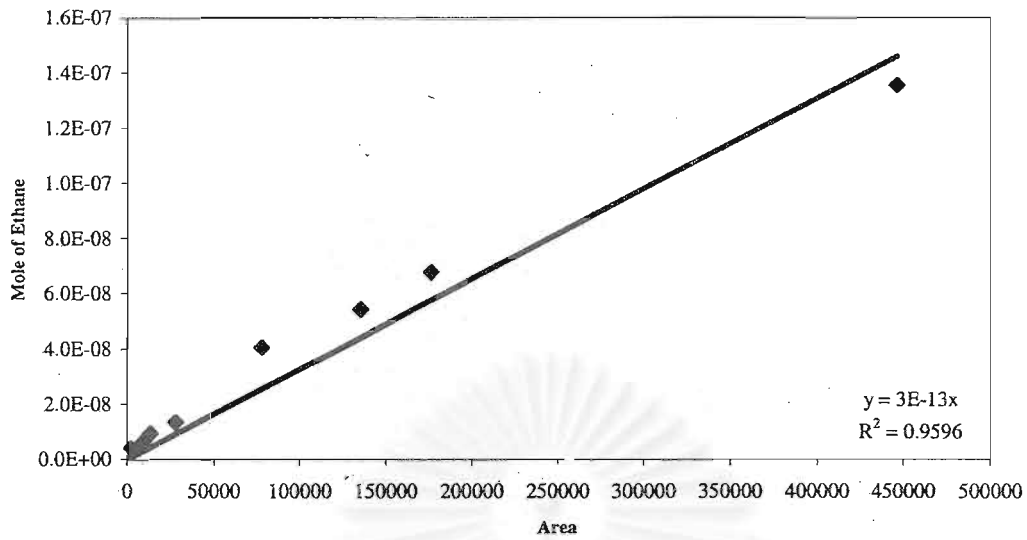$R^2 = 0.9999$

Figure E.3 The calibration curve of ethane.

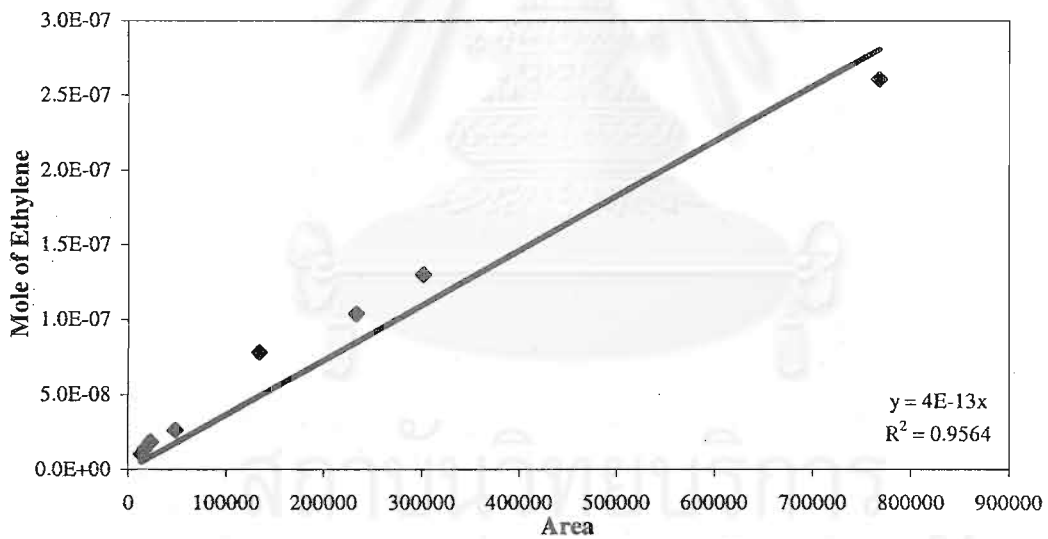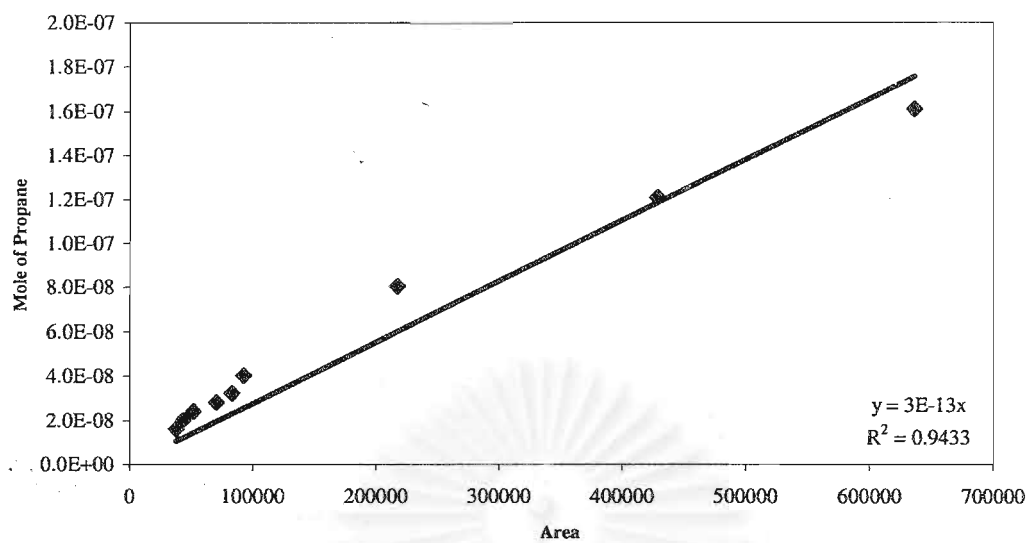**Figure E.4** The calibration curve of ethylene.
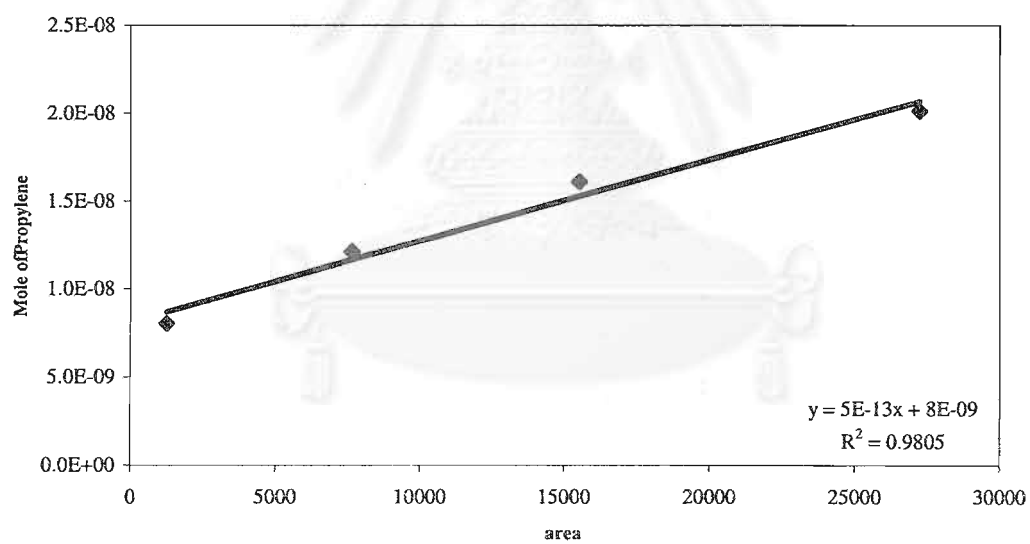
Figure E.5 The calibration curve of propane.
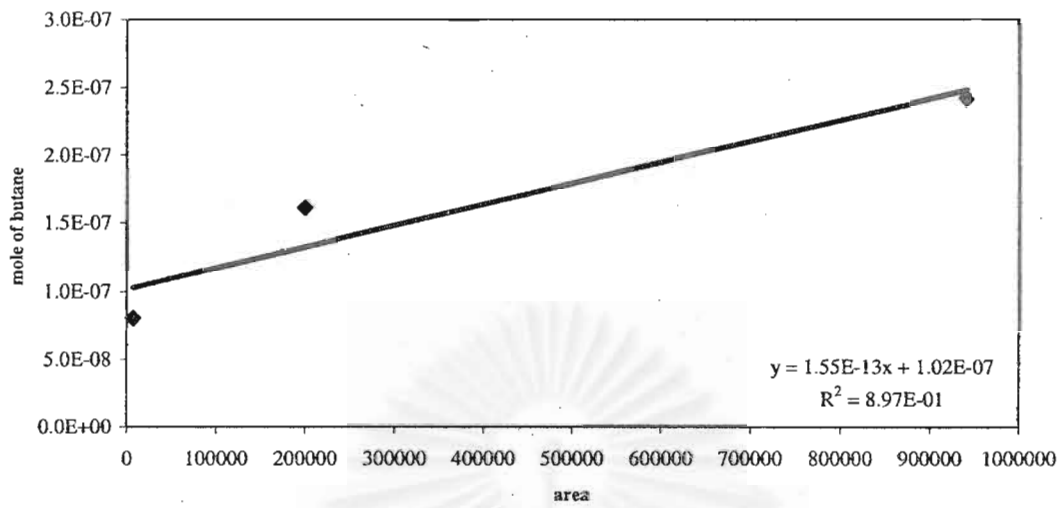

Figure E.6 The Calibration curve of propylene.

Figure E.7 The calibration curve of butane.

APPENDIX F

CALCULATION OF CO CONVERSION, REACTION RATE AND SELECTIVITY

The catalyst performance for the CO hydrogenation was evaluated in terms of activity for CO conversion reaction rate and selectivity.

Activity of the catalyst performed in term of carbon monoxide conversion and reaction rate. Carbon monoxide conversion is defined as moles of CO converted with respect to CO in feed:

$$\text{CO conversion (\%)} = \frac{100 \times [\text{mole of CO in feed} - \text{mole of CO in product}]}{\text{mole of CO in feed}} \quad \text{(i)}$$

where mole of CO can be measured employing the calibration curve of CO in Figure E.1, Appendix E.,i.e.,

$$\text{mole of CO} = (\text{area of CO peak from integrator plot on GC-8A}) \times 3 \times 10^{-11} \quad \text{(ii)}$$

Reaction rate was calculated from CO conversion that is as follows:

Let the weight of catalyst used	=	W	g
Flow rate of CO	=	2	cc/min
Reaction time	=	60	min
Weight of CH_2	=	14	g
Volume of 1 mole of gas at 1 atm	=	22400	cc

$$\text{Reaction rate (g } CH_2/\text{g of catalyst/h)} = \frac{[\% \text{ conversion of CO/100}] \times 60 \times 14 \times 2}{W \times 22400} \quad \text{(iii)}$$

Selectivity of product is defined as mole of product (B) formed with respect to mole of CO converted:

$$\text{Selectivity of B (\%)} = 100 \times [\text{mole of B formed/mole of total products}] \quad \text{(iv)}$$

Where B is product, mole of B can be measured employing the calibration curve of products such as methane, ethane, ethylene, propane, propylene and butane in Figure E.2-E.7, Appendix E.,i.e.,

mole of CH_4 = (area of CH_4 peak from integrator plot on GC-14B)$\times 6\times10^{-13}$ (ii)

APPENDIX G

LIST OF PUBLICATIONS

1. Bunjerd Jongsomjit, Chitlada Sakdamnuson, James G. Goodwin, Jr. and Piyasan Praserthdam, "Co-Support Compound Formation in Titania-Supported Cobalt Catalyst", Catalysis Letters, 94 (2004): 209-214.

CATALYSIS LETTERS

Gabor A. Somorjai - Editors - John M. Thomas

Gabor A. Somorjai
Professor of Chemistry, UC Berkeley
University Professor, UC Berkeley
058 Hildebrand Hall #1460
Department of Chemistry
University of California
Berkeley, CA 94720-1460
U.S.A.

Tel: (510) 642-4053
Fax: (510) 643-9668
E-mail: CatLett@socrates.berkeley.edu

Dr. Bunjerd Jongsomjit
Department of Chemical Engineering
Faculty of Engineering
Chulalongkorn University
Bangkok, 10330
Thailand

2/25/4

Dear Dr. Jongsomjit,

Thank you for returning your revised manuscript with the diskette entitled

"Co-Suport Compound Formation . . ."

The paper has been accepted for publication in *Catalysis Letters* and it was forwarded to the publisher. I am including a reprint order form for your convenience.

With best personal regards.

Sincerely,

Gabor A. Somorjai

Co-support compound formation in titania-supported cobalt catalyst

Bunjerd Jongsomjit[a,*], Chitlada Sakdamnuson[a], James G. Goodwin Jr[b], and Piyasan Praserthdam[a]

[a]*Center of Excellence on Catalysis and Catalytic Reaction Engineering, Department of Chemical Engineering, Faculty of Engineering, Chulalongkorn University, Bangkok 10330, Thailand*
[b]*Department of Chemical Engineering, Clemson University, Clemson, SC 29634, USA*

Co-support compound formation (Co-SCF) in Co/TiO_2 was found during standard reduction resulting in a lower reducibility of the catalyst. The compound formed is considered to be non-reducible at temperatures <800 °C during TPR and different from $CoTiO_3$. The characteristics of Co-SCF were investigated using BET surface area, XRD, Raman spectroscopy, SEM/EDX, and TPR.

KEY WORDS: supported catalyst; cobalt catalyst; cobalt-support compound; titania support; Co/TiO_2; reducibility; CO hydrogenation.

1. Introduction

In Fischer–Tropsch synthesis (FTS), supported cobalt catalysts are preferred because of their high activity for FTS based on natural gas [1], high selectivity to linear long-chain hydrocarbons and low activity for the water–gas shift (WGS) reaction [2,3]. However, compound formation between cobalt and the supports can occur during the catalyst activation and/or reaction conditions resulting in irreversible catalyst deactivation [4–6].

Besides alumina (Al_2O_3) and silica (SiO_2), titania (TiO_2) has been widely studied as the support for cobalt catalysts by many authors [7–20], especially for the application of FTS in a continuously stirred tank reactor (CSTR) [11,15]. It was reported that Co-SCF in SiO_2 [21] and Al_2O_3 [4–6,22] can occur during standard reduction and resulted in a lower degree of reduction. However, titania was the first support where strong metal support interaction was observed [19]. In the present research, the nature of Co-SCF in titania-supported cobalt catalyst and its effect on the characteristics of the catalysts were the main focus. In this study, the Co/TiO_2 catalyst was prepared, pretreated under various conditions, and characterized using BET surface area, XRD, TPR, SEM/EDX, and Raman spectroscopy to identify the nature of compounds formed. The main objectives of this research were to develop a better understanding of Co-SCF in titania-supported cobalt catalyst and to better identify the compounds formed. Based on information obtained from the present research, the strategies to minimize such a compound formation can be further developed.

2. Experimental

2.1. Catalyst preparation

A 20 wt% of Co/TiO_2 was prepared by the incipient wetness impregnation. A designed amount of cobalt nitrate $[Co(NO_3) \cdot 6H_2O]$ was dissolved in deionized water and then impregnated onto TiO_2 (anatase form calcined at 600 °C obtained from Ishihara Sangyo, Japan). The catalyst precursor was dried at 110 °C for 12 h and calcined in air at 500 °C for 4 h.

2.2. Catalyst pretreatments

Standard reduction of the calcined catalyst was conducted in a fixed-bed flow reactor under differential conditions at 1 atm using a temperature ramp from ambient to 350 °C at 1 °C/min and holding at 350 °C for 10 h in a gas flow having a space velocity of 16,000 h^{-1} and consisting of H_2 or mixtures of H_2 and water vapor (5–10 vol%). The high space velocity of the H_2 flow when water vapor was not added insured that the partial pressure of water vapor in the catalyst bed produced by cobalt oxide reduction would be essentially zero in that case. The reduced catalyst was then passivated at room temperature with air for 30 min.

2.3. Catalyst nomenclature

The nomenclature used for the catalyst samples in this study is following:

- Co–C: the calcined catalyst sample
- Co–RW0: the calcined catalyst sample reduced in H_2
- Co–RW5: the calcined catalyst sample reduced in a mixture of H_2 with 5 vol% water vapor added during reduction
- Co–RW10: the calcined catalyst sample reduced in a mixture of H_2 with 10 vol% water vapor added during reduction

* To whom correspondence should be addressed.
E-mail: bunjerd.j@chula.ac.th

2.4. Catalyst characterization

2.4.1. BET surface area

BET surface area of the samples after various pretreatments was performed to determine if the total surface area changes upon the various pretreatment conditions. It was determined using N_2 adsorption at 77 K in a Micromeritics ASAP 2010.

2.4.2. X-ray diffraction

XRD was performed to determine the bulk crystalline phases of catalyst following different pretreatment conditions. It was conducted using a SIEMENS D–5000 X-ray diffractometer with CuK_α ($\lambda = 1.54439$ Å). The spectra were scanned at a rate of 2.4 °/min in the range $2\theta = 20$–$80°$.

2.4.3. Scanning electron microscopy and energy dispersive X-ray spectroscopy

SEM and EDX were used to determine the catalyst morphologies and elemental distribution throughout the catalyst granules, respectively. The SEM of JEOL mode JSM–5800LV was applied. EDX was performed using Link Isis series 300 program.

2.4.4. Raman spectroscopy

The Raman spectra of the samples were collected by projecting a continuous wave laser of argon ion (Ar^+) green (514.532 nm) through the samples exposed to air at room temperature. A scanning range of 100–1000 cm^{-1} with a resolution of 2 cm^{-1} was applied. The data were analyzed using the Renishaw WiRE (Windows-based Raman Environment) software, which allows Raman spectra to be captured, calibrated, and analyzed using system 2000 functionality via Galactic GRAMS interface with global imaging capacity.

2.4.5. Temperature-programmed reduction

TPR was used to determine the reduction behaviors and reducibilities of the samples. It was carried out using 50 mg of a sample and a temperature ramp from 35 to 800 °C at 5 °C/min. The carrier gas was 5% H_2 in Ar. A cold trap was placed before the detector to remove water produced during the reaction. A thermal conductivity detector (TCD) was used to determine the amount of H_2 consumed during TPR. The H_2 consumption was calibrated using TPR of Ag_2O at the same conditions. The reduced samples were recalcined at the original calcination conditions prior to performing TPR. The calculation of reducibilities was described elsewhere [4–6,21,22,23].

2.5. Reaction

CO hydrogenation ($H_2/CO = 10/1$) was performed to determine the overall activity of the catalyst samples reduced at various conditions. Hydrogenation of CO was carried out at 220 °C and 1 atm. A flow rate of $H_2/$ CO/He = 20/2/8 cc/min in a fixed-bed flow reactor under differential conditions was used. A relatively high H_2/CO ratio was used to minimize deactivation due to carbon deposition during reaction. Typically, 20 mg of a catalyst sample was re-reduced in situ in flowing H_2 (30 cc/min) at 350 °C for 10 h prior to the reaction. Reactor effluent samples were taken at 1 h intervals and analyzed by GC. In all cases, steadystate was reached within 5 h.

3. Results and discussion

3.1. Evidence of Co-SCF in Co/TiO₂ catalyst

It can be observed that Co-SCF in Co/TiO_2 essentially occurred during standard reduction resulting in lower reducibilities of the reduced samples during TPR at temperatures 35–800 °C as shown in table 1. The reducibilities ranged from 92% to 64% upon the various pretreatments of catalyst samples. Essentially, TPR of the TiO_2 support only (table 1) was also conducted at the same condition and no hydrogen consumption was detected. It should be noted that the loss in the degree of reduction was attributed to the compound formation of cobalt and the titania support. The suggested conceptual diagram of reducibility loss during standard reduction is illustrated in figure 1. First, when performing TPR on a fresh calcined sample, the reducibility gain was 92%. However, when the calcined sample was reduced with and without water vapor addition (5–10 vol%) during reduction, then recalcined it back to the oxide form prior to performing TPR, the reducibilities obviously decreased. The reducibilities loss during the reduction process were found to be in the range of 22–28% indicating the non-reducible (at temperatures < 800 °C) "Co-titanate" compound formed. The term "Co-titanate" is used here to refer to the surface compound formed during standard reduction of cobalt and the titania support.

It should be mentioned that a decrease in the degree of reduction of reduced samples slightly changed upon

Table 1
Reducibilities and surface areas of samples after various pretreatments

Sample	Reduction gas mixture (P_{H2}/P_{H2O})	Reducibility (%) during TPR at 35–800 °C[a,b]	Surface area (m^2/g)[b]
TiO_2	--	–	70
Co–C	–	92	52
Co–RW0	1/0	70	49
Co–RW5	0.95/0.05	68	46
Co–RW10	0.90/0.10	64	46

[a]The reduced samples were recalcined at the original calcination conditions prior to performing TPR.
[b]Measurement error is ±5%.
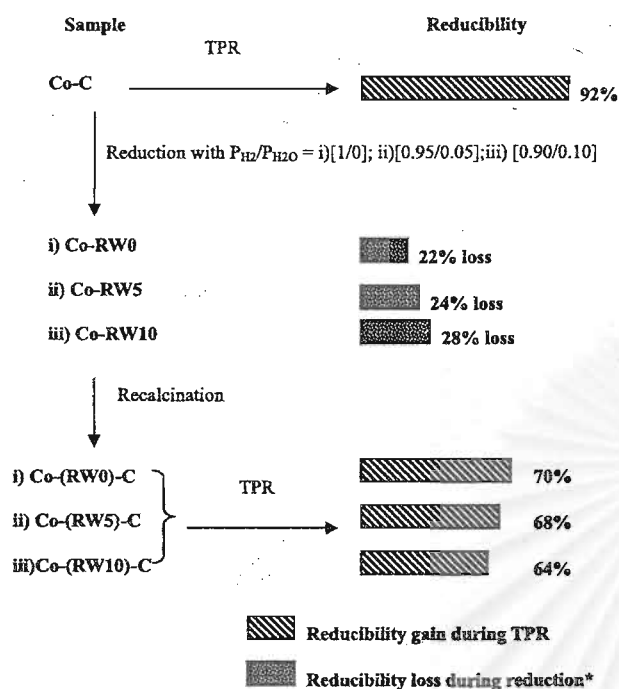
Figure 1. Suggested conceptual diagram for the reducibility loss during reduction process.

* The difference in reducibility gain from a fresh calcined sample and the reducibility gain from a reduced and recalcined sample.

Figure 2. TPR profiles of bulk Co_3O_4 and the catalyst samples after various pretreatment conditions.

increasing the partial pressures of water vapor during the reduction process. Zhang *et al.* [22] investigated the reducibilities of $CoRu/\gamma$-Al_2O_3 during standard reduction and TPR in the presence of added water vapor. They reported that water has a significant effect on the reduction behavior of $CoRu/\gamma$-Al_2O_3. It was suggested that water vapor present during reduction leads to a decrease in the degree of reduction of the cobalt perhaps in two ways: (i) inhibition of the reduction of well-dispersed CoO interacting with the alumina support, possibly by increasing the cobalt–alumina interaction, and (ii) facilitation of the migration of cobalt ions into probable tetrahedral sites of γ-Al_2O_3 to form a non-reducible (at temperatures < 900 °C) spinel. However, considering the Co-SCF in Co/TiO_2, the effect of water vapor added during standard reduction was essentially less pronounced compared to that on the alumina support. The only slight effect of water vapor on Co-SCF in Co/TiO_2 is also listed in table 1 indicating that the reducibilities of the reduced samples only slightly decreased within experimental error when water vapor (5–10 vol%) was added during standard reduction. Besides the reducibility measurement, TPR also provides information on the reduction behaviors of the catalyst samples pretreated under various conditions.

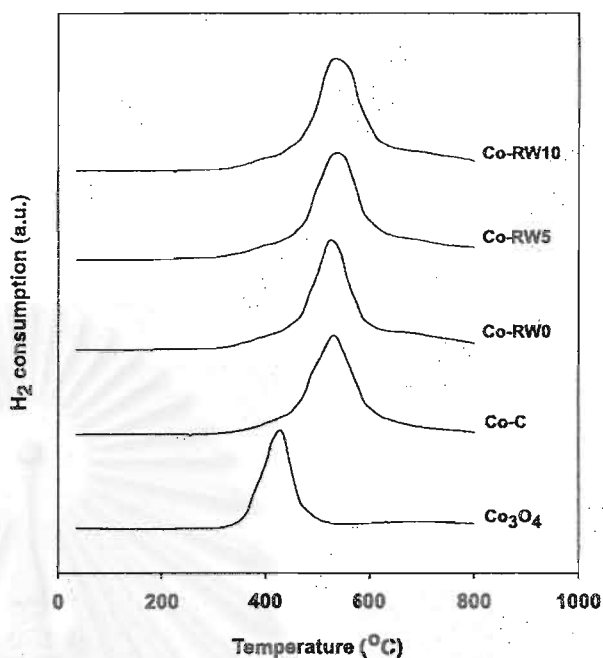TPR profiles of bulk Co_3O_4 and the catalyst samples after various pretreatment conditions are shown in figure 2. Only one strong reduction peak can be observed for bulk Co_3O_4 and all the samples regardless of various pretreatment conditions used. This peak can be assigned to the overlap of two-step reduction of Co_3O_4 to CoO and then to Co^0 [22,24,25]. Upon the TPR conditions, the two reduction peaks based on the two-step reduction may or may not be observed. The TPR profile of the titania support (not shown) showed no reduction peak. There was only one reduction peak located at ca. 370–620 °C (max. at 520 °C) for the calcined sample (Co–C) indicated that no residual cobalt nitrates remain on the calcined sample of Co/TiO_2 upon the calcination condition used in this study. In some cases, the peak of the decomposition of cobalt nitrates during TPR of supported cobalt catalysts can be observed at temperatures between 200 and 300 °C, especially with silica and alumina supports [4–6,23,26,27]. However, prolonged calcination or reduction and recalcination results in complete decomposition of any cobalt nitrates present [23].

TPR profiles of all reduced samples were also similar exhibiting only one reduction peak as shown in figure 2. TPR peak located at ca. 400–620 °C (max. at 520 °C) for Co-RW0 sample was slightly shifted about 10 °C higher when the partial pressure of water vapor was increased during reduction indicating slightly stronger interaction between cobalt and titania support. However, the much stronger interaction between cobalt and the supports such as silica and alumina can be usually observed leading to an observation of two separated peaks during TPR of the reduced and recalcined samples [4–6,21,23]. The higher temperature reduction peak can be assigned to the reduction of cobalt strongly interacting with the

supports, i.e. Co_xO_y–Al_2O_3 and Co_xO_y–SiO_2, which can not be observed in the reduced and recalcined Co/TiO_2 catalyst. Based on the TPR results, it should be noted that a degree of reduction of the reduced Co/TiO_2 catalyst was found to decrease during standard reduction due to "Co-titanate" formed. However, the reduction behaviors of samples reduced in various conditions were similar upon the TPR measurement conditions used in this study. This can be concluded that "Co-titanate" formed in a Co/TiO_2 catalyst resulted in only a decrease in the reducibility without changing the reduction behaviors of it. The effect of partial pressures of water vapor during reduction on the formation of "Co-titanate" seemed to be less pronounced.

3.2. Characteristics of "Co-titanate"

In order to identify the characteristics of "Co-titanate" formed during reduction, several characterization techniques were conducted. BET surface areas of TiO_2 and the catalyst samples after various pretreatments are also shown in table 1. BET surface areas of samples were slightly less than the titania (anatase form) support (70 m^2/g). Since all surface areas of the samples in this study ranged between 46 and 52 m^2/g, there was no significant change in surface areas after the various pretreatments within experimental errors. This indicated that "Co-titanate" formed did not cause any change in surface areas of the catalyst.

SEM and EDX were performed to study the morphologies of the catalyst samples and elemental distributions of the catalyst samples, respectively. There was no significant change in morphologies of catalyst samples due to the "Co-titanate" formed. By observation on the external surface of the catalyst granules, cobalt patches (the term "patches" is used to refer to the entities rich in cobalt supported on the catalyst granules) can be seen all over the external surface of samples. In general, all of them were similar regardless of the pretreatment conditions used. The typical morphology in an external area of catalyst granules with different magnification for Co-RW10 is shown in figure 3. It can be observed that cobalt patches (white spots) were well distributed all over the external surface of catalyst granules. The elemental distributions can be clearly seen by EDX. Figure 4 shows the typical elemental distribution for a cross section of a granule of Co-RW10. The distribution of cobalt was well dispersed throughout the catalyst granule as also seen by SEM. Thus, there was no significant change in catalyst morphologies and elemental distribution upon the formation of "Co-titanate".

The bulk crystalline phases of samples were determined using XRD. XRD patterns of TiO_2, $CoTiO_3$ (synthesized, based on reference [28]) and catalyst samples after various pretreatments are shown in figure 5. XRD patterns of TiO_2 showed strong diffrac-
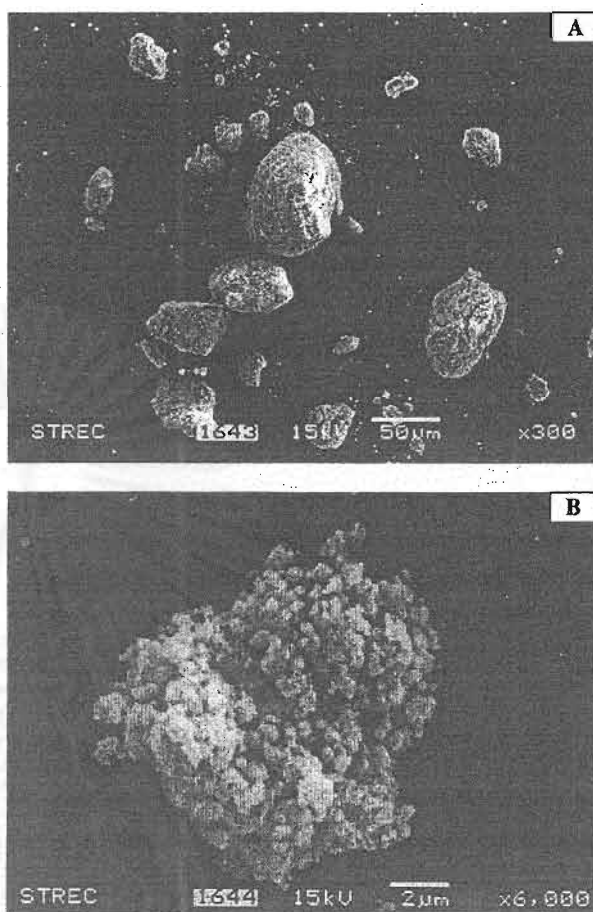

Figure 3. SEM micrographs of Co-RW10 catalyst granule at the external surface; (a) at 300× magnification and (b) at 6000× magnification.

tion peaks at 26°, 37°, 48°, 55°, 56°, 62°, 69°, 71° and 75° indicating the TiO_2 in the anatase form. After calcination, the diffraction peaks of Co_3O_4 at 36°, 46°, and 65° can be observed. Apparently, the relative intensity of those peaks is much lower compared to the TiO_2 peaks. To identify the XRD peaks of samples, XRD peaks of $CoTiO_3$ were also collected and it showed the diffraction peaks at 23°, 32°, 35°, 49°, 52°, 62° and 64° as also shown in figure 5. Kraum et al. [29] reported the observation for XRD peaks of $CoTiO_3$ phase along with Co_3O_4 on the calcined Co/TiO_2 catalyst using cobalt (III) acetyl acetonate as a precursor for cobalt. They suggested that the formation of $CoTiO_3$ by the use of cobalt (III) acetyl acetonate as a precursor can be attributed to the migration of cobalt ions into the support lattice, with the consecutive formation of titanate. However, based on differences in the cobalt precursor, the amounts of cobalt loading and the calcination condition used in the present study, the formation of $CoTiO_3$ was not observed in the calcined Co/TiO_2 catalyst. After reduction at various conditions and passivation, the diffraction peaks of CoO were
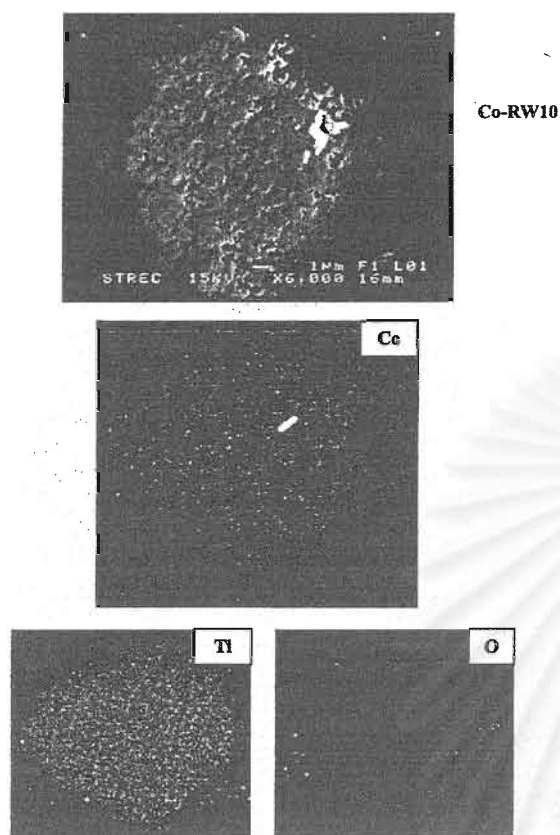
Figure 4. SEM micrograph and EDX mapping of Co-RW10 catalyst granule (cross section).

Figure 5. XRD patterns of TiO_2, $CoTiO_3$ and the catalyst samples after various pretreatment conditions.

present at 37° and 63°. This indicated that Co_3O_4 in the calcined samples was reduced to highly dispersed cobalt metal and CoO during standard reduction at 350 °C. Any Co_3O_4 formed during passivation was present in only very thin surface layers and was consequently XRD invisible. No XRD peaks for "Co-titanate" formed were detected for any of the catalyst samples. In order to investigate the structure of non-reducible (at temperatures < 800 °C during TPR) "Co-titanate", XRD was also conducted on the samples after performing TPR up to 800 °C. XRD patterns of samples after TPR measurement up to 800 °C are shown in figure 6. The similar trend as shown in figure 5 was found except for the observation of cobalt metal peaks at 44° and 52° due to sintering. No phase change, i.e from anatase to rutile form of TiO_2 was observed. XRD results revealed that the "Co-titanate" formed was in a highly dispersed form, thus, it is invisible in XRD after either standard reduction or TPR.

Raman spectra of TiO_2, CoO, Co_3O_4, $CoTiO_3$ and the catalyst samples after various pretreatments are shown in figure 7. To identify Raman bands of samples, the Raman spectra of Co_3O_4, CoO and $CoTiO_3$ were collected. The Raman bands of $CoTiO_3$ exhibited bands at 695, 604, 455, 382, 336 and 266 cm^{-1} which are similar to the ones reported by Brik et al. [30]. The strong Raman
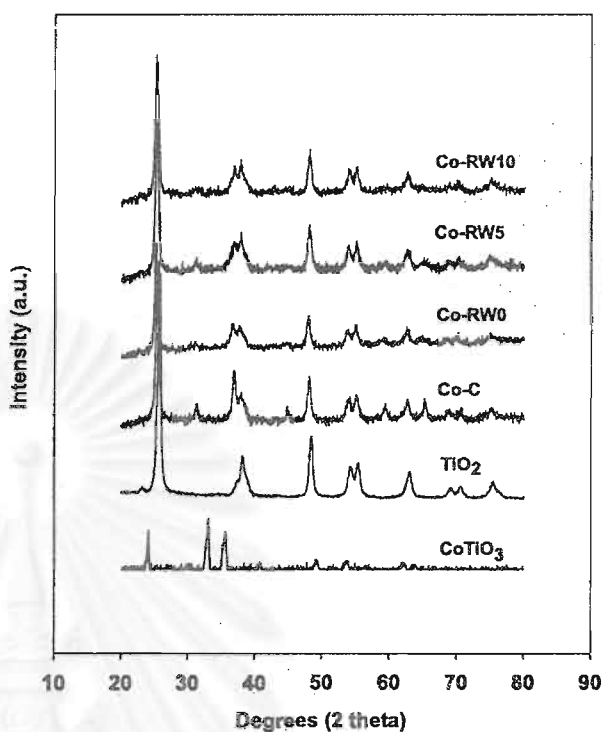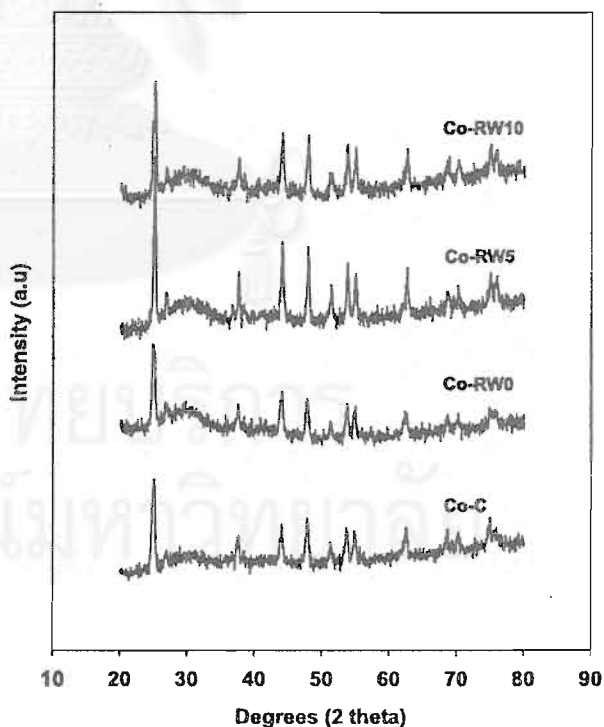

Figure 6. XRD patterns of the catalyst samples after TPR measurement up to 800 °C.

bands for TiO_2 were observed at 640, 514, and 397 cm^{-1} indicating the TiO_2 in its anatase form [9]. The Raman spectrum of the calcined sample exhibited Raman bands
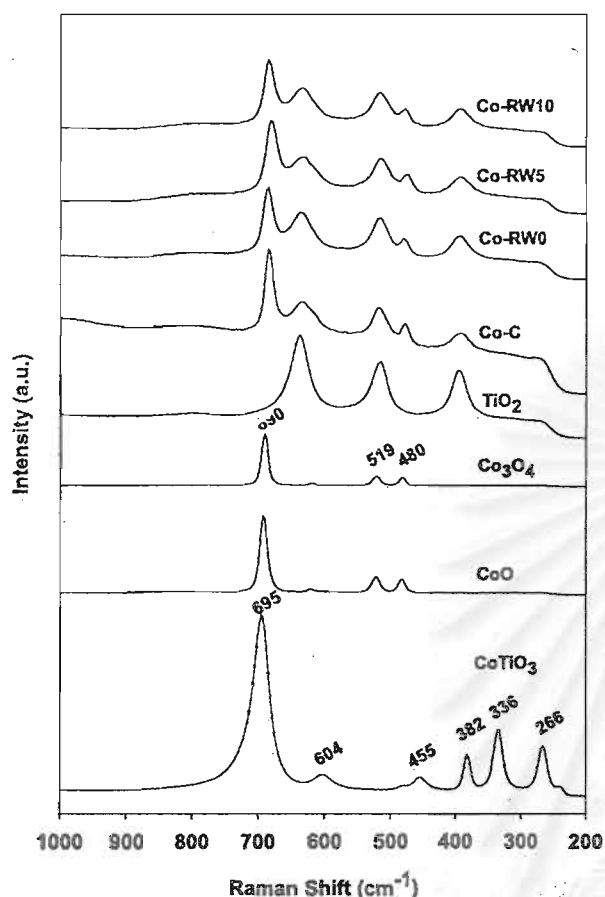
Figure 7. Raman spectra of TiO_2, Co_3O_4, CoO, $CoTiO_3$ and the catalyst samples after various pretreatment conditions.

Figure 8. Raman spectra of Co_3O_4, CoO, $CoTiO_3$, the calcined sample and the reduced with a lesser degree of passivation samples.

at 640, 514, and 397 cm^{-1} as seen in those for TiO_2 including two shoulders at 690 and 480 cm^{-1}, assigned to Co_3O_4 [4–6]. Raman spectra of all reduced samples showed the Raman bands of TiO_2 support and the shoulders at 690 and 480 cm^{-1}. These can be assigned to Co_3O_4 present on catalyst surface rather than CoO (detected in the bulk by XRD) since Raman spectroscopy is more of surface technique [5]. This indicated that "Co-titanate" formed during reduction was different from $CoTiO_3$ and invisible in Raman spectroscopy. The invisible "Co-titanate" bands was probably caused by (i) its highly dispersed form and (ii) the Raman signals were hindered due to the highly strong Raman intensities of TiO_2 support. It was reported that reduced samples of $Co/\gamma–Al_2O_3$ at high partial pressure of water vapor during reduction exhibited the broad Raman bands between 400–700 cm^{-1} [4]. This was suggested that these broad Raman bands represent a surface cobalt compound related to cobalt strongly interacting with the alumina support as a "Co-aluminate". The identified "Co-alumiante" was suggested to be different from $CoAl_2O_4$ (spinel) due to being a non-stoichiometric surface "Co-aluminate" compound. This highly dispersed "Co-aluminate" may be formed, possibly by
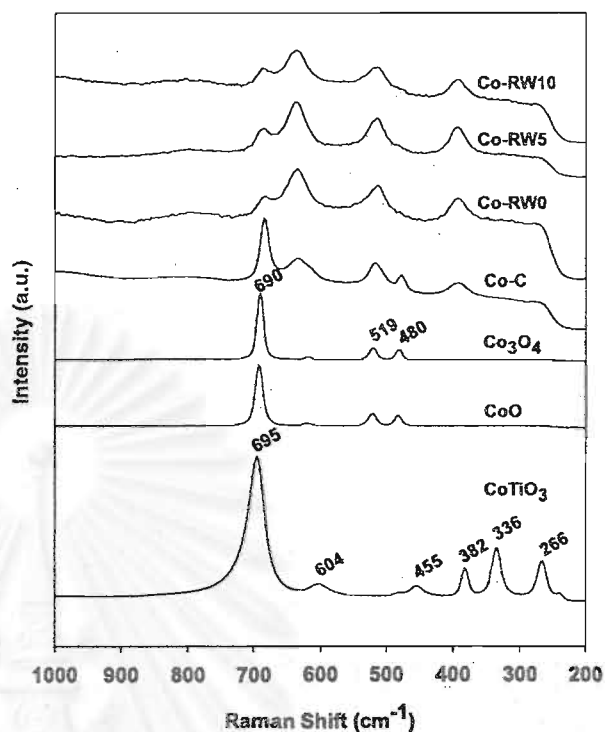
cobalt migration into the alumina matrix and was detectable using Raman spectroscopy, but not XRD. In addition, the alumina support itself does not exhibit any of Raman bands between 100 and 1000 cm^{-1}, thus, the Raman bands of "Co-aluminate" can be clearly detected. However, in the present study, the highly strong Raman intensities of the titania support may result in a hindrance of the Raman bands, if present, of the highly dispersed "Co-titanate" formed. Besides the strong signal of TiO_2, the signal of CoO and Co_3O_4 is likely to hinder the observation of surface "Co-titanate" as well. In order to eliminate that interference, we also conducted Raman spectroscopy on the reduced samples with a lesser degree of passivation and the Raman spectra of samples are shown in figure 8. It can be observed that the characteristic peaks of the reduced samples were similar to each other, but deviated from the characteristic peaks of Co_3O_4 as seen in figure 7. The Raman band of the reduced samples at 397 cm^{-1} of the TiO_2 became broader. This perhaps resulted from the overlap between the peaks of 397 cm^{-1} of the TiO_2 and 382 cm^{-1} of $CoTiO_3$ due to the formation of surface "Co-titanate". However, to elucidate all kinds of hindrances, rigorous surface techniques may be needed for further investigation. Nevertheless, Raman spectroscopy revealed that the "Co-titanate" formed was different from $CoTiO_3$ probably due to it also being non-stoichiometric (cobalt deficiency) surface "Co-titanate" compound.

CO hydrogenation was performed to determine the overall activity of the catalyst samples reduced at

Table 2
Reaction rate for CO hydrogenation on catalyst samples reduced at various conditions

Sample	CO conversion (%)[a]		Rate (μmol/gcat.s)[b]		CH$_4$ selectivity (%)	
	Initial[c]	SS[d]	Initial	SS	Initial	SS
Co–C	3.71	2.09	1.39	0.79	99	99
Co–RW0	1.53	0.73	0.58	0.27	99	99
Co–RW5	0.83	0.46	0.31	0.17	99	99
Co–RW10	0.34	0.08	0.13	0.03	98	98

[a] CO hydrogenation was carried out at 220 °C, 1.8 atm, and $H_2/CO/He = 20/2/8$ cc/min).
[b] Error $\pm 5\%$.
[c] After 5 min of reaction.
[d] After 5 h of reaction.

various conditions. The results are shown in table 2. It indicated that the CO conversion ranged between 3.71 and 0.34% (initial) and 2.09 to 0.08% (steady state). The reaction rate ranged between 1.39 and 0.13 μmol/g cat.s (initial) and 0.79–0.03 μmol/g cat.s (steady). This suggested that the "Co-titanate" formed in the reduced samples resulted in decreased activities of catalyst. However, there was no significant difference in selectivity for any of samples based on reaction conditions used in this study.

4. Conclusions

We have shown that Co-support compound formation (Co-SCF) in titania-supported cobalt catalyst can occur during standard reduction resulting in a lower reducibility of catalyst. The compound of cobalt and titania formed referred as "Co-titanate" was considered to be non-reducible at temperatures <800 °C. The "Co-titanate" formed resulted in a decrease in the degree of reduction without any significant change in the reduction behaviors. It was found that the partial pressures of water vapor during reduction probably had only a slight effect on an increase in the "Co-titanate" formation. Due to its highly dispersed form, it can not be detected by XRD. However, Raman spectroscopy revealed that this highly dispersed "Co-titanate" formed was likely to be different from CoTiO$_3$ and present as a non-stoichiometric surface "Co-titanate" compound. The "Co-titanate" formed also resulted in decreased activities of catalyst without any changes in selectivity.

Acknowledgments

References

[1] H.P. Wither Jr., K.F. Eliezer and J.W. Michell, Ind. Eng. Chem. Res. 29 (1990) 1807.
[2] E. Iglesia, Appl. Catal. A 161 (1997) 59.
[3] R.C. Brady and R.J. Pettit, J. Am. Chem. Soc. 103 (1981) 1287.
[4] B. Jongsomjit, J. Panpranot and J.G. Goodwin Jr., J. Catal. 204 (2001) 98.
[5] B. Jongsomjit and J.G. Goodwin Jr., Catal. Today 77 (2002) 191.
[6] B. Jongsomjit, J. Panpranot and J.G. Goodwin Jr., J. Catal. 205 (2003) 66.
[7] W.S. Epling, P.K. Cheekaamarla and A.M. Lane, Chem. Eng. J. 93 (2003) 61.
[8] A. Voß, D. Borgmann and G. Wedler, J. Catal. 212 (2002) 10.
[9] Y. Brik, M. Kacimi, F. Bozon-Verduraz and M. Ziyad, J. Catal. 211 (2002) 470.
[10] D.J. Duvenhage and N.J. Coville, Appl. Catal. A 233 (2002) 63.
[11] J.L. Li, G. Jacobs, T. Das and B.H. Davis, Appl. Catal. A 233 (2002) 255.
[12] K. Nakaoka, K. Takanabe and K. Aika, Chem. Commun. 9 (2002) 1006.
[13] N.N. Madikizela and N.J. Coville, J. Mol. Catal. A-Chem. 181 (2002) 129.
[14] N.J. Coville and J.L. Li, Catal. Today 71 (2002) 403.
[15] J.L. Li, L.G. Xu, R. Keogh and B. Davis, Catal. Lett. 70 (2000) 127.
[16] D.G. Wei, J.G. Goodwin Jr., R. Oukaci and A.H. Singleton, Appl. Catal. A 210 (2001) 137.
[17] J.L. Li and N.J. Coville, Appl. Catal. A 208 (2001) 177.
[18] R. Zennaro, M. Tagliabue and C.H. Bartholomew, Catal. Today 58 (2000) 309.
[19] R. Riva, H. Miessuer, R. Vitali and G. Del Piero, Appl. Catal. A 196 (2000) 111.
[20] J.L. Li and N.J. Coville, Appl. Catal. A 181 (1999) 201.
[21] A. Kogelbauer, J.C. Weber and J.G. Goodwin Jr., Catal. Lett. 34 (1995) 269.
[22] Y. Zhang, D. Wei, S. Hammache and J.G. Goodwin Jr., J. Catal. 188 (1999) 281.
[23] A. Kogelbauer, J.G. Goodwin Jr. and R. Oukaci, J. Catal. 160 (1996) 125.
[24] D. Schanke, S. Vada, E.A. Blekkan, A. Hilmen, A. Hoff and A. Holmen, J. Catal. 156 (1995) 85.
[25] B.A. Sexton, A.E. Hughes and T.W. Turney, J. Catal. 97 (1986) 390.
[26] P. Arnoldy and J.A. Moulijn, J. Catal. 93 (1985) 38.
[27] A.M. Hilmen, D. Schanke and A. Holmen, Catal. Lett. 38 (1996) 143.
[28] B. Brezny and A. Muan, J. Inorg. Nucl. Chem. 31 (1969) 649.
[29] M. Kraum and M. Baerns, Appl. Catal. A 186 (1999) 189.
[30] Y. Brik, M. Kacimi, M. Ziyad and F. Bozon-Verduraz, J. Catal. 202 (2001) 118.

VITAE

Miss Chitlada Sakdamnuson was born on October 20th, 1979 in Singburi, Thailand. She received the Bachelor degree of Science with a major in Chemical Technology from Chulalongkorn University in May 2002. She continued her Master's study at the department of Chemical Engineering, Chulalongkorn University in June 2002.